Proceedings of Anticancer Research

BIO-BYWORD SCIENTIFIC PUBLISHING PTY LTD
(619 649 400)
Level 10
50 Clarence Street
SYDNEY NSW 2000

ISSN (ONLINE): 2208-3553
ISSN (PRINT): 2208-3545

Proceedings of Anticancer Research

Focus and Scope

Proceedings of Anticancer Research is an international peer-reviewed and open access journal, which is devoted to the rapid publication of high quality original articles, reviews, case reports, short communication and letters on all aspects of experimental and clinical oncology.

- Cellular research and bio-markers
- Identification of bio-targets and agents with novel mechanisms of action
- Preventative and integrated treatment for cancer patients
- Radiation and surgery
- Palliative care
- Patient adherence, quality of life, satisfaction
- Anticancer medicine

About Publisher

Bio-Byword Scientific Publishing is a fast-growing, peer-reviewed and open access journal publisher, which is located in Sydney, Australia. As a dependable and credible corporation, it promotes and serves a broad range of subject areas for the benefit of humanity. By informing and educating a global community of scholars, practitioners, researchers and students, it ndeavors to be the world's leading independent academic and professional publisher. To realize it, it keeps creative and innovative to meet the range of the authors' needs and publish the best of their work.

By cooperating with University of Sydney, University of New South Wales and other world-famous universities, Bio-Byword Scientific Publishing has established a huge publishing system based on hundreds of academic programs, and with a variety of journals in the subjects of medicine, construction, education and electronics.

PublisherHeadquarter

BIO-BYWORD SCIENTIFIC PUBLISHING PTYLTD Level 10
50 Clarence Street
Sydney NSW 2000
Website: www.bbwpublisher.com Email: info@bbwpublisher.com

2024, Volume 8, Issue 2

Table of Contents

Proceedings of Anticancer Research, 2024, Volume 8, Issue 2
http://ojs.bbwpublisher.com/index.php/PAR
ISSN Online: 2208-3553
ISSN Print: 2208-3545

Study on the Application Value of Liver Function and Serological Index Levels in the Diagnosis of Fatty Liver

Gaopeng Lu*

Wuxi Ziwang Rehabilitation Hospital, Wuxi 214191, China

***Corresponding author:** Gaopeng Lu, 444501868@qq.com

Abstract: *Objective:* To explore the application value of liver function and serological index detection in diagnosing fatty liver. *Methods:* Ninety patients with fatty liver disease (disease group) and ninety healthy subjects (healthy group) were selected as the subjects of this study. They all underwent liver function index testing and serological index testing. Test results were compared, and the diagnostic accuracy of single and combined tests was evaluated. *Results:* Liver function indicators of patients in the disease group were higher than those in the healthy group, with severe patients exhibiting higher levels than moderate patients and mild patients ($P < 0.05$). Serological indicators in patients in the disease group were higher than those in the healthy group, with severe patients showing higher levels than moderate patients and mild patients ($P < 0.05$). The diagnostic accuracy of liver function index testing was higher than that of serological index testing, and the accuracy of combined testing was higher than that of single testing ($P < 0.05$). *Conclusion:* In diagnosing fatty liver, combining liver function testing and serological testing enables the initial diagnosis of the disease and facilitates the accurate assessment of its severity.

Keywords: Fatty liver; Clinical diagnosis; Liver function test; Serological test

Online publication: February 23, 2024

1. Introduction

Fatty liver is a liver disease with a high clinical incidence, often associated with daily dietary habits, such as high-sugar and high-calorie intake. With people's living standards improving, the incidence of fatty liver continues to rise, making it the second most common liver disease and significantly impacting physical health. The primary pathogenesis of fatty liver involves the accumulation of excess fat within liver cells. Early stages of the disease typically present no obvious symptoms, although symptoms resembling gastrointestinal issues may manifest [1]. Consequently, early screening poses challenges. As the disease progresses, patients may experience liver area pain, lower limb edema, jaundice, lethargy, and other related symptoms [2]. Treatment becomes more difficult at this stage, often with less-than-ideal prognoses.

Early diagnosis of fatty liver is crucial for determining disease severity and implementing appropriate

treatment strategies. Serological index testing is a standard clinical examination procedure, while liver function index testing plays a significant role in liver disease diagnosis and management. This study aims to analyze the combined examination of these two approaches in fatty liver disease to assess their diagnostic value. To investigate this, 90 patients with fatty liver and 90 healthy subjects were included.

2. Materials and methods

2.1. General information

From January 2021 to December 2023, 90 patients with fatty liver were screened and admitted. During the same period, 90 healthy subjects who underwent physical examinations were selected to form a disease group and a healthy group, respectively.

Healthy group: 52 males and 38 females, aged 36 to 75 years (mean age 57.45 ± 5.23 years).

Disease group: 50 males and 40 females, aged 35 to 77 years (mean age 57.20 ± 5.41 years); disease duration 2 to 10 years (mean duration 6.05 ± 1.14 years); disease severity comprised 21 mild cases, 32 moderate cases, and 37 severe cases.

Gender and age comparisons between the two groups showed no significant difference ($P > 0.05$).

2.2. Inclusion and exclusion criteria

Inclusion criteria:

(1) The disease group consisted of 90 patients meeting clinical diagnostic criteria for fatty liver, while the physical examination results of the healthy group were normal;
(2) No recent intake of drugs affecting liver function or serological indicators;
(3) Willingness to cooperate with examination procedures;
(4) Consciousness and normal cognition;
(5) Complete clinical information.

Exclusion criteria:

(1) Presence of other liver diseases;
(2) Organ dysfunction or concomitant physical illnesses such as malignant tumors;
(3) Mental illness;
(4) Participation in other concurrent medical research projects.

2.3. Methods

Both research subjects underwent testing for liver function and serological indicators. Participants adjusted their diet three days prior by abstaining from pig blood or liver, alcohol, and high-fat and high-protein foods, maintaining a light diet. Fasting for a minimum of eight hours before the examination was ensured. On the examination day, 5 mL of venous blood was collected between 7 a.m. and 9 a.m., and serum was separated for testing. Liver function index levels, including aspartate aminotransferase (AST; normal range: 0–50 μmol/L), alanine aminotransferase (ALT; normal range: 0–40 μmol/L), and γ-glutamyl transpeptidase (γ-GT; normal range: 0–40μ/L), were measured using the rate method. Serological index levels, including total cholesterol (TC; normal range: 3.0–5.7 mmol/L), triglyceride (TG; normal range: 0.5–1.7 mmol/L), low-density lipoprotein cholesterol (LDL-C; normal range: 2.1–3.1 mmol/L), and high-density lipoprotein cholesterol (HDL-C; normal range: 0.9–1.8 mmol/L), were measure using the enzyme-linked method.

2.4. Observation indicators

Comparison of liver function and serological test results between the two research subjects and evaluation of the diagnostic accuracy of single and combined tests.

2.5. Statistical analysis

Data were analyzed using SPSS version 25.0 statistical software. Measurement data conforming to normal distribution were expressed as mean ± standard deviation (SD) and underwent either *t*-tests or F-tests (for three or more groups). Count data were presented as [*n* (%)] and underwent χ^2 tests. A significance level of $P < 0.05$ indicated statistical significance.

3. Results

3.1. Comparison of liver function indicators

As shown in **Table 1**, the levels of AST, ALT, and γ-GT in patients in the disease group were significantly higher than those in the healthy group ($P < 0.05$). As the severity of the disease increased, the levels of each liver function index gradually increased ($P < 0.05$).

3.2. Comparison of blood routine indicators

Table 2 shows that the TC and TG levels of patients in the disease group were significantly higher than those of the healthy group ($P < 0.05$). The difference in LDL-C and HDL-C levels between the two groups was insignificant ($P > 0.05$). As the severity of the disease increased, the levels of TC and TG continued to increase ($P < 0.05$), while the levels of LDL-C and HDL-C had no significant changes ($P > 0.05$).

3.3. Diagnostic effect

As presented in **Table 3**, the accuracy of liver function testing is higher than that of serological testing ($P < 0.05$), and the accuracy of combined testing is higher than that of single testing ($P < 0.05$).

Table 1. Comparison of liver function indicators (mean ± SD)

Group name	*n*	AST (μmol/L)	ALT (μmol/L)	γ-GT (μ/L)
Healthy group	90	15.34 ± 5.28	19.20 ± 5.13	26.35 ± 6.14
Disease group	90	56.96 ± 12.17	61.85 ± 12.18	81.45 ± 20.31
t	-	29.763	30.615	24.636
P	-	0.000	0.000	0.000
Mild	21	51.63 ± 5.28	46.69 ± 10.18	53.64 ± 9.47
Moderate	32	54.96 ± 8.15	52.74 ± 9.51	71.05 ± 12.28
Severe	37	59.04 ± 7.54	68.41 ± 15.08	90.45 ± 17.04
F	-	10.631	13.245	11.057
P	-	0.000	0.000	0.000

Table 2. Comparison of blood routine indicators (mean ± SD, mmol/L)

Group name	*n*	TC	TG	LDL-C	HDL-C
Healthy group	90	4.79 ± 0.54	1.89 ± 0.41	3.31 ± 0.45	1.22 ± 0.25
Disease group	90	7.12 ± 1.13	3.19 ± 0.54	3.27 ± 0.51	1.19 ± 0.27
t	-	17.650	18.190	0.558	0.773
P	-	0.000	0.000	0.578	0.440
Mild	21	5.91 ± 1.08	2.23 ± 0.65	3.21 ± 0.48	1.15 ± 0.22
Moderate	32	6.79 ± 1.14	2.98 ± 0.51	3.25 ± 0.44	1.17 ± 0.23
Severe	37	7.78 ± 1.23	3.64 ± 0.47	3.30 ± 0.50	1.21 ± 0.30
F	-	14.528	12.645	0.418	0.516
P	-	0.000	0.000	0.423	0.411

Table 3. Diagnosis results [*n* (%)]

Detection method	*n*	Confirmed	Missed diagnosis / misdiagnosis
Liver function test	90	72 (80.00)	18 (20.00)
Serological testing	90	54 (60.00)	36 (40.00)
Combined testing	90	87 (96.67)	3 (3.33)
χ^2 / *P* single testing comparison	-	8.571 / 0.003	
Comparison of χ^2 / *P* combined detection and single detection	-	36.427 / 0.000	

4. Discussion

The liver, being a vital metabolic organ, is susceptible to various liver diseases. Statistics indicate that the incidence rate of fatty liver in China is approximately 20% [3], with economically developed regions exhibiting higher rates. For instance, in first-tier cities like Beijing, Shanghai, and Guangzhou, the incidence ranges between 25% and 30% [4]. Fatty liver is more prevalent in men than in women, often associated with excessive alcohol consumption and poor dietary habits. It is both a stress-related condition and influenced by genetic factors. Dietary composition and lifestyle choices play pivotal roles in its development. Factors such as alcohol abuse, overeating, and obesity disrupt the body's fat metabolism balance, leading to the accumulation of excess fat in liver cells. Hepatocyte degeneration occurs when the fat weight in liver cells surpasses 5% of the liver's wet weight [5], progressing to liver fibrosis and potentially culminating in cirrhosis or liver failure. Apart from impacting liver function, fatty liver can also trigger cardiovascular diseases such as stroke and diabetes. Importantly, fatty liver is reversible [6]; early detection and symptomatic treatment can impede liver fibrosis progression and gradually restore liver function. Early diagnosis, therefore, forms the cornerstone of effective treatment, with liver biopsy traditionally considered the gold standard. However, due to its invasiveness and associated health risks, liver biopsy is not widely favored and may compromise patient well-being. Non-invasive diagnostic techniques, including imaging studies and serum biochemical testing, are thus recommended.

This study comprised 90 patients diagnosed with fatty liver and 90 healthy subjects, forming disease and healthy groups, respectively. Results revealed that both groups underwent liver function index testing

and serological index testing, procedures that entail minimal invasiveness by requiring only serum collection. Liver function indicators, including AST, ALT, and γ-GT, play crucial roles in diagnosing fatty liver. AST and ALT, secreted by mitochondria and cytoplasm of human cells, enter the bloodstream during pathological liver cell reactions, leading to elevated levels. γ-GT is released from the intrahepatic bile duct epithelium and liver cytoplasm when liver tissue is damaged [7,8]. The findings indicated higher levels of these liver function indicators in the disease group compared to the healthy group, with severity correlating with higher levels, underscoring their diagnostic and prognostic significance. As a bile-synthesizing organ, the liver influences lipid emulsification. Fatty liver disrupts this process, leading to elevated TC and TG levels, particularly after prolonged consumption of high-fat diets [9]. While LDL-C and HDL-C levels remained relatively stable between groups, TC and TG levels were significantly higher in the disease group, with severity correlating with elevated levels. This suggests that routine blood lipid indicators, namely TC and TG, can aid in fatty liver diagnosis and severity assessment. A comparison of single and combined liver function and serological index testing indicated higher accuracy with combined testing, highlighting the synergistic benefits of utilizing both methods.

In the early stages, fatty liver symptoms are often subtle, becoming more pronounced as the disease progresses, with specific manifestations linked to underlying causes. Early-stage symptoms may include fatigue, loss of appetite, and hepatosplenomegaly [10], progressing to nosebleeds, melena, and lower limb edema in advanced stages. While liver biopsy remains the gold standard for diagnosis, its invasive nature, associated risks, and low reproducibility limit its utility [11]. Liver function and serological index testing, on the other hand, are routine clinical procedures requiring minimal venous blood collection and boasting high patient acceptance rates [12].

In conclusion, this study's analysis underscores the prevalence of fatty liver as a common clinical condition. Liver function and blood routine index testing exhibit significant diagnostic utility in fatty liver diagnosis and merit widespread adoption.

Disclosure statement

The author declares no conflict of interest.

References

[1] Zhang Y, Tong Y, Liu X, et al., 2023, Expression Changes and Diagnostic Value of miRNA-223 in Elderly Patients with Non-Alcoholic Fatty Liver. Gerontology and Health Care, 29(5): 885–888.

[2] Wang Y, Zhao J, Zhou S, et al., 2021, Analysis of the Diagnostic Efficacy of Forns Index, FIB-4, APRI, and GPR for Liver Fibrosis in Patients with HBV Infection and Non-Alcoholic Fatty Liver Disease. Journal of PLA Medicine, 33(7): 72–77.

[3] Ye Y, Pan L, Bao D, et al., 2021, Diagnostic Value of Golgi Protein 73 and FIB4 Index in Non-Alcoholic Fatty Liver Disease Cirrhosis. Zhejiang Clinical Medicine, 23(11): 1575–1577.

[4] Huang Y, Ren Y, Yang Y, et al., 2022, Effect of Blood Lipid Concentration on Diagnosing Fatty Liver with MRI In-Phase and Reverse-Phase Imaging. Chinese Physician Journal, 24(5): 753–755.

[5] Huang M, Qin Q, Yan S, et al., 2022, Research on the Diagnostic Efficacy of Obesity-Related Indicators for Non-Alcoholic Fatty Liver Disease. Chinese Journal of Preventive Medicine, 23(4): 255–259.

[6] Zhang D, Sun F, Wang G, et al., 2023, Preliminary Study on the Quantitative Assessment of IDEAL-IQ and Its Correlation with Blood Lipid Content in Patients with Non-Alcoholic Fatty Liver Disease. Journal of Practical Radiology, 39(1): 66–69.

[7] Lin J, Liang Z, Zhang Y, et al., 2023, Research on Influencing Factors Related to the Onset of Non-Alcoholic Fatty Liver – Based on Subjects from a Physical Examination Center in Nanning, Guangxi. Guangxi Science, 30(4): 821–828.

[8] Li X, Liu M, Yin X, et al., 2023, Diagnostic Value of Ultrasound-Guided Percutaneous Liver Tissue Biopsy in Early Liver Cancer. Guizhou Medicine, 47(3): 443–444.

[9] Peng X, Gong X, Guo Y, et al., 2023, Predictive Value of Liver Biochemical Indicators Combined with MRI In-Phase and Anti-Phase for Fat Quantification in Non-Alcoholic Fatty Liver. Liver, 28(6): 711–715.

[10] Ze N, Mima T, Tashi D, 2023, Analysis of the Correlation between Serum A1AT Levels and Type 2 Diabetes Combined with Non-Alcoholic Fatty Liver and Liver Fibrosis. Chinese Clinical New Medicine, 16(8): 816–820.

[11] Wu C, Zhang C, Xu H, et al., 2023, Analysis of the Epidemiological Research and Diagnosis Status of Non-Alcoholic Fatty Liver Disease in China. China Medical Herald, 20(11): 158–161.

[12] Fang D, Xiao Q, Yang L, et al., 2023, Study on Serum Lipidomics Analysis and Diagnostic Value of Patients with Type 2 Diabetes Complicated with Non-Alcoholic Steatohepatitis. Journal of Modern Laboratory Medicine, 38(3): 159–164.

Proceedings of Anticancer Research, 2024, Volume 8, Issue 2
http://ojs.bbwpublisher.com/index.php/PAR
ISSN Online: 2208-3553
ISSN Print: 2208-3545

VEGF, HIF-1α, and Metabolic Indicators in Esophageal Squamous Cell Carcinoma

Yangyan Chen*

Shanghai Zhangjiang Institute of Medical Innovation, Shanghai 201204, China

***Corresponding author:** Yangyan Chen, chenyangyan6@126.com

Abstract: *Objective:* To explore and analyze the expression and clinical significance of vascular endothelial growth factor (VEGF), hypoxia-inducible factor 1α (HIF-1α), and metabolic indicators in esophageal squamous cell carcinoma (ESCC). *Methods:* Sixty ESCC patients admitted to the hospital from October 2021 to October 2023 were selected as the ESCC group. Sixty normal healthy patients from the same period were chosen as the control group. Their serum samples and tissue samples were collected. Metabolic indicators of all study subjects were obtained based on the basic biochemical results upon admission. RT-PCR was utilized to detect the expression of VEGF and HIF-1α in ESCC tissues. *Results:* The expression of VEGF and HIF-1α in the ESCC T3+T4 group was significantly higher than that of the carcinoma *in situ* (Tis) group, T1+T2 group, and control group. Furthermore, the expression of HIF-1α was found to be related to the expression of VEGF, showing a significant correlation between the quantities. Significant differences in the levels of metabolic indicators were observed between the ESCC group and the control group ($P < 0.05$). *Conclusion:* Metabolic indicators are associated with the onset of ESCC in patients. Abnormal lipid metabolism plays a crucial role in the occurrence and development of tumors. The expression of VEGF and HIF-1α in ESCC tissues significantly correlates with the tumor stage, providing a new reference for the diagnosis and treatment of ESCC.

Keywords: VEGF; HIF-1α; Metabolic index; Esophageal squamous cell carcinoma (ESCC)

Online publication: March 28, 2024

1. Introduction

Esophageal squamous cell carcinoma (ESCC) is a malignant tumor of the esophagus caused by esophageal squamous epithelial dysplasia. It represents a common disease, yet its primary cause remains incompletely understood, possibly attributed to factors such as diet, lifestyle, genetics, infection, and other diseases. The clinical presentation typically involves symptoms such as dysphagia, pain, regurgitation, hoarseness, and weight loss, often leading to complications such as infection, fluid imbalance, and psychological disorders [1]. Tumor markers play a crucial role in clinical examinations, providing essential guidance for the detection, diagnosis, treatment, and prognosis of diseases, including esophageal cancer. Most clinically detected tumor markers manifest in malignant tumors, benign tumors, embryonic tissues, and even normal tissues. Studies have highlighted the

significance of elevated vascular endothelial growth factor (VEGF) expression as an indicator of poor prognosis in esophageal cancer [2].

Hypoxia-inducible factor 1α (HIF-1α) is a component of HIF-1 that exhibits widespread expression in tissue cells during hypoxia, including the kidney, liver, lung, brain, heart, and various cell lines [3]. Hypoxia represents the most common physiological response of the body. HIF-1α plays a pivotal role in ischemic-hypoxic brain injury, hypoxic lung disease, ischemic-hypoxic myocardial disease, tumors, and inflammation. Consequently, dynamic monitoring of tumor markers and comprehensive serum index examinations hold greater value [4]. This study focuses on 60 ESCC patients treated at the hospital from October 2021 to October 2023, aiming to explore the expression and clinical significance of VEGF, HIF-1α, and metabolic indicators in ESCC.

2. Materials and methods

2.1. General information

Sixty ESCC patients admitted to the hospital between October 2021 and October 2023 were selected as the ESCC group, from whom serum and tissue samples were collected. Among them, there were 39 males and 21 females, with an average age of 62.76 ± 4.08 years. This group comprised 12 cases of carcinoma *in situ* (Tis), 32 cases of T1+T2 stage, and 16 cases of T3+T4 stage. Additionally, 60 normal healthy patients from the same period were chosen as the control group. Basic information such as age and gender was comparable across the four groups, with no significant differences noted ($P > 0.05$). This study was approved by the local ethics committee.

2.2. Methods

Fasting blood glucose (FBG), triglycerides (TG), total cholesterol (TC), low-density lipoprotein (LDL), high-density lipoprotein (HDL), and blood uric acid (BUA) levels were obtained for all subjects based on the basic biochemical results upon admission. Additionally, albumin (ALB) was included as a key metabolic indicator for statistical analysis. The expression of VEGF and HIF-1α in ESCC tissues was detected using real-time polymerase chain reaction (RT-PCR). Mouse anti-human HIF-1α monoclonal antibody, rabbit anti-human VEGF monoclonal antibody, and immunoassay kits were procured from Beijing Kerimei Technology Co., Ltd., and strictly followed the instructions provided with the kits.

2.3. Observation indicators

Metabolic indicators and the expression of VEGF and HIF-1α in ESCC tissue were analyzed to investigate their clinical significance in ESCC.

2.4. Statistical analysis

SPSS 26.0 statistical software was utilized for analysis. Measurement data were expressed as mean ± standard deviation (SD). The *t*-test was employed, and the correlation analysis of VEGF and HIF-1α expression was conducted using Spearman rank correlation analysis. A significance level of $P < 0.05$ indicated statistical significance.

3. Results

3.1. Comparison of metabolic index levels between the two groups

Table 1 shows that there were significant differences in the levels of metabolic indicators TC, HDL, LDL, and ALB between the ESCC group and the control group. Patients in the esophageal squamous cell carcinoma group had higher TC (3.76 ± 1.24 mmol/L) and LDL (2.98 ± 0.75 mmol/L) as compared to the control group of 3.46 ± 1.12 mmol/L TC and 2.33 ± 0.97 mmol/L LDL ($P < 0.05$). The ESCC group also exhibited lower HDL (0.76 ± 0.23 mmol/L) and ALB (32.86 ± 4.53 g/L) as compared to the control group of 1.12 ± 0.21 mmol/L HDL and 39.25 ± 2.83 g/L ALB ($P < 0.05$).

Table 1. Comparison of metabolic index levels between the two groups

Indicator	Control group ($n = 60$)	ESCC group ($n = 60$)	t value	P value
FBG (mmol/L)	5.82 ± 4.35	5.37 ± 2.46	2.863	0.285
TG (mmol/L)	0.62 ± 0.45	0.53 ± 0.31	1.924	0.369
TC (mmol/L)	3.46 ± 1.12	3.76 ± 1.24	8.935	0.003
LDL (mmol/L)	2.33 ± 0.97	2.98 ± 0.75	10.427	0.000
HDL (mmol/L)	1.12 ± 0.21	0.76 ± 0.23	15.982	0.000
BUA (μmol/L)	310.26 ± 54.37	342.15 ± 60.94	1.025	0.682
ALB (g/L)	39.25 ± 2.83	32.86 ± 4.53	8.058	0.005

3.2. Comparison of the expression of VEGF and HIF-1α between the two groups

As shown in **Figure 1**, VEGF and HIF-1α in the ESCC T3+T4 group were significantly higher than that in the carcinoma *in situ* (Tis) group, T1+T2 group, and control group. There is a significant correlation between VEGF expression and HIF-1α expression ($P < 0.05$).

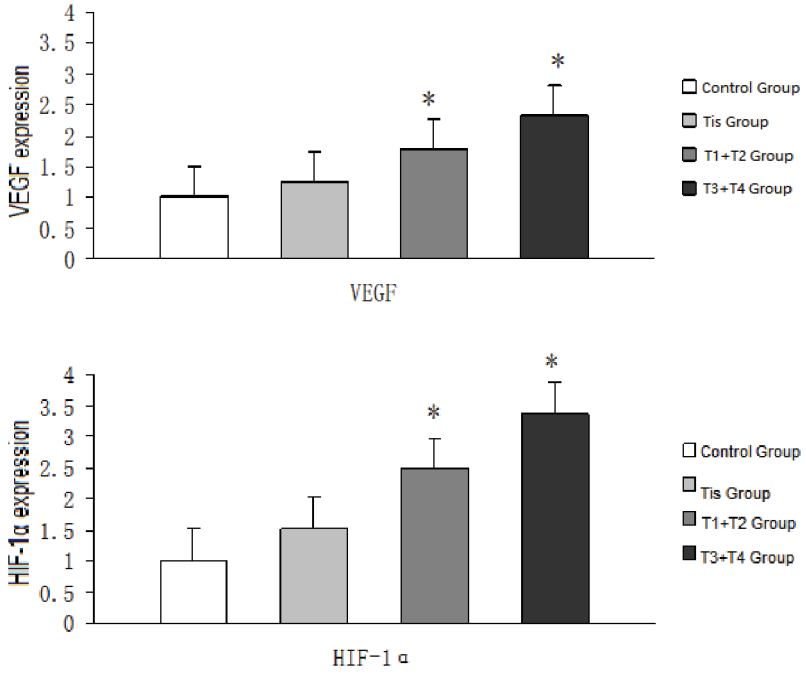

Figure 1. Comparison of the expression of VEGF and HIF-1α between the two groups. *$P < 0.05$

4. Discussion

ESCC ranks among the most common malignant tumors of the digestive tract, characterized by complex and diverse mechanisms driving its occurrence and progression. Often detected in advanced stages with high metastatic potential, its prognosis remains poor [5,6]. Diagnosis typically involves various modalities such as endoscopy, imaging studies, and laboratory tests. Notably, nodular or cauliflower-like tumors are observed in middle to late stages via endoscopy, along with ulcers and esophageal lumen stenosis. Chromoendoscopy enhances the detection rate of early ESCC [7]. Additionally, endoscopic ultrasonography can display changes in the esophageal wall's hierarchical structure, the cancer's infiltration depth, and its relationship with surrounding tissues. CT examination can clarify the staging of esophageal squamous cell carcinoma and can also be used to judge prognosis. PET-CT scans provide valuable insights into primary tumor extent, lymph node involvement, metastasis, and tumor staging [8-10]. Laboratory investigations, including blood and urine analyses, liver and kidney function tests, and tumor marker assessments, play pivotal roles in evaluating patients' overall condition and aiding in ESCC diagnosis. Serum tumor markers, renowned for their convenience, minimal invasiveness, and prompt disease status reflection, are widely employed in diagnosing, evaluating treatment efficacy, and assessing prognosis across various cancers [11,12]. In clinical practice, combining multiple tumor markers enhances diagnostic sensitivity, compensating for individual marker limitations and enabling early detection and intervention.

ESCC is frequently diagnosed at intermediate to advanced stages. Early screening and prompt identification of suspicious or asymptomatic individuals are pivotal for improving survival rates and prolonging patient survival. Notably, VEGF exhibits elevated production during the transition of ESCC to solid tumors, particularly evident in the Tis and T1 stages, making it a prime candidate for tumor screening using existing clinical methods. Other tumor markers are mostly produced in the T3 and T4 stages of ESCC and are of little significance for early screening [13]. VEGF's role in promoting tumor angiogenesis is well-established, with implications for tumor growth and metastasis. Moreover, studies have implicated VEGF in mediating vascular permeability, enhancing malignant extravasation, and facilitating endothelial progenitor cell mobilization to foster tumor neovascularization [14]. Targeting VEGF pathways holds promise for novel therapeutic strategies. Hypoxia, a hallmark of aggressive tumors, underscores the importance of investigating new HIF-1α target genes to develop targeted therapies that impede disease progression. Additionally, hypoxia within the tumor microenvironment triggers inflammatory responses, further exacerbating tumorigenesis, with HIF-1α potentially mediating inflammatory effects [15,16]. This study reveals significantly elevated expression levels of VEGF and HIF-1α in the ESCC T3+T4 group compared to the Tis and T1+T2 groups, with a notable correlation between HIF-1α and VEGF expression levels. This highlights the prognostic and therapeutic relevance of heightened VEGF and HIF-1α expression levels. Elevated tumor marker levels are implicated in tumor initiation and progression.

This study's findings demonstrate significant differences in metabolic indicator levels, including TC, HDL, LDL, and ALB, between the ESCC and control groups. Specifically, ESCC patients exhibited high TC (3.76 ± 1.24 mmol/L) and LDL (2.98 ± 0.75 mmol/L) levels but lower HDL (0.76 ± 0.23 mmol/L) and ALB (32.86 ± 2.83 g/L) compared to the control group (TC: 3.46 ± 1.12 mmol/L; LDL: 2.33 ± 0.97 mmol/L; HDL: 1.12 ± 0.21 mmol/L; ALB: 39.25 ± 2.83 g/L). These metabolic changes influence ESCC progression, with proliferating carcinoma cells driving increased cholesterol demand and LDL serving as a key cholesterol transporter, contributing to elevated levels. Conversely, HDL primarily facilitates cholesterol transport to the liver for degradation, hence its decreased levels in ESCC patients. Consequently, abnormal lipid metabolism plays a pivotal role in tumor development. The significant correlation between VEGF and HIF-1α expression and tumor stage underscores their potential as diagnostic and therapeutic targets for ESCC.

Disclosure statement

The author declares no conflict of interest.

References

[1] Li X, Yang J, Wang J, 2020, Research Status of Genomics, Proteomics, and Metabolomics Application in Esophageal Cancer Screening and Early Diagnosis. Chinese Journal of Cancer Prevention and Treatment, 27(6): 493–498.

[2] Cui Y, Chen H, Xi R, et al., 2022, Whole-Genome Sequencing of 508 Patients Identifies Key Molecular Features Associated with Poor Prognosis in Esophageal Squamous Cell Carcinoma. Cell Res, 30(10): 902–913. https://doi.org/10.1038/s41422-020-0333-6

[3] Wan P, Shen W, Peng Z, et al., 2022, Characteristic Intestinal Flora and Associated Biomarkers in Esophageal Cancer Based on PacBio SMRT Sequencing. Journal of Environmental and Occupational Medicine, 39(9): 1011–1020. https://doi.org/10.11836/JEOM22065

[4] Yang L, Miao Z, Kang X, 2023, Changes and Clinical Significance of Peripheral Serum VEGF Before and After Chemotherapy in Patients with Esophageal Squamous Cell Carcinoma. Hebei Medicine, 45(21): 3226–3229.

[5] Liu Z, Zhao Y, Kong P, et al., 2023, Integrated Multi-Omics Profiling Yields a Clinically Relevant Molecular Classification for Esophageal Squamous Cell Carcinoma. Cancer Cell, 41(1): 181–195.e9. https://doi.org/10.1016/j.ccell.2022.12.004

[6] Tang L, Liu T, Jia X, et al., 2022, Effect and Prognosis Analysis of Intensity-Modulated Radiotherapy Combined with Concurrent CF Regimen on IGF-1 and VEGF in Esophageal Squamous Cell Carcinoma. Zhongnan Journal of Medical Sciences, 50(2): 245–248.

[7] Chen X, Yu L, Zhou J, et al., 2023, Inhibition of p62 and/or NFE2L2 Induced Autophagy Impaired Esophageal Squamous Cell Cancer Metastasis by Reversing EMT. Gene, 858: 147194. https://doi.org/10.1016/j.gene.2023.147194

[8] Guo J, Alimujiang M, Idelis A, et al., 2023, The Role and Changes of Lymphatic Vessels and Endothelial Cells in Esophageal Cancer's Lymphatic Metastasis. Chinese Clinic of Thoracic and Cardiovascular Surgery Magazine, 30(5): 766–772.

[9] Chen D, Di Y, 2021, The Influence of Blood Lipid Levels and Metabolic Indicators on the Incidence of Esophageal Cancer. Modern Oncology, 29(21): 3770–3772.

[10] Wang X, Yang H, Fan J, et al., 2023, Exploration of Esophageal Squamous Cell Carcinoma Metabolomic Markers Based on the Lin County Nutritional Intervention Trial Population. Chinese Oncology, 32(2): 154–160.

[11] Li Y, Xing S, Chen F, et al., 2023, Intracellular *Fusobacterium nucleatum* Infection Attenuates Antitumor Immunity in Esophageal Squamous Cell Carcinoma. Nat Commun, 14(1): 5788. https://doi.org/10.1038/s41467-023-40987-3

[12] Cui S, McGranahan N, Gao J, et al., 2023, Tracking the Evolution of Esophageal Squamous Cell Carcinoma Under Dynamic Immune Selection by Multi-Omics Sequencing. Nat Commun, 14(1): 892. https://doi.org/10.1038/s41467-023-36558-1

[13] Cao Z, Yang J, 2023, The Value of Serum SCC-Ag, VEGF, and UHRF1 Levels in Predicting the Recurrence of Esophageal Squamous Cell Carcinoma After Radical Surgery. Henan Medical Research, 32(6): 1024–1029.

[14] Hua Y, He K, Zhang J, et al., 2023, Effects of High Expression of Hypoxia-Inducible Factors and Angiogenic Factors Induced by *Fusobacterium nucleatum* on Survival Prognosis of Patients with Esophageal Squamous Cell Carcinoma. Journal of Shandong University (Medical Edition), 61(11): 59–67.

[15] Peng M, Zhou X, Jiang L, 2020, Effect of VEGF and HIF-1α Expression on the Efficacy of Radiotherapy in Patients with Esophageal Squamous Cell Carcinoma. Journal of Practical Cancer, 35(10): 1631–1634.

[16] Liu X, Liu Y, Fan Z, et al., 2022, Expression and Clinical Significance of Hypoxia-Inducible Factor-1α and Vascular

Endothelial Growth Factor in Esophageal Squamous Cell Carcinoma Tissue. Journal of Xinjiang Medical University, 45(10): 1099–1103.

Proceedings of Anticancer Research, 2024, Volume 8, Issue 2
http://ojs.bbwpublisher.com/index.php/PAR
ISSN Online: 2208-3553
ISSN Print: 2208-3545

Evaluation of Phytochemical Analysis and Total Phenol Content of Proso Millet and Barnyard Millet

Deepa Priya Ramadoss[1], Kirubanandan Shanmugam[2]*

[1]Department of Biotechnology, School of Bioengineering, SRM Institute of Science and Technology, Kattankulathur 603203, Kancheepuram, Tamil Nadu, India
[2]Independent Research Professional, Chennai, Tamil Nadu, India

***Corresponding author:** Kirubanandan Shanmugam, Kirubanandan.shanmugam@gmail.com

Abstract: Whole grains of proso and barnyard millets were sequentially extracted using different solvents (hexane, chloroform, ethyl acetate, and methanol). Phytochemical analysis was performed qualitatively, and the total phenolic content in the extracts of proso and barnyard millets was quantified. Alkaloids and cardiac glycosides were identified in all solvent extracts of both millets. Anthraquinone and glycosides yielded negative results in all solvent extracts of both millets. Among all the solvent extracts, methanol extracts of proso and barnyard millets showed the presence of major compounds such as flavonoids, terpenoids, amino acids, tannins, and phenolics compounds. The maximum amount of phenols was found in methanolic extracts of proso and barnyard millets (0.669 ± 0.003 and 0.625 ± 0.003), followed by the chloroform extract of proso and barnyard millets (0.284 ± 0.002 and 0.257 ± 0.003). The minimum amount of phenolics was found in the acetone extract of proso and barnyard millets. The methanol extract of both millets showed the presence of major compounds with high phenolic content.

Keywords: Proso millet; Barnyard millet; Sequential solvent extraction; Phytochemical analysis; Total phenolic content

Online publication: March 28, 2024

1. Introduction

For thousands of years, humans have relied on natural products as valuable sources of medicines and inspiration for drug development [1]. In several countries, particularly in India, China, and Egypt, traditional medicinal systems have been based on plant-derived natural products. Food-derived natural products have been shown to be potential candidates for medicinal use [2]. More than 1 million Americans and more than 10 million people worldwide are expected to be diagnosed with cancer, a disease commonly believed to be preventable. Only 5 to 10% of all cancer cases are attributed to genetic defects, whereas the remaining 90 to 95% are caused by environmental and lifestyle factors. The lifestyle factors include cigarette smoking, diet (fried foods, red meat. Millet grains, compared to other grains like wheat, rice, and sorghum, are known for their health benefits and medicinal properties. The types of millets include finger millet, foxtail millet, proso millet, pearl millet, and little millet.

Millet seeds are rich sources of nutraceuticals and phytochemicals, which are used to prevent various health issues [3-5]. In recent years, whole grain cereals have garnered significant attention due to their fiber content and the presence of a diverse array of bioactive compounds such as antioxidants and phytochemicals [6]. Millets contain a variety of phytochemicals including polyphenols, phytosterols, phytates, sterols, carotenoids, flavonoids, and alkaloids. Among these, phenolic acids and tannins are the main polyphenols, while flavonoids play important roles in the body's immune system and act as antioxidants [7].

The health benefits of consuming whole grains, which are rich in phytochemicals, are well-documented[8] the phytochemical contents in grains have been commonly underestimated in the literature, because bound phytochemicals were not included. This study was designed to investigate the complete phytochemical profiles in free, soluble conjugated, and insoluble bound forms, as well as their antioxidant activities in uncooked whole grains. Corn had the highest total phenolic content (15.55 ± 0.60 μmol of gallic acid equivalent to per gram of grain. However, the presence of antioxidants and phytochemicals in whole grains has not been given as much attention as those in vegetables and fruits. It has been suggested that the health benefits of consuming whole grains are due to the presence of unique bioactive compounds [9]. Based on these observations, this study aims to quantify the presence of phytochemicals and total phenolic content in proso and barnyard millets.

2. Materials and methods

2.1. Plant materials

Whole grains of proso millet (Panivaragu, CO(PV)5, *Panicum miliaceum* L.) and barnyard millet (Kudiraivali, CO(KV)2, *Echinochloa frumentacea (Roxb.) Link*) were purchased and authenticated from the Department of Millet, Tamil Nadu Agriculture University, Coimbatore, Tamil Nadu, India. The seeds were thoroughly washed with running water, rinsed twice with sterile distilled water, and then left to dry at room temperature. Subsequently, the dried seeds were powdered using a blender before proceeding to the extraction process.

2.2. Sequential solvent extraction or preparation of plant extract

Fifty grams of powdered whole grains of proso millet (PM) and barnyard millet (BM) were macerated with 50 mL of hexane (1:5 v/w) at room temperature for 72 hours with intermittent stirring or shaking. After 72 hours, the solvent was collected and filtered through Whatman filter paper No. 1, and the residues were dried. The residues were then re-macerated with chloroform, ethyl acetate, acetone, and methanol after 72 hours each. Finally, the filtrates were evaporated to remove excess solvent residue in the extracts using a rotor vacuum evaporator. The extracts were dried for further investigation.

2.3. Qualitative phytochemical analysis of proso and barnyard millet solvent extracts

All the solvent extracts obtained from PM and BM were subjected to identify the presence of various bioactive constituents in both millets using several phytochemical analyzing tests (**Table 1**) [10-12].

2.4. Quantitative estimation of total phenolic content

The total phenolic content of sequential solvent extraction of PM and BM was determined by the Folin-Ciocalteu reagent method as described earlier by Singleton *et al.* [13]. Each solvent extract of PM and BM was dissolved in methanol (10 mg/mL). To 1 mL of each extract, 2 mL of Folin-Ciocalteu reagent and 2.5 mL of 20% Na_2CO_3 solution were added, and the mixture was incubated at room temperature for 30 minutes. After the incubation period, the absorbance of each sample was measured at 725 nm using a UV-spectrophotometer.

Table 1. Preliminary phytochemical analysis of proso and barnyard millet extracts

Phytochemical constituents	Methods and observation
Test for alkaloids (Mayer's test)	6 drops of Mayer's reagents + 1% HCl + steam to 1 mL of the extract Cream cloud precipitate indicated the presence of alkaloids
Test for flavonoids (Alkaline reagent test)	2–3 drops of dilute NaOH to 1 mL of the extract A deep yellow color appeared but gradually became colorless by adding a few drops of dilute HCl indicating the presence of flavonoids
Test for steroids (Liebermann-Burchard test)	2 mL of acetic anhydride + concentrated H_2SO_4 to 1 mL of the extract A green or green-blue color formation indicated the presence of steroids
Test for tannins and phenolics (Ferric chloride test)	2 mL of 5% neutral ferric chloride solution to 1 mL of the extract A dark blue or greenish-black precipitate indicated the presence of tannins
Test for terpenoids	2 mL of chloroform and concentrated H_2SO_4 to 1 mL of the extract Observed for reddish-brown color interface
Test for cardiac glycosides (Keller-Kiliani test)	1 mL of glacial acetic acid containing one drop of $FeCl_3$ + concentrated H_2SO_4 to 1 mL of the extract Brown ring formation at the junction indicated the presence of cardiac glycosides
Test for glycosides (Legal test)	Sodium nitroprusside in pyridine and sodium hydroxide to 1 mL of the extract The formation of pink to blood-red coloration indicated the presence of glycoside
Test for saponins (Froth test)	5 mL distilled water to 0.5 mL of extract, shaken well for 15 min Frothing persistence indicated the presence of saponins
Test for amino acids (Ninhydrin test)	A few drops of Ninhydrin reagent to 1 mL of the extract The formation of blue or violet coloration indicated the presence of amino acids.
Test for anthraquinone	Benzene was added to 1 mL of the extract and shaken, followed by the addition of 1 mL of diluted ammonia The formation of pink, red, or violet coloration indicated the presence of anthraquinones in the ammonia phase

3. Results

3.1. Preliminary phytochemical analysis of sequential solvent extraction of PM and BM

PM and BM whole grains were sequentially extracted using different solvents ranging from non-polar to polar (hexane, chloroform, ethyl acetate, acetone, and methanol). The yield percentage of crude extracts of PM and BM ranged from 1 to 4%.

Qualitative phytochemical analysis of different solvent extracts of PM and BM is presented in **Tables 2** and **3**. All solvent extracts of PM and BM indicated the presence of alkaloids and cardiac glycosides. Anthraquinone and glycosides yielded negative results in all solvent extracts of both millets. Steroids and saponins were detected in methanol and chloroform extracts of PM. Tannins and phenolic compounds were identified in methanol and ethyl acetate extracts of PM. Methanol extracts of PM showed the presence of flavonoids, terpenoids, amino acids, tannins, and phenolic compounds, except in other solvent extracts. Similar results were detected with minor variations in extracts of BM.

It was found that phytochemicals content varies widely due to differences in the polarity of the solvents used for extraction. When compared with other solvent extracts, methanol, a moderately polar organic solvent, yielded the most phytoconstituents. This indicates the presence of the polar nature of the phytochemicals in methanol extracts, all of which possess different medicinal properties.

Table 2. Phytochemical analysis of sequential extraction of proso millet

Phytochemical	Hexane	Chloroform	Ethyl acetate	Acetone	Methanol
Alkaloids	+	+	+	+	+
Flavonoids	-	-	-	-	+
Steroids	-	-	-	+	+
Tannins and phenolics	-	-	-	-	+
Terpenoids	-	-	+	-	+
Cardiac glycosides	+	+	+	+	+
Glycosides	-	-	-	-	-
Saponins	-	+	-	-	+
Amino acids	+	-	-	-	+
Anthraquinone	-	-	-	-	-

Note: + indicated the presence of the compound, and - indicated the absence of the compound.

Table 3. Phytochemical analysis of sequential extraction of barnyard millet

Phytochemical	Hexane	Chloroform	Ethyl acetate	Acetone	Methanol
Alkaloids	+	+	+	+	+
Flavonoids	-	-	+	-	+
Steroids	+	-	-	+	+
Tannins and phenolics	-	-	-	-	+
Terpenoids	-	+	+	-	+
Cardiac glycosides	+	+	+	+	+
Glycosides	-	-	-	-	-
Saponins	-	+	-	-	+
Amino acids	+	-	-	-	+
Anthraquinone	-	-	-	-	-

Note: + indicated the presence of the compound, and - indicated the absence of the compound.

3.2. Total phenol content of extracts of PM and BM

Phenolics are prominent antioxidants that play several important roles in preventing numerous diseases. It is one of the major classes of phytonutrients that have been widely studied in phytochemical research [14]. The total phenolic content was estimated from different solvent extracts (hexane, chloroform, ethyl acetate, acetone, and methanol) of PM and BM. The phenolic content of the five different solvent extracts displayed vast differences, ranging from 0.120 ± 0.002 to 0.569 ± 0.003 in both millets (**Table 4**). The maximum amount of phenols was found in methanol extracts of PM and BM (0.669 ± 0.003 and 0.625 ± 0.003), followed by chloroform extract of PM and BM, which showed 0.284 ± 0.002 and 0.257 ± 0.003. The minimum amount of phenolics was found in acetone extracts of PM and BM.

Table 4. Total phenol content of proso and barnyard millet extracts (mean ± SD of three determinations)

Extract	Proso millet (g)	Barnyard millet (g)
Hexane	0.162 ± 0.002	0.156 ± 0.003
Chloroform	0.284 ± 0.002	0.257 ± 0.003
Ethyl acetate	0.156 ± 0.002	0.144 ± 0.002
Acetone	0.122 ± 0.003	0.120 ± 0.002
Methanol	0.669 ± 0.003	0.625 ± 0.003

Based on the preliminary results of quantitative phytochemical analysis and estimation of phenolic content in different solvent extracts of PM and BM, methanol extracts of both millets showed the presence of major compounds and the highest phenolic content. Therefore, methanol was further used for the isolation of bioactive compounds by supercritical fluid extraction.

4. Discussion

Since ancient times, plants have served as a significant reservoir of drugs, bioactive compounds, and remedies for various diseases worldwide. The majority of bioactive components in plants consist of flavonoids, alkaloids, tannins, and phenolic compounds, which have been shown to be crucial sources of main compounds in the development of new anticancer drugs.

For over 3,500 years, constituents derived from plants have been used in cancer treatment. It has been reported that between 1981 and 2014, globally, 75% of new chemical entities introduced as anticancer drugs were derived from natural products or inspired by them [15]. Despite the successful utilization of synthetic chemicals as drugs for many diseases over the years, pharmaceutical industries have not achieved complete success in certain diseases (such as cancer, diabetes, cardiac diseases, and AIDS) due to the complexity of these diseases.

Previous literature suggests that preparing extracts using different solvents has a potent healing effect. Phytochemical screening of the sequential solvent extracts of PM and BM whole grains showed the presence of flavonoids, terpenoids, alkaloids, steroids, tannins, and phenolic compounds, among others, in the methanolic extract. Rao *et al.* reported the presence of phenols, tannins, alkaloids, flavonoids, and saponins in small millets (proso millet, finger millet, foxtail millet, and kodo millet) [16]. Suma and Urooj reported the presence of flavonoids, alkaloids, phenolics, and reducing sugars in methanolic and aqueous extracts of foxtail millet [17]. Differences in the presence of compounds might be attributed to the polarity of the extracting solvents, accounting for the observed variation in phytochemical identification in the extracts. This study suggests that the presence of these phytochemical constituents in PM and BM extracts possesses various medicinal properties, including metabolic activity, antitoxic, antioxidant, anti-inflammatory, anti-cancer, anti-carcinogenic properties, and cholesterol-lowering activity.

Total phenolic content (TPC) in the millets examined in this study was found to be higher than the TPC in other cereals including *Triticum turgidum* subsp. *durum* (Durum wheat) [8,18,19]. Among all the solvent extracts of PM and BM, the maximum amount of phenol was detected in the methanolic extract of PM and BM. Kim *et al.* demonstrated that PM contains 18–26.5 mg GAE/g of TPC [20]. It was reported that Khodo millet exhibited a maximum of 10.3% phenolic content in the methanolic extract [16]. Abraham *et al.* reported that among different varieties of PM, whole grains of red-coloured millet exhibited higher TPC

compared to whole grains of light-coloured millet [21]. Whole grain soluble extracts of Khodo millet contained higher TPC than other small millet varieties [22], namely kodo millet and finger millet. Zhang *et al.* stated that a higher amount was estimated in bound phenol content than free phenol content of PM, ranging between 83.44–456.95 mg GAE/g [23], as well as the antioxidant activity and anti-proliferative properties of three diverse proso millet varieties. Panwar *et al.* corroborated that BM demonstrated a greater phenolic content than finger millet [24].

Acknowledgments

The authors would like to acknowledge the Department of Biotechnology, School of Bioengineering, SRM Institute of Science and Technology for the financial support.

Disclosure statement

The authors declare no conflict of interest.

References

[1] Harvey AL, 2007, Natural Products as a Screening Resource. Curr Opin Chem Biol, 11(5): 480–484. https://doi.org/10.1016/j.cbpa.2007.08.012

[2] Anand P, Kunnumakara AB, Sundaram C, et al., 2008, Cancer is a Preventable Disease that Requires Major Lifestyle Changes. Pharm Res, 25(9): 2097–2116. https://doi.org/10.1007/s11095-008-9661-9

[3] Holtekjølen AK, Kinitz C, Knutsen SH, 2006, Flavanol and Bound Phenolic Acid Contents in Different Barley Varieties. J Agric Food Chem, 54(6): 2253–2260. https://doi.org/10.1021/jf052394p

[4] Rice-Evans C, Miller N, Paganga G, 1997, Antioxidant Properties of Phenolic Compounds. Trends Plant Sci, 2(4): 152–159. https://doi.org/10.1016/S1360-1385(97)01018-2

[5] Yao LH, Jiang YM, Shi J, et al., 2004, Flavonoids in Food and Their Health Benefits. Plant Foods Hum Nutr, 59(3): 113–122. https://doi.org/10.1007/s11130-004-0049-7

[6] Diplock AT, Charleux JL, Crozier-Willi G, et al., 1998, Functional Food Science and Defence Against Reactive Oxidative Species. Br J Nutr, 80 Suppl 1: S77–S112. https://doi.org/10.1079/bjn19980106

[7] Chandrasekara A, Shahidi F, 2010, Content of Insoluble Bound Phenolics in Millets and Their Contribution to Antioxidant Capacity. J Agric Food Chem, 58(11): 6706–6714. https://doi.org/10.1021/jf100868b

[8] Adom KK, Liu RH, 2002, Antioxidant Activity of Grains. J Agric Food Chem, 50(21): 6182–6187. https://doi.org/10.1021/jf0205099

[9] Gani A, Wani SM, Masoodi FA, et al., 2012, Whole-Grain Cereal Bioactive Compounds and Their Health Benefits: A Review. J Food Process Technol, 3(3): 146.

[10] Harborne JB, 1973, Phytochemical Methods. Chapman and Hall Ltd., London.

[11] Trease GE, Evans WC, 2002, Pharmacognosy, 15th edition. Saunders Publishers, London.

[12] Ogunyemi A, 1979, The Origin of Herbal Cure and Its Spread, in Proceedings of the Conference on African Medicinal Plants. Ile-Ife University Press, 20–22.

[13] Singleton VL, Rossi JA, 1965, Colorimetry of Total Phenolics with Phosphomolybdic-Phosphotungstic Acid Reagents. Am J Enol Vitic, 16(3): 144–158.

[14] Ismail A, Marjan ZM, Foong CW, 2004, Total Antioxidant Activity and Phenolic Content in Selected Vegetables. Food Chem, 87(4): 581–586. http://dx.doi.org/10.1016/j.foodchem.2004.01.010

[15] Newman DJ, Cragg GM, 2016, Natural Products as Sources of New Drugs from 1981 to 2014. J Nat Prod, 79(3): 629–661. https://doi.org/10.1021/acs.jnatprod.5b01055

[16] Rao BR, Nagasampige MH, Ravikiran M, 2011, Evaluation of Nutraceutical Properties of Selected Small Millets. J Pharm Bioallied Sci, 3(2): 277–279. https://doi.org/10.4103/0975-7406.80775

[17] Suma PF, Urooj A, 2012, Antioxidant Activity of Extracts from Foxtail Millet (*Setaria italica*). J Food Sci Technol, 49(4): 500–504. https://doi.org/10.1007/s13197-011-0300-9

[18] Liyana-Pathirana C, Dexter J, Shahidi F, 2006, Antioxidant Properties of Wheat as Affected by Pearling. J Agric Food Chem, 54(17): 6177–6184. https://doi.org/10.1021/jf060664d

[19] Madhujith T, Shahidi F, 2007, Antioxidative and Antiproliferative Properties of Selected Barley (*Hordeum vulgarae* L.) Cultivars and Their Potential for Inhibition of Low-Density Lipoprotein (LDL) Cholesterol Oxidation. J Agric Food Chem, 55(13): 5018–5024. https://doi.org/10.1021/jf070072a

[20] Kim J, Hyun TK, Kim M, 2010, Anti-Oxidative Activities of Sorghum, Foxtail Millet and Proso Millet Extracts. African J Biotechnol, 9(18): 2683–2690.

[21] Ábrahám ÉB, Öri N, Szabó S, et al., 2012, Quality of Grain of Different Proso Millet (*Panicum miliaceum* L.) Varieties. Eur J Plant Sci Biotechnol, 6(Special Issue 2): 132–134.

[22] Chandrasekara A, Shahidi F, 2011, Antioxidant Phenolics of Millet Control Lipid Peroxidation in Human LDL Cholesterol and Food Systems. J Am Oil Chem Soc, 89(2): 275–285. https://doi.org/10.1007/s11746-011-1918-5

[23] Zhang L, Liu R, Niu W, 2014, Phytochemical and Antiproliferative Activity of Proso Millet. PLoS One, 9(8): e104058. https://doi.org/10.1371/journal.pone.0104058

[24] Panwar P, Dubey A, Verma AK, 2016, Evaluation of Nutraceutical and Antinutritional Properties in Barnyard and Finger Millet Varieties Grown in Himalayan Region. J Food Sci Technol, 53(6): 2779–2787. https://doi.org/10.1007/s13197-016-2250-8

Proceedings of Anticancer Research, 2024, Volume 8, Issue 2
http://ojs.bbwpublisher.com/index.php/PAR
ISSN Online: 2208-3553
ISSN Print: 2208-3545

Role of TSH Inhibition Therapy in the Postoperative Management of Patients with Differentiated Thyroid Cancer

Xudong Gao[1], Bo Zhao[1], Ya Su[2], Shenglin He[2]*

[1]Department of Otorhinolaryngology, Head and Neck Surgery, Shaanxi Provincial People's Hospital, Xi'an 710068, China
[2]Department of Endocrinology, Shaanxi Provincial People's Hospital, Xi'an 710068, China

***Corresponding author:** Shenglin He, heshenglin2008@126.com

Abstract: *Objective:* To investigate the effect of TSH inhibition therapy in the postoperative management of patients with differentiated thyroid cancer. *Methods:* Seventy patients diagnosed with differentiated thyroid cancer were selected for the study. TSH inhibition therapy was administered to the research group, while thyroxine replacement therapy was provided to the control group during the postoperative management phase. This allowed for a comparative analysis between the two groups. *Results:* In comparison with the control group, the research group exhibited significant decreases in serum TSH, T3, and T4 levels after treatment, while FT4 and FT3 levels significantly increased ($P < 0.05$). Additionally, significant decreases in Tg, VEGF, TSGF, CD44V6, and sIL-2R levels were observed in the research group after treatment ($P < 0.05$). No significant differences were found in pre-treatment thyroid function between the two groups ($P > 0.05$). *Conclusion:* The application of TSH inhibition therapy in the postoperative management of patients with differentiated thyroid cancer demonstrates promising outcomes.

Keywords: TSH inhibition therapy; Differentiated thyroid cancer; Postoperative management; Effect

Online publication: March 28, 2024

1. Introduction

Thyroid cancer is a prevalent malignant tumor that is typically managed through surgical resection, radiation therapy, and thyroid hormone replacement therapy. Differentiated thyroid cancer (DTC) represents the most common subtype [1], and patients commonly undergo postoperative treatment following surgical resection. Thyroid-stimulating hormone (TSH) suppression therapy has emerged as a pivotal therapeutic approach in postoperative management. This paper aims to explore the role of TSH suppression therapy in the postoperative management of patients with DTC.

2. General information and methods

2.1. Data

Fifty patients diagnosed with DTC, selected between January 2018 and December 2019, were divided into two groups of 25 cases each. In the research group, there were 10 males and 15 females with an age range of 29 to 58 years (mean age 45.26 ± 5.29 years), while in the control group, there were 11 males and 14 females with an age range of 25 to 57 years (mean age 45.21 ± 5.22 years). A comparison of data between the two groups revealed no significant difference ($P > 0.05$).

2.2. Methods

During the postoperative management period, the control group received thyroxine replacement therapy at a dosage of 1.5–2.5 μg/kg of thyroxine per day. In the postoperative management period, the research group underwent TSH suppression therapy, using levothyroxine sodium tablets at a dosage of 1.5–2.5 μg/kg per day to achieve the desired level of control, with this dosage maintained throughout. The criteria for suppression were as follows: postoperative TSH suppression recommended to be below 0.1 mIU/L in patients with high-risk DTC, below 0.1–0.5 mIU/L in patients with intermediate-risk DTC, and between 0.5–2.0 mU/L in patients with low-risk DTC. Both groups received treatment for a duration of 1 year.

2.3. Observation indexes

(1) Comparison of serum TSH, triiodothyronine (T3), thyroxine (T4), free T4 (FT4), and free T3 (FT3) levels between the two groups.

(2) Comparison of thyroglobulin (Tg), vascular endothelial growth factor (VEGF), tumor-specific growth factor (TSGF), CD44 containing variable exon 6 (CD44V6), and soluble interleukin-2 receptor (sIL-2R) levels between the two groups.

2.4. Data analysis

This study utilized SPSS 25.0 software to conduct χ^2 tests and *t*-tests, with results presented in the form of percentage and mean ± standard deviation (SD), and statistical significance indicated by $P < 0.05$.

3. Results

Table 1 shows that the serum TSH, T3, and T4 levels were significantly reduced in the research group after treatment, while the serum FT4 and FT3 levels were significantly increased after treatment, as compared to the control group ($P < 0.05$). **Table 2** shows that the research group had significantly reduced levels of Tg, VEGF, TSGF, CD44V6, and sIL-2R after treatment as compared to the control group ($P < 0.05$). There were no significant differences in all the indicators between the two groups ($P > 0.05$).

Table 1. Comparison of thyroid function between the two groups before and after treatment

Groups	TSH (mU/L)		T3 (nmol/L)		T4 (nmol/L)		FT4 (ρmol/L)		FT3 (ρmol/L)	
	Before	After	Before	After	Before	After	Before	After	Before	After
Research group ($n = 25$)	2.33 ± 0.52	0.15 ± 0.04	1.81 ± 0.15	0.62 ± 0.26	106.72 ± 3.77	74.75 ± 4.72	16.55 ± 0.52	27.17 ± 0.03	4.71 ± 0.13	6.72 ± 1.65
Control group ($n = 25$)	2.34 ± 0.66	1.62 ± 0.15	1.83 ± 0.44	1.25 ± 0.53	107.35 ± 3.74	89.77 ± 3.91	16.62 ± 0.45	7.66 ± 0.65	4.66 ± 0.14	1.85 ± 0.04
t	0.06	47.35	0.22	5.34	0.59	12.25	0.51	149.92	1.31	14.75
P	> 0.05	< 0.05	> 0.05	< 0.05	> 0.05	< 0.05	> 0.05	< 0.05	> 0.05	< 0.05

Table 2. Comparison of Tg, VEGF, TSGF, CD44V6, and sIL-2R levels between the two groups before and after treatment

Groups	Tg (ng/mL)		VEGF (pg/mL)		TSGF (μg/mL)		CD44V6 (ng/mL)		sIL-2R (μg/mL)	
	Before	After	Before	After	Before	After	Before	After	Before	After
Research group (n = 25)	45.77 ± 11.75	12.77 ± 2.52	27.55 ± 5.65	13.66 ± 2.42	73.65 ± 6.84	50.51 ± 4.72	520.68 ± 23.62	306.51 ± 13.51	552.75 ± 28.36	372.28 ± 67.88
Control group (n = 25)	45.25 ± 11.61	19.76 ± 6.55	27.42 ± 5.33	20.62 ± 4.51	72.82 ± 7.85	64.25 ± 6.75	523.66 ± 22.37	399.62 ± 15.26	550.61 ± 25.27	458.26 ± 35.22
t	0.16	4.98	0.08	6.80	0.40	8.34	0.46	22.84	0.28	5.62
P	> 0.05	< 0.05	> 0.05	< 0.05	> 0.05	< 0.05	> 0.05	< 0.05	> 0.05	< 0.05

4. Discussion

TSH inhibition therapy has the potential to diminish the stimulation of residual thyroid tissue or thyroid cancer cells [2-4], thereby reducing the risk of cancer recurrence. This study's analysis indicates that TSH inhibition therapy presents an optimal approach in the postoperative management of patients with DTC:

(1) Decreased recurrence rate: TSH inhibition therapy mitigates the risk of cancer recurrence by diminishing the stimulation of residual thyroid tissue by TSH. Studies have demonstrated that TSH inhibition therapy significantly lowers the likelihood of postoperative recurrence in high-risk patients [5-8].

(2) Enhanced survival: Several studies have indicated that patients with DTC undergoing TSH inhibition therapy exhibit superior long-term survival rates [9-12]. This outcome is attributed to the therapy's inhibition of residual thyroid tissue function, thereby reducing the probability of cancer cell recurrence [13,14].

The experimental findings revealed:

(1) Alterations in thyroid hormone levels: Following treatment, serum TSH, T3, and T4 levels in the research group significantly decreased, while FT4 and FT3 levels significantly increased ($P < 0.05$). This suggests that TSH inhibition therapy notably influences patients' thyroid hormone levels post-treatment, primarily by reducing TSH levels and increasing FT4 and FT3 levels.

(2) Changes in tumor markers and growth factors: Tg, VEGF, TSGF, CD44V6, and sIL-2R levels significantly decreased in the research group after treatment ($P < 0.05$). This indicates that TSH inhibition therapy exerts an inhibitory effect on the tumor markers and growth factors of thyroid cancer patients, thereby aiding in the inhibition of cancer cell growth and proliferation [15].

(3) Pre-treatment comparison: Comparative analysis of thyroid function, tumor markers, and growth factors before treatment between the two groups yielded $P > 0.05$. This suggests no significant difference in these indicators between the two groups before treatment.

In conclusion, the application of TSH suppression therapy in the postoperative management of patients with DTC is deemed optimal, resulting in significant improvements in thyroid function, tumor markers, and growth factors.

Disclosure statement

The authors declare no conflict of interest.

References

[1] Wang X, Zhao F, Yan S, 2022, Effects of Thyrotropin Suppression Therapy on Bone Metabolism, CD44V6 and sIL-2R Levels in Patients with Differentiated Thyroid Cancer. Chinese Journal of Modern Medicine, 32(23): 34–38.

[2] Zhang X, Chen D, 2023, Research Progress on Osteoporosis Caused by Thyrotropin Suppression Therapy After Surgery for Differentiated Thyroid Cancer. Primary Chinese Medicine, 2(2): 108–113.

[3] Bai N, Liu C, Zhang X, et al., 2021, Application of TSH Inhibition Therapy in Differentiated Thyroid Cancer Patients After Surgery. Journal of Qiqihar Medical College, 42(24): 2145–2148.

[4] Wang X, Zhao Y, 2021, Study on the Effect of Thyrotropin Suppression Regimen on Prognosis and T-Cell Immune Factors in Elderly Thyroid Cancer Patients. Chinese Journal of Practical Internal Medicine, 41(11): 978–980.

[5] Mei Y, Wang Q, Zhao L, et al., 2021, Effect of TSH Inhibition Therapy on Immune Function and Bone Metabolism in Postoperative Patients with Differentiated Thyroid Cancer. Chongqing Medicine, 50(8): 1381–1384.

[6] Wu W, Jing J, Gao J, et al., 2022, Effects of Thyrotropin Suppression Therapy on TRAb, TPOAb, and TgAb in Postoperative Patients with Differentiated Thyroid Cancer. Chinese Journal of Gerontology, 42(6): 1340–1342.

[7] Cheng R, 2023, Current Status and Thoughts on Postoperative Thyrotropin Suppression Therapy for Differentiated Thyroid Cancer. Chinese Journal of Practical Surgery, 43(4): 391–396.

[8] Zhang R, Guan Y, 2022, Analysis of the Application Effect of Thyrotropin Suppression Therapy after Total Thyroidectomy. Chinese and Foreign Medicine Research, 20(28): 111–115.

[9] Kong X, Liu Q, Xu W, et al., 2021, Effects of Different TSH Inhibitory Treatments on TSH, FT3, and FT4 in Differentiated Thyroid Cancer After Surgery. China Medical Innovation, 18(7): 155–158.

[10] Ding Y, Jiang L, Zhang Z, 2022, Correlation Analysis of TSH and Tg Levels and Long-Term Prognosis in Patients with Differentiated Thyroid Cancer After 131I Treatment. Health Research, 42(2): 227–230 + 233.

[11] Lin Y, 2022, Controversy and Exploration of 131I Therapy for Differentiated Thyroid Cancer. International Journal of Radiation Medicine and Nuclear Medicine, 46(7): 389–391.

[12] Zhang L-D, Xi Y-C, You L-Q, et al., 2018, Effect of TSH Inhibition Therapy on Serum Tg, VEGF, TSGF, CD44V6, sIL-2R, and T Lymphocyte Subpopulation Levels in Patients with Differentiated Thyroid Cancer After Surgery. Journal of Hainan Medical College, 24(2): 242–245.

[13] Wu W, Jing J, Gao J, et al., 2022, Effects of Thyrotropin Suppression Therapy on TRAb, TPOAb, and TgAb in Postoperative Patients with Differentiated Thyroid Cancer. Chinese Journal of Gerontology, 42(6): 1340–1342.

[14] Jin W, Yao X, 2022, Exploring the Efficacy of Thyroid-Stimulating Hormone (TSH) Suppression Therapy in Postoperative Thyroid Cancer Patients. China Medical Digest: Otolaryngology, 37(1): 97–99.

[15] Zhao F-L, Kang Y-L, Ma Y-J, et al., 2021, Efficacy of TSH Inhibition Therapy in Elderly Thyroid Cancer Patients After Total Thyroidectomy and Its Effect on Serum Tg, TSH, and CEA Levels. Journal of Practical Cancer, 2021(12): 36.

Proceedings of Anticancer Research, 2024, Volume 8, Issue 2
http://ojs.bbwpublisher.com/index.php/PAR
ISSN Online: 2208-3553
ISSN Print: 2208-3545

Research Progress of circRNAs during Epithelial-Mesenchymal Transition of Hepatocellular Carcinoma

Yuqing Li[1], Cuicui Ren[1], Yu Cai[2], Chang Tian[2], Yuanyuan Jia[2], Ge Wu[1]*

[1]Xi'an Medical University, Xi'an 710000, China
[2]Faculty Development and Teaching Evaluation Office, The First Affiliated Hospital of Xi'an Medical University, Xi'an 710000, China

***Corresponding author:** Ge Wu, WG73212021@163.com

Abstract: Hepatocellular carcinoma is prone to invasion and metastasis. It often receives a low diagnosis rate in the early stage but has an extremely high mortality rate. Epithelial-mesenchymal transformation (EMT) is a key factor in promoting tumor cell invasion and metastasis. Circular RNA (circRNA) is involved in regulating EMT in hepatocarcinoma cells through multiple pathways, thereby affecting the occurrence and progression of hepatocellular carcinoma. This article mainly reviews the research progress of circRNA related to EMT core transcription factors, circRNA that promotes EMT in liver cancer, and circRNA that inhibits EMT in liver cancer.

Keywords: circRNA; Epithelial-mesenchymal transformation (EMT); Hepatocellular carcinoma (HCC)

Online publication: March 28, 2024

1. Introduction

China is one of the countries with the highest incidence and mortality rates of liver cancer. More than 50% of newly diagnosed and deceased hepatocellular carcinoma (HCC) patients worldwide occur in China, ranking fourth in the incidence of common malignant tumors and second in tumor-related mortality [1,2]. In 2020, there were 905,700 new cases and 830,200 deaths from liver cancer globally, ranking sixth in the incidence of malignant tumors and third in tumor-related mortality. Primary liver cancer is a diverse group of tumors, including HCC, intrahepatic cholangiocarcinoma, and mixed hepatocellular carcinoma-cholangiocarcinoma, with significant differences in etiology, clinical characteristics, histopathology, treatment, and prognosis. Among them, HCC accounts for 85% to 90% of all cases [3].

Currently, although liver ultrasound imaging and serum alpha-fetoprotein (AFP) testing have been widely used for early screening of clinical liver cancer, the sensitivity and specificity of AFP detection are limited. At the same time, the accuracy of the ultrasound examination is greatly influenced by the operator's subjective judgment, and traditional ultrasound examination often struggles to accurately differentiate the nature of liver

focal lesions [4].

The treatment strategy for HCC varies depending on the patient's disease stage, liver function status, and individual differences. Only a few early-stage liver cancer patients can achieve a better prognosis through surgical resection, radiofrequency ablation, or liver transplantation. However, most patients are diagnosed at an advanced stage, limiting treatment options, and the efficacy of traditional chemotherapy and radiotherapy is poor. In recent years, emerging therapies such as targeted therapy and immunotherapy have brought new hope to advanced-stage patients [5].

Therefore, in-depth exploration of the pathogenesis of HCC and the search for novel biomarkers to improve the early detection rate of HCC is of great significance for the early diagnosis and treatment of HCC patients. This not only helps improve patient prognosis and survival rates but also enhances their quality of life.

Circular RNA (circRNA), first discovered in viruses in the 1970s, is a type of RNA with a unique natural closed-loop structure. It lacks the 5'-3' polarity and polyA tail commonly found in linear RNAs, making it more stable and resistant to degradation by RNA exonucleases. However, due to the limitations of early knowledge and technological capabilities, circRNA was initially regarded as a non-coding RNA without biological functions. It was considered to be a byproduct of RNA transcription and splicing processes, which led to a lack of in-depth research on circRNA. In recent years, with the application of high-throughput sequencing technology and bioinformatics analysis in clinical diagnostics and basic research, our understanding of circRNA has undergone profound changes. Nowadays, circRNA is recognized as a group of molecules with diverse biological functions, playing important roles in gene expression regulation, cellular physiology, and disease development. Furthermore, numerous studies have identified circRNAs associated with HCC, suggesting their potential as novel diagnostic markers and targets for drug development in HCC [6].

Based on these prospects, this article aims to provide a comprehensive review of the research progress on circRNA in the context of hepatocellular carcinoma epithelial-mesenchymal transition.

2. Circular RNA

The typical splicing pattern of linear RNA involves joining the 3' end of one exon with the 5' end of an adjacent exon. In contrast, circRNAs are formed by back-splicing, where the 3' end of an RNA molecule is joined to its 5' end, creating a closed-loop structure. This splicing pattern can occur at any position in the genome, including introns, exons, and the antisense strand. Based on their formation mechanisms, circRNAs can be categorized into four types: circular intronic RNAs (ciRNAs), exonic circRNAs (EciRNAs), exon-intron circRNAs (EIciRNAs), antisense circRNAs, and circRNAs derived from intergenic or unannotated genomic sequences (intergenic circular RNAs). EciRNAs consist solely of exonic sequences and represent approximately 80% of all identified circRNAs. They are associated with RNA polymerase II and promote gene transcription, mainly located in the cytoplasm. ciRNAs are composed entirely of intronic sequences and primarily reside in the nucleus. EIciRNAs contain sequences from both exons and introns, and they can interact with small nucleolar ribonucleoprotein U1snRNP to form complexes that further enhance parental gene transcription [7,8].

There are three proposed models for the circular formation of circRNAs: intron pairing-driven circularization, RNA binding protein (RBP)-driven circularization, and lariat-driven circularization [9]. The functions of circRNAs mainly include:

(1) miRNA sponge activity: circRNAs have abundant miRNA binding sites, allowing them to interact with miRNAs and act as molecular sponges that sequester miRNAs, thereby relieving the inhibitory effect of miRNAs on their target genes and increasing the expression levels of these target genes. This

mechanism, known as the competitive endogenous RNA (ceRNA) mechanism, plays a crucial role in cellular growth, differentiation, and disease regulation [10].

(2) Regulation of protein binding: Some circRNAs contain specific binding sites for RNA binding proteins (RBPs) and can act as sponges for these protein molecules. They can inhibit the specific functions of RBPs and the transcription of parental genes by forming RNA-protein complexes [11].

(3) Encoding peptides: Although circRNAs were initially considered non-coding RNAs, recent research has shown that some circRNAs have the ability to encode peptides. These short peptides can be translated by ribosomes in specific cellular environments, participating in cellular regulatory networks.

(4) Influencing transcriptional regulation of host genes: circRNAs can interact with small nucleus ribonucleoprotein U1, affecting the transcriptional regulation of host genes. After U1 binds to circRNA, it forms a complex with RNA polymerase II, which interacts with the transcription factor IIH gene, thereby affecting the activity of RNA polymerase II and influencing the expression of the parental gene [12].

The closed-loop structure of circRNAs allows them to evade degradation by RNA enzymes, enhancing their stability. As a result, circRNAs can be detected in various body fluids such as saliva, blood, and urine. Additionally, circRNAs exhibit high tissue specificity, with ciRS-7 being specifically expressed in brain tissue and rarely expressed in other tissues, making them potential biomarkers for specific diseases [13,14].

3. Epithelial-mesenchymal transition

Epithelial-mesenchymal transition (EMT) is an important cellular biological phenomenon in which epithelial cells gradually acquire the characteristics and functions of mesenchymal cells through molecular regulation (**Figure 1**). Depending on the specific biological context in which EMT occurs, it can be categorized into three distinct types. Type 1 EMT primarily functions during embryonic development, promoting cellular diversity through mesenchymal-epithelial transition (MET). Type 2 EMT plays a critical role in physiological processes such as wound healing, tissue regeneration, and organ fibrosis. Type 3 EMT primarily enhances the invasive and metastatic capabilities of tumor cells, thereby promoting tumor progression [15].

Notably, Type 3 EMT plays a crucial role in the migration, invasion, and distant metastasis of malignant tumor cells. The specific regulatory mechanisms of tumor EMT are not yet fully understood. Multiple signaling pathways, such as Wnt, NK-κB, PI3K, triacylglycerol (TG), and epidermal growth factor (EGF), are involved in the induction of EMT. The occurrence of epithelial-mesenchymal transition in tumor cells often signifies the initiation of the malignant stage of tumor progression [16].

This process is typically accompanied by the downregulation of E-cadherin expression and the upregulation of molecules such as N-cadherin and Vimentin [17]. At the same time, inhibitory transcription factors such as Snail, Slug, ZEB1, ZEB2, and E47 are upregulated, coordinating the expression levels of E-cadherin. Through EMT, tumor cells lose polarity and tight intercellular connections, acquire enhanced invasive and migratory potential, and gradually resemble mesenchymal cells, making them more prone to local infiltration or distant metastasis [18]. Therefore, EMT can mediate the occurrence of invasive, migratory, immune evasion, and therapy resistance characteristics in tumor cells, playing a significant role in HCC metastasis and recurrence. Early detection of changes in relevant indicators associated with EMT is of great clinical significance in guiding patient treatment and improving survival rates.

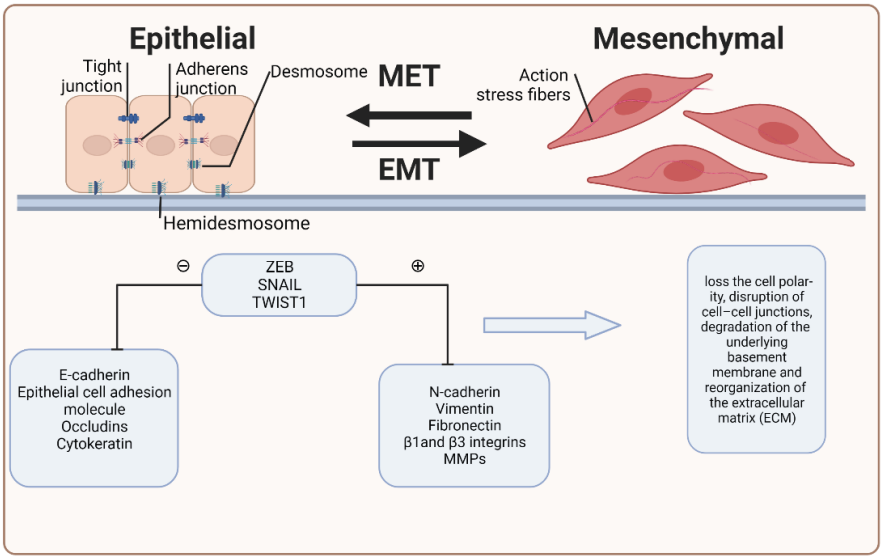

Figure 1. Outline of a typical EMT program

4. circRNA related to epithelial-mesenchymal transition in hepatocellular carcinoma

4.1. circRNA related to EMT-inducing transcription factors

The induction of EMT is initiated by a network of transcription factors (EMT-TFs). Currently, Snail, TWIST, and ZEB are widely recognized as core transcription factors in EMT. These factors can initiate the EMT process by directly or indirectly inhibiting the expression of epithelial markers [19]. Recent studies have reported various circRNAs that regulate the progression of liver cancer by targeting EMT core transcription factors (**Figure 2**).

Previous studies have clearly indicated that the pathogenesis of hepatocellular carcinoma (HCC) is closely associated with the regulatory relationship between has_circ_CYP24A1, miR-506, and Snail2. Specifically, this regulatory mechanism is mainly manifested in the competitive binding of has_circ_CYP24A1 with miR-506, leading to a decrease in the expression level of miR-506, thereby indirectly triggering the high expression of Snail2. This chain reaction rapidly promotes the EMT process in HCC, thereby driving the malignant progression of HCC [20].

has_circ_SEC62 enhances the expression of SNRPA in HCC cells by acting as a sponge for miR-625-5p. SNRPA activates the NOTCH1/Snail pathway both in vivo and in vitro, promoting the epithelial-mesenchymal transition (EMT)-like process in HCC cells, thereby accelerating metastasis [21].

Furthermore, has_circ_KIAA1429 maintains the expression of Zeb1 in HCC by regulating the m6A-YTHDF3-Zeb1 mechanism. This accelerates the EMT process in HCC, promoting the proliferation, migration, and invasion of HCC cells [22].

Twist1 directly binds to Cul2 and its promoter, leading to the abnormal formation of Cul2 circRNA. This promotes the expression of Twist1 through sponge targeting of miRNAs, thereby promoting the EMT process in HCC and enhancing the proliferation, migration, and invasion of HCC cells [23].

Has_circ_IFT80 downregulates the expression of miR-1236-3p, thereby increasing the expression of Twist2 and promoting the proliferation and metastasis of liver cancer cells [24]. These findings suggest that circRNAs can influence the progression of liver cancer by regulating the expression of EMT core transcription factors.

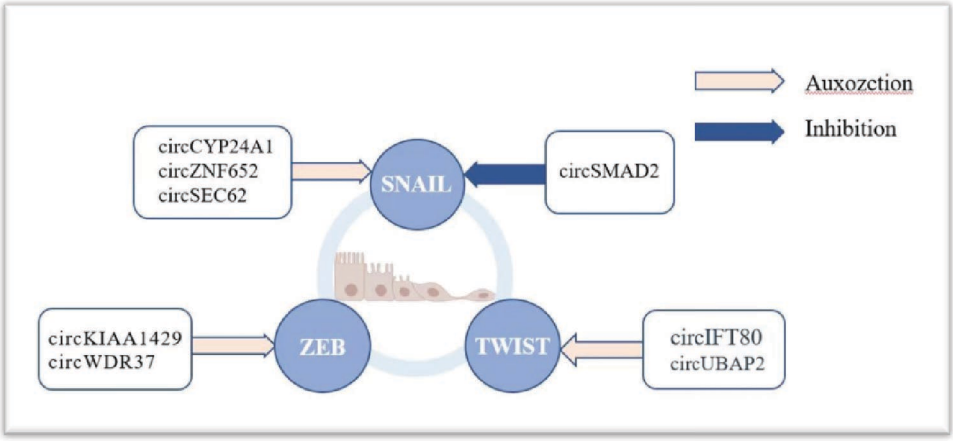

Figure 2. Interaction network between circRNA and EMT-related transcription factors

4.2. circRNA that promotes epithelial-mesenchymal transition in hepatocellular carcinoma

4.2.1. Hsa_circ_0003288 (circBIRC6)

Hsa_circ_0003288 is a circular RNA that has been shown to play a role in HCC. Programmed cell death ligand-1 (PD-L1) is a ligand expressed on the surface of tumor cells that interacts with programmed death receptor-1 (PD-1) expressed on the surface of lymphocytes. This interaction leads to the death of lymphocytes that can kill tumor cells, thereby mediating tumor immune evasion [25]. A previous study indicated that higher expression levels of hsa_circ_0003288 were associated with a poor prognosis in HCC patients [26]. In a study by Xu *et al*., it was found that the expression level of circ_0003288 was significantly increased in HCC, and its overexpression significantly promoted the proliferation and migration of HCC cells, correlating positively with PD-L1 expression levels. The study used RT-PCR to detect the expression levels of hsa_circ_0003288, miR-145, and multiple functional genes and analyzed cell viability, colony formation, apoptosis, cell migration, and invasion using various experimental methods. It was found that hsa_circ_0003288 acts as a sponge for miR-145, upregulating PD-L1 expression levels, and promoting EMT and invasion of HCC through the PI3K/AKT signaling pathway. This suggests its carcinogenic role in the development of HCC. Targeting hsa_circ_0003288 may provide a therapeutic strategy for the treatment of HCC [27].

4.2.2. Has_circ_0001459 (circNEIL3)

Insulin-like growth factor-I receptor (IGF-IR) is a cell surface tyrosine kinase receptor encoded by a gene located on chromosome 15q26.3. Recent studies have found that abnormal activation of IGF-IR can promote the malignant transformation of liver cells and induce EMT through various mechanisms. Akt, activated by IGF-IR, can stabilize slug, a negative regulator of E-cadherin expression. Additionally, IGF-IR may trigger EMT through pathways such as STAT3, FAK, and NF-kB [28,29]. Shen *et al*. found that has_circ_0001459 is significantly upregulated in liver cancer tissues. Dual-luciferase reporter assays confirmed the interaction between has_circ_0001459 and miR-6165, as well as between miR-6165 and IGF-1R. This confirmed that has_circ_0001459 can sponge miR-6165 and induce upregulation of its downstream target IGF-1R, thereby promoting invasion, migration, and EMT of HCC cells and significantly advancing the progression of HCC [30]. This suggests that has_circ_0001459 may serve as a prognostic factor and therapeutic target in hepatocellular carcinoma.

4.2.3. Has_circ_0003998 (circARFGEF2)

Has_circ_0003998 has been found to be highly expressed in non-small cell lung cancer (NSCLC) and breast cancer, promoting cell invasion and migration [31]. Poly(rC) binding protein 1 (PCBP1) is an RNA-binding protein that suppresses tumor formation and metastasis by translational silencing, mRNA alternative splicing, or transcriptional regulation of oncogenes. Importantly, PCBP1 has been reported to be involved in the EMT pathway in cancer, particularly in the TGF-β pathway [32]. PCBP1 can selectively splice the EMT-associated gene CD44v6, thus inhibiting invasion and EMT in HCC.

In a recent study by Song *et al*., it was revealed that has_circ_0003998 acts as a competing endogenous RNA (ceRNA) for microRNA-143-3p, relieving its inhibitory effect on the EMT-related transcription factor FOSL2. Considering that the interaction with RNA-binding proteins (RBPs) is an important part of circRNA function, pull-down experiments and protein mass spectrometry analysis were performed, revealing that has_circ_0003998 can bind with PCBP1 to enhance the expression of CD44v6, thus accelerating EMT progression in HCC. Therefore, the has_circ_0003998/miR-143-3p/FOSL2 axis and the has_circ_0003998/PCBP1/CD44v6 axis were discovered to regulate EMT in HCC. Therefore, has_circ_0003998 holds promise as a novel marker or therapeutic target in liver cancer.

4.2.4. Has_circ_0004277 (circWDR37)

Studies have shown that has_circ_0004277 is overexpressed in colorectal cancer and is involved in the malignant phenotype of colorectal cancer by sponging miR-512-5p to upregulate PTMA expression [33]. ZO-1, a tight junction protein, is not only involved in regulating cell substance transport and maintaining epithelial polarity but is also closely related to the information transmission and regulation of processes such as cell proliferation, differentiation, tumor cell metastasis, and gene transcription [34]. Similarly, significant upregulation of has_circ_0004277 has been detected in HCC cells, leading to the upregulation of N-cadherin and ZEB-1 expression and downregulation of E-cadherin expression at both the protein and RNA levels.

HuR protein consists of three RNA recognition motifs (RRMs) and one flexible hinge region, with RRMs primarily recognizing adenine/uridine-rich elements (AREs) in the 3'UTR of target mRNAs, stabilizing them, and promoting their translation. Recent studies have found that HuR can be secreted by various cells in the human body, but its expression levels are lower in some normal tissues and higher in various malignant tumor tissues, showing an association with poor prognosis. This suggests that HuR is closely related to the occurrence and development of various tumors, and its overexpression can enhance tumor cell proliferation and invasion.

A recent study by Zhu *et al*. demonstrated through *in vitro* and *in vivo* experiments that upregulation of has_circ_0004277 significantly promotes HCC cell proliferation and migration. Furthermore, its overexpression significantly induces N-cadherin and ZEB-1 expression while reducing E-cadherin expression at both the protein and RNA levels, indicating that has_circ_0004277 acts as an important positive regulatory factor in HCC cell growth and exhibits an oncogenic role. Subsequently, target prediction was performed using bioinformatics software, revealing that has_circ_0004277 may block the binding between HuR and ZO-1 mRNA by competitively binding with HuR, thereby inhibiting ZO-1 and stimulating EMT progression. Further experiments confirmed this hypothesis. Additionally, enhanced expression of has_circ_0004277 was observed in HCC cells, tissues, and plasma exosomes [35]. This suggests that it may serve as a potential prognostic marker for HCC patients.

4.2.5. Has_circ_0084922 (circKIAA1429)

M6A modification plays a role in various cellular physiological processes, including mRNA maturation, protein translation, and molecular structural changes, and has become a hot research topic. Increasing evidence

suggests that dysregulation of m6A can lead to various cancers, including HCC [36]. Previous studies have found that hsa_circ_0084922 from KIAA1429 is significantly upregulated in HCC tissues, promoting HCC migration, invasion, and EMT. Conversely, the downregulation of its expression leads to the opposite results. Moreover, Zeb1 has been identified as a downstream target of circKIAA1429, and YTHDF3 enhances the stability of Zeb1 mRNA in an m6A-dependent manner, prolonging the lifespan of Zeb1 mRNA in HCC, thereby accelerating HCC progression. This provides a new potential target for the treatment of liver cancer.

4.3. circRNA that inhibits epithelial-mesenchymal transition in hepatocellular carcinoma

4.3.1. circRNA CDR1as

Cerebellar degeneration-related protein 1 antisense RNA (CircCDR1as) is a circular RNA molecule associated with the occurrence of various cancers and neurodegenerative diseases. It contains over 70 binding sites for miR-7 and can regulate multiple signaling pathways through the sponge effect of binding miR-7, thereby participating in the regulation of tumor growth. For example, miR-7 acts as a tumor suppressor and regulates cell proliferation and various biological processes by triggering signal transduction of growth factors. It is abnormally expressed in various tumors such as colorectal cancer, cholangiocarcinoma, and osteosarcoma, playing an important role in the development of tumors [37]. The study by Yang *et al*. demonstrated that CDR1as changes EGFR signal regulation and cell proliferation by controlling miR-7 expression, proposing a molecular interaction network of the CDR1as/miR-7/EGFR axis in HCC cells [38]. By replacing the miR-7 binding sites in CDR1as with specific base sequences that bind mmu-miR-21 or mmu-miR-130b and transfecting them into Hepa1-6 cells, it was found that the protein levels of Vimentin and N-cadherin significantly decreased compared to the control and negative control groups ($P < 0.01$), while the protein levels of E-cadherin significantly increased ($P < 0.01$). This demonstrated that M-CDR1as can inhibit EMT in mouse Hepa1-6 liver cancer cells by binding and sequestering miR-21 and miR-130b *in vitro* [39].

4.3.2. Has_circ_0000098 (circSLC30A7)

Previous studies have found that ALX4 expression is decreased in HCC tissues, and overexpression of ALX4 inhibits HCC cell proliferation, invasion, and EMT processes [40]. However, the specific mechanism of ALX4 downregulation in liver cancer tissues remains unclear. Further research by Li *et al*. revealed that has_circ_0000098 positively regulates ALX4 expression by competitively binding with miR-1204. Additionally, the study found that the knockdown of ALX4 counteracted the inhibitory effect of downregulated miR-1204 on HCC cell proliferation, migration, invasion, and EMT. Therefore, it can be concluded that the has_circ_0000098/miR-1204/ALX4 regulatory network is involved in the progression of EMT in HCC, and low expression levels of has_circ_0000098 are associated with larger tumor volume and later stage [41]. With further research, has_circ_0000098 holds promise as a reference marker for prognostic prediction in HCC patients.

4.3.3. Has_circ_0008305 (circPTK2)

The PTK2 gene expresses two types of circRNA: circ_0003221 and circ_0008305. Both of these circRNAs are associated with cell proliferation and migration processes in cancer. In NSCLC, has_circ_0008305 targets miR-429/miR-200b-3p and inhibits their activation of the TGF-β-induced EMT pathway through targeting TIF1-γ [42]. In ovarian cancer, circ-PTK2 enhances tumor cell proliferation and migration through a cascade regulatory mechanism involving miR-639 and FOXC1. However, its role in HCC is not yet clear [43]. MiR-92a-3p is a core member of the miR-17-92 cluster, which is overexpressed in human cancers and is believed to be involved in cancer development [44]. The study by Gong *et al*. found that miR-92a-3p acts as an oncogene in HCC by targeting E-cadherin and reducing its expression. Further experiments demonstrated that has_circ_0008305

inhibits the expression of miR-92a as a competing endogenous RNA (ceRNA), upregulating the expression of E-cadherin in liver cancer cells and suppressing the EMT process in HCC (**Table 1**) [45].

Table 1. The EMT-related circRNAs in HCC

Type	CircRNA	Target/pathway
EMT-inducing circRNAs in HCC	circBIRC (hsa_circ_0003288)	circBIRC/miR-145/PD-L1/PI3K/AKT signal pathway
	circNEIL3 (hsa_circ_0001459)	circNEIL3/miR-6165/IGF-1R axis
	circARFGEF2 (hsa_circ_0003998)	circARFGEF2/miR-143-3p/FOSL2 axis circARFGEF2/ PCBP1/CD44v6 axis
	circWDR37 (hsa_circ_0004277)	circWDR37/HuR/ZO-1 axis
	circKIAA1429 (hsa_circ_0084922)	circKIAA1429/m (6)A-YTHDF3/Zeb1 axis
EMT-suppressive circRNAs in HCC	circCDR1as	circCDR1as/miR-21、miR-130b
	circSLC30A7 (hsa_circ_0003288)	circSLC30A7/miR-1204/ALX4 axis
	circPTK2 (hsa_circ_0008305)	circPTK2/miR-92a/E-cadherin axis

5. Conclusion

In summary, a large number of circRNAs are involved in the regulation of EMT in HCC, and they mainly regulate the EMT process through the following mechanisms:

(1) Acting as miRNA sponges: circRNAs can act as miRNA sponges by containing miRNA binding sites, thus binding to miRNAs and inhibiting their regulatory effects on target genes. In liver cancer, certain circRNAs have miRNA binding sites that can bind and inhibit EMT-related miRNAs, thereby releasing target genes and promoting EMT onset and progression.

(2) Interaction with RNA-binding proteins: Some circRNAs can interact with RNA-binding proteins to form circRNA-RBP complexes. These complexes can affect the EMT characteristics of liver cancer cells by regulating the expression of key EMT factors such as transcription factors, cell adhesion molecules, and signaling pathways.

(3) Regulation of transcription levels: Certain circRNAs can interact with transcription factors, affecting their expression and activity. These transcription factors may influence the EMT process in liver cancer cells by regulating the expression of genes involved in EMT.

(4) Regulation of the splicing process: Some circRNAs may be involved in regulating splicing, affecting the splicing forms of EMT-related genes in liver cancer cells. Alterations in splicing can lead to changes in the structure and function of transcript products and thus have an impact on the EMT process.

(5) Regulation of cell cycle and apoptosis: Certain circRNAs influence the onset and progression of EMT in liver cancer cells by regulating the cell cycle and apoptosis.

These circRNAs can regulate the expression of genes associated with the cell cycle and apoptosis and thus influence the EMT characteristics of liver cancer cells. They are mainly distributed in the cytoplasm or stored in extracellular vesicles and can be released into body fluids via the exosome pathway. Monitoring circRNA levels in body fluids is a promising biomarker for assessing early metastasis of liver cancer and plays a crucial role in the diagnosis of the disease.

The relationship between EMT and tumor prognosis is complex and varied, depending on factors such as tumor type, patient characteristics, and treatment strategies. However, previous research has shown that

EMT is associated with malignant features such as invasion, metastasis, and drug resistance in tumors. Studies have shown that cells undergoing EMT have increased migration and invasion capabilities, which can lead to the spread of tumor cells from the primary tumor to distant organs, resulting in the formation of metastatic tumors. In addition, EMT can contribute to drug resistance in tumor cells, thereby reducing the effectiveness of treatment. EMT is also associated with the properties of cancer stem cells (CSCs). CSCs are a small subset of tumor cells that have the potential for self-renewal and multilineage differentiation and are thought to play a critical role in tumor growth, metastasis, and recurrence.

Although further research and validation are needed to understand the relationship between EMT and tumor prognosis, existing evidence suggests that EMT may be an important indicator of poor tumor prognosis. Therefore, the assessment of EMT may have significant implications for determining tumor prognosis and selecting treatment strategies.

6. Outlook

Studies have shown that targeted intervention of circRNAs can effectively interfere with the initiation of EMT, thereby slowing down the invasive and metastatic abilities of liver cancer cells. This strategy may have potential value in preventing hepatocellular carcinoma recurrence and improving patient survival rates. Despite recognizing the importance of circRNAs in the EMT process of liver cancer, the exact regulatory mechanisms remain unclear. Currently, only a limited number of studies have extensively investigated circRNAs in liver cancer cell lines and animal models, and many molecular mechanisms of circRNA regulation of cancer EMT remain to be elucidated. Therefore, it is necessary to further explore the precise role of circRNAs in the regulation of EMT in liver cancer, which will provide a solid basis for their potential as diagnostic and therapeutic targets for cancer. The continued development of advanced technologies will deepen our understanding of the functions and mechanisms of circRNAs, further improving our understanding of biology and its applications in disease mechanisms. Researchers are encouraged to conduct further basic research on circRNAs to uncover their pathological and physiological functions. Additionally, studies on treatment strategies based on circRNAs should be conducted to safely and successfully integrate them into clinical practice.

Funding

Medical Research Project of Xi'an Science and Technology Bureau (Project No. 22YXYJ0134)

Disclosure statement

The authors declare no conflict of interest.

References

[1] Sung H, Ferlay J, Siegel RL, et al., 2021, Global Cancer Statistics 2020: Globocan Estimates of Incidence and Mortality Worldwide for 36 Cancers in 185 Countries. CA Cancer J Clin, 71(3): 209–249. https://doi.org/10.3322/caac.21660

[2] Zhou M, Wang H, Zeng X, et al., 2019, Mortality, Morbidity, and Risk Factors in China and Its Provinces, 1990–2017: A Systematic Analysis for the Global Burden of Disease Study 2017. Lancet, 394(10204): 1145–1158. https://

doi.org/10.1016/S0140-6736(19)30427-1

[3] Siegel RL, Miller KD, Jemal A, 2020, Cancer Statistics, 2020. CA Cancer J Clin, 70(1): 7–30. https://doi.org/10.3322/caac.21590

[4] Wang M, Wang Y, Feng X, et al., 2017, Contribution of Hepatitis B Virus and Hepatitis C Virus To Liver Cancer in China North Areas: Experience of the Chinese National Cancer Center. Int J Infect Dis, 65: 15–21. https://doi.org/10.1016/j.ijid.2017.09.003

[5] Wang T, Chen D, 2021, Clinical Diagnosis and Treatment of Hepatocellular Carcinoma: From Guidelines to Clinical Practice. Journal of Clinical Hepatology, 37(8): 1745–1747. https://doi.org/10.3969/j.issn.1001-5256.2021.08.001

[6] Li X, Yang L, Chen L-L, 2018, The Biogenesis, Functions, and Challenges of Circular RNAs. Mol Cell, 71(3): 428–442. https://doi.org/10.1016/j.molcel.2018.06.034

[7] Rybak-Wolf A, Stottmeister C, Glažar P, et al., 2015, Circular RNAs in the Mammalian Brain are Highly Abundant, Conserved, and Dynamically Expressed. Mol Cell, 58(5): 870–885. https://doi.org/10.1016/j.molcel.2015.03.027

[8] Li Z, Huang C, Bao C, et al., 2015, Exon-Intron Circular RNAs Regulate Transcription in the Nucleus. Nat Struct Mol Biol, 22: 256–264. https://doi.org/10.1038/nsmb.2959

[9] Meng X, Li X, Zhang P, et al., 2017, Circular RNA: An Emerging Key Player in RNA World. Brief Bioinform, 18(4): 547–557. https://doi.org/10.1093/bib/bbw045

[10] Li J, Yang J, Zhou P, et al., 2015, Circular RNAs in Cancer: Novel Insights into Origins, Properties, Functions and Implications. Am J Cancer Res, 5(2): 472–480.

[11] Pamudurti NR, Bartok O, Jens M, et al., 2017, Translation of CircRNAs. Mol Cell, 66(1): 9–21.e7. https://doi.org/10.1016/j.molcel.2017.02.021

[12] Huang A, Zheng H, Wu Z, et al., 2020, Circular RNA-Protein Interactions: Functions, Mechanisms, and Identification. Theranostics, 10(8): 3503–3517. https://doi.org/10.7150/thno.42174

[13] Memczak S, Jens M, Elefsinioti A, et al., 2013, Circular RNAs are a Large Class of Animal RNAs with Regulatory Potency. Nature, 495(7441): 333–338. https://doi.org/10.1038/nature11928

[14] Chen B, Huang S, 2018, Circular RNA: An Emerging Non-Coding RNA as a Regulator and Biomarker in Cancer. Cancer Letters, 418: 41–50. https://doi.org/10.1016/j.canlet.2018.01.011

[15] Dongre A, Weinberg RA, 2019, New Insights into the Mechanisms of Epithelial-Mesenchymal Transition and Implications for Cancer. Nat Rev Mol Cell Biol, 20(2): 69–84. https://doi.org/10.1038/s41580-018-0080-4

[16] Zhang CL, Tan XS, Huang ZS, 2021, Effect of Oxymatrine on Epithelial-Mesenchymal Transition and Cell Biological Characteristics of Human Hepatoma Carcinoma Cell Line Hepg2 by Upregulating Mir-204. Journal of Youjiang Medical University for Nationalities, 43(1): 11–16.

[17] Ou H, Chen Z, Xiang L, et al., 2019, Frizzled 2-Induced Epithelial-Mesenchymal Transition Correlates with Vasculogenic Mimicry, Stemness, and Hippo Signaling in Hepatocellular Carcinoma. Cancer Sci, 110(4): 1169–1182. https://doi.org/10.1111/cas.13949

[18] Giannelli G, Koudelkova P, Dituri F, et al., 2016, Role of Epithelial to Mesenchymal Transition in Hepatocellular Carcinoma. J Hepatol, 65(4): 798–808. https://doi.org/10.1016/j.jhep.2016.05.007

[19] Peinado H, Olmeda D, Cano A, 2007, Snail, Zeb and bHLH Factors in Tumour Progression: An Alliance Against the Epithelial Phenotype? Nat Rev Cancer, 7(6): 415–428. https://doi.org/10.1038/nrc2131

[20] Yan L, 2020, The Role of CircCYP24A1 in HBx Induced Epithelial-Mesenchymal Transition and Tumor Invasion and Metastasis in Human Hepatocellular Carcinoma, thesis, China Medical University.

[21] Mo Z, Li R, Cao C, et al., 2023, Splicing Factor SNRPA Associated with Microvascular Invasion Promotes Hepatocellular Carcinoma Metastasis through Activating NOTCH1/Snail Pathway and is Mediated by circSEC62/miR-625-5p Axis. Environ Toxicol, 38(5): 1022–1037. https://doi.org/10.1002/tox.23745

[22] Wang M, Yang Y, Yang J, et al., 2020, circ_KIAA1429 Accelerates Hepatocellular Carcinoma Advancement through the Mechanism of m^{6}A-YTHDF3-Zeb1. Life Sci, 257: 118082. https://doi.org/10.1016/j.lfs.2020.118082

[23] Meng J, Chen S, Han J-X, et al., 2018, Twist1 Regulates Vimentin through Cul2 Circular RNA to Promote EMT in Hepatocellular Carcinoma. Cancer Res, 78(15): 4150–4162. https://doi.org/10.1158/0008-5472.CAN-17-3009

[24] Chen J, Qi Z, 2022, The Elevated circ_0067835 Could Accelerate Cell Proliferation and Metastasis via miR-1236-3p/Twist2 Axis in Hepatocellular Carcinoma. Biomed Res Int, 2022: 2825172. https://doi.org/1155/2022/2825172

[25] Buchbinder EI, Desai A, 2016, CTLA-4 and PD-1 Pathways: Similarities, Differences, and Implications of Their Inhibition. Am J Clin Oncol, 39(1): 98–106. https://doi.org/10.1097/COC.0000000000000239

[26] Yang G, Wang X, Liu B, et al., 2019, circ-BIRC6, a Circular RNA, Promotes Hepatocellular Carcinoma Progression by Targeting the miR-3918/Bcl2 Axis. Cell Cycle, 18(9): 976–989. https://doi.org/10.1080/15384101.2019.1601477

[27] Xu G, Zhang P, Liang H, et al., 2021, Circular RNA hsa_circ_0003288 Induces EMT and Invasion by Regulating hsa_circ_0003288/miR-145/PD-L1 Axis in Hepatocellular Carcinoma. Cancer Cell Int, 21(1): 212. https://doi.org/10.1186/s12935-021-01902-2

[28] Taliaferro-Smith L, Oberlick E, Liu T, et al., 2015, FAK Activation is Required for IGF1R-Mediated Regulation of EMT, Migration, and Invasion in Mesenchymal Triple Negative Breast Cancer Cells. Oncotarget, 6(7): 4757–4772. https://doi.org/10.18632/oncotarget.3023

[29] Kim HJ, Litzenburger BC, Cui X, et al., 2007, Constitutively Active Type I Insulin-Like Growth Factor Receptor Causes Transformation and Xenograft Growth of Immortalized Mammary Epithelial Cells and is Accompanied by an Epithelial-to-Mesenchymal Transition Mediated by NF-κB and Snail. Mol Cell Biol, 27(8): 3165–3175. https://doi.org/10.1128/MCB.01315-06

[30] Shen D, Zhao H, Zeng P, et al., 2022, Circular RNA circ_0001459 Accelerates Hepatocellular Carcinoma Progression via the miR-6165/IGF1R Axis. Ann N Y Acad Sci, 1512(1): 46–60. https://doi.org/10.1111/nyas.14753

[31] Yu W, Jiang H, Zhang H, et al., 2018, hsa_circ_0003998 Promotes Cell Proliferation and Invasion by Targeting miR-326 in Non-Small Cell Lung Cancer. Onco Targets Ther, 11: 5569–5577. https://doi.org/10.2147/OTT.S174750

[32] Tripathi V, Sixt KM, Gao S, et al., 2016, Direct Regulation of Alternative Splicing by SMAD3 through PCBP1 is Essential to the Tumor-Promoting Role of TGF-β. Mol Cell, 64(3): 549–564. https://doi.org/10.1016/h.molcel.2016.09.013

[33] Yang L, Sun H, Liu X, et al., 2020, Circular RNA hsa_circ_0004277 Contributes to Malignant Phenotype of Colorectal Cancer by Sponging miR-512-5p to Upregulate the Expression of PTMA. J Cell Physiol, Early View. https://doi.org/10.1002/jcp.29484

[34] Hsu Y-L, Hung J-Y, Chang W-A, et al., 2017, Hypoxic Lung Cancer-Secreted Exosomal miR-23a Increased Angiogenesis and Vascular Permeability by Targeting Prolyl Hydroxylase and Tight Junction Protein ZO-1. Oncogene, 36(34): 4929–4942. https://doi.org/10.1038/onc.2017.105

[35] Zhu C, Su Y, Liu L, et al., 2021, Circular RNA hsa_circ_0004277 Stimulates Malignant Phenotype of Hepatocellular Carcinoma and Epithelial-Mesenchymal Transition of Peripheral Cells. Front Cell Dev Biol, 8: 585565. https://doi.org/10.3389/fcell.2020.585565

[36] Wang S, Chai P, Jia R, et al., 2018, Novel Insights on m^{6}A RNA Methylation in Tumorigenesis: A Double-Edged Sword. Mol Cancer, 17: 101. https://doi.org/10.1186/s12943-018-0847-4

[37] Jiang C, Zeng X, Shan R, et al., 2020, The Emerging Picture of the Roles of circRNA-CDR1as in Cancer. Front Cell Dev Biol, 8: 590478. https://doi.org/10.3389/fcell.2020.590478

[38] Yang X, Xiong Q, Wu Y, et al., 2017, Quantitative Proteomics Reveals the Regulatory Networks of Circular RNA CDR1as in Hepatocellular Carcinoma Cells. J Proteome Res, 16(10): 3891–3902. https://doi.org/10.1021/acs.jproteome.7b00519

[39] Sun F, Wang JZ, Luo JJ, et al., 2018, miR-21 and miR-130b Targeted Artificial Modification of circRNA can Inhibit the Epithelial-Mesenchymal Transition of Hepatocellular Carcinoma Cells. China Medical Devices, 33(S1): 43–45.

[40] Shi Y, Sun X, He X, 2017, Overexpression of Aristaless-Like Homeobox-4 Inhibits Proliferation, Invasion, and EMT in Hepatocellular Carcinoma Cells. Oncol Res, 25(1): 11–18. https://doi.org/10.3727/096504016X14685034103833

[41] Li M, Yue W, Li Q, et al., 2021, Circular RNA circ_0000098 Elevates ALX4 Expression via Adsorbing miR-1204 to Inhibit the Progression of Hepatocellular Carcinoma. Front Oncol, 11: 696078. https://doi.org/10.3389/fonc.2021.696078

[42] Wang L, Tong X, Zhou Z, et al., 2018, Circular RNA hsa_circ_0008305 (circPTK2) Inhibits Tgf-β-Induced Epithelial-Mesenchymal Transition and Metastasis by Controlling TIF1γ in Non-Small Cell Lung Cancer. Mol Cancer, 17(1): 140. https://doi.org/10.1186/s12943-018-0889-7

[43] Wu SG, Zhou P, Chen JX, et al., 2021, circ-PTK2 (hsa_circ_0008305) Regulates the Pathogenic Processes of Ovarian Cancer via miR-639 and FOXC1 Regulatory Cascade. Cancer Cell Int, 21(1): 277. https://doi.org/10.1186/s12935-021-01985-x

[44] Tsuchida A, Ohno S, Wu W, et al., 2011, miR-92 is a Key Oncogenic Component of the miR-17-92 Cluster in Colon Cancer. Cancer Sci, 102(12): 2264–2271. https://doi.org/10.1111/j.1349-7006.2011.02081.x

[45] Gong T-T, Sun F-Z, Chen J-Y, et al., 2020, The Circular RNA circPTK2 Inhibits EMT in Hepatocellular Carcinoma by Acting as a ceRNA and Sponging miR-92a to Upregulate E-cadherin. Eur Rev Med Pharmacol Sci, 24(18): 9333–9342. https://doi.org/10.26355/eurrev_202009_23015

Proceedings of Anticancer Research, 2024, Volume 8, Issue 2
http://ojs.bbwpublisher.com/index.php/PAR
ISSN Online: 2208-3553
ISSN Print: 2208-3545

Surgical Reconstruction of a Large Defect after Excision of Infiltrative Squamous Cell Carcinoma in the Scalp and Occipital Region: A Case Report

Chi Zhang, Tiehui Zhang, Peiyu Cong, Hongzhu Lv, Chengzhi Cui*

Department of Neurosurgery, Dalian Central Hospital, Dalian 116000, China

***Corresponding author:** Chengzhi Cui, cuichengzhi2001@sina.com

Abstract: Squamous cell carcinoma (SCC) of the scalp is the second most prevalent skin cancer, following basal cell carcinoma. Notably, it has the capability to infiltrate the skull, dura mater, and even brain tissue. The cornerstone of treatment is the surgical removal of the lesion, with a particular focus on the depth of invasion, which is directly correlated with recurrence rates. Post-surgical strategies may involve immediate or delayed cranial bone reconstruction and repair of scalp defects using either artificial dermis or skin grafts. In the case presented, a substantial defect necessitated more than a single flap for primary repair. Hence, a single pedicle double-island flap was designed for reconstructing the occipital area. Due to increased tension on the flap following cranial bone repair, the bone repair was temporarily deferred. Postoperative care included adjuvant chemotherapy and radiotherapy to mitigate the risk of SCC recurrence.

Keywords: Squamous cell carcinoma; Intracranial invasion; Single pedicle double-island flap; Case report

Online publication: March 28, 2024

1. Introduction

Squamous cell carcinoma (SCC) originates from keratinocytes in the epidermis or its appendages, including sebaceous gland ducts, hair follicles, and sweat gland ducts [1]. This malignancy is notorious for its high potential to invade deeply into brain tissue, consequently heightening the risk of recurrence. Various etiological factors contribute to its development, such as exposure to ultraviolet (UV) radiation, chemical agents, racial factors, pre-cancerous skin conditions, and scars. Early detection and prompt, complete surgical excision can significantly improve prognosis [2]. This report details a case involving the surgical removal of a large, infiltrative SCC in the scalp and occipital region, resulting in a massive defect. The reconstruction was achieved using a pedicled flap with branches from the anterior lateral thigh [3].

2. Clinical data

The patient, a 41-year-old individual, presented with a two-year history of recurrent ulceration and a recent one-

month history of increased swelling accompanied by headaches. A previous scalp burn in the occipital region 40 years ago had left scar tissue, which was covered by a wig. The ulcerations were recurrent, producing a foul odor and causing blurry vision. Physical examination revealed a 7×4 cm skin ulceration with white purulent discharge in the occipital region (**Figure 1.1**), along with barrel-shaped visual field impairment. Other physical findings were unremarkable.

For auxiliary examinations, cranial magnetic resonance imaging (MRI) with contrast enhancement displayed a localized defect in the right occipital region, involving both the skull bone and scalp soft tissue, presenting as irregular clusters of abnormal signal intensity. The lesion exhibited hypointensity on T1-weighted images and hyperintensity on T2-weighted/FLAIR images, with indistinct margins. The cross-sectional dimension of the lesion was 2.8×1.3 cm. Post-contrast administration, the lesion showed enhanced uptake, with adjacent dura mater thickening and enhancement, and partial encasement of the adjacent superior sagittal sinus. No significant abnormal signal changes were observed in the adjacent brain parenchyma (**Figure 2**). Magnetic resonance angiography (MRA) revealed the involvement of the superior sagittal sinus (**Figure 3.1**). Cranial bone thin-layer imaging and three-dimensional reconstruction demonstrated the involvement of the occipital region skull bone (**Figure 3.2**). The pathological diagnosis indicated squamous cell carcinoma (**Figure 1.2**).

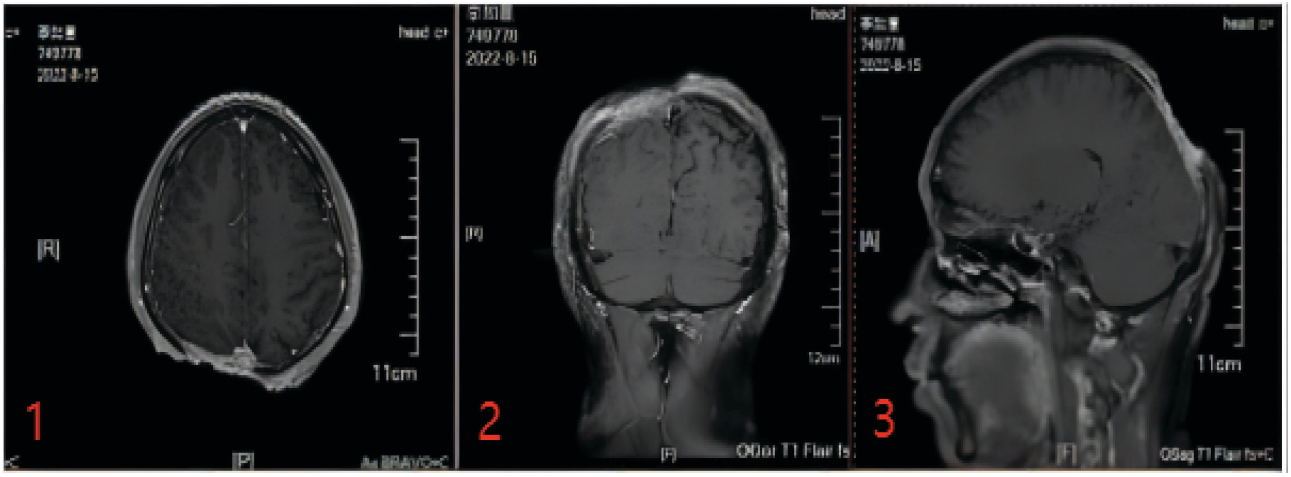

Figure 1. The occipital region ulceration and pathological diagnosis

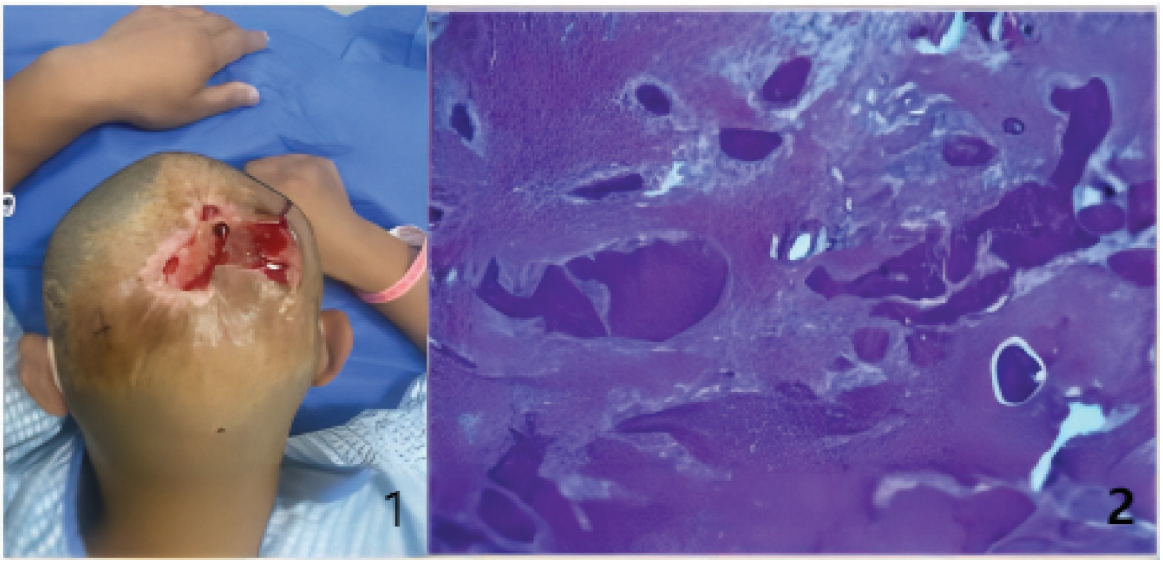

Figure 2. Signal display of lesion site on MRI

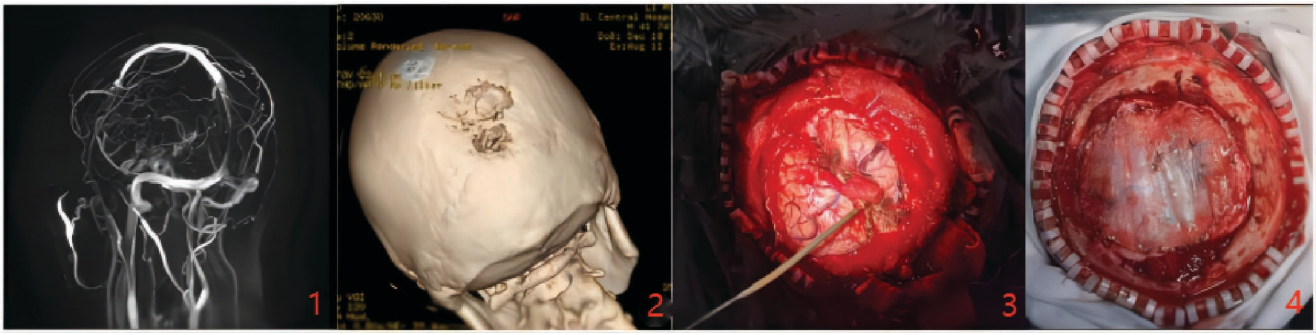

Figure 3. From left to right are the three-dimensional imaging of MRI and the actual situation in the operation

The multidisciplinary team (MDT) conducted an extensive resection of the tumor, involving the scalp, invaded skull bone, dura mater, brain tissue, and a pedicled flap graft from the anterior-lateral perforator branches of the right thigh (**Figure 3.3**). Intraoperatively, a 2 cm margin was excised from the tumor-involved areas. Intraoperative pathology confirmed the absence of tumor cells at the margins. A portion of the fascia lata from the outer side of the left thigh was utilized for dura mater repair (**Figure 3.4**).

Preoperatively, color Doppler flow imaging was employed to identify the perforator vessels in the donor and recipient areas, determining their positions and numbers. The recipient area's defect exceeded the blood supply area of a single flap. After deliberation, the hand and foot surgery team decided to repair using a pedicled flap from the anterior-lateral perforator branches of the right thigh. Notably, there is significant anatomical variation in these vessels, often with a longer intramuscular course. Accurate identification and preparation of a single pedicle double-island free flap were critical. The patient had the rare intramuscular type of perforator vessels, present in only 5% of the population. This anatomical variation posed considerable surgical challenges, as each millimeter of dissection risked damaging the vessels and accompanying veins, potentially leading to inadequate blood supply, restricted venous outflow, and flap necrosis.

Nonetheless, the surgical team successfully created a single pedicle double-island flap (**Figure 4.1**), and anastomosis was performed between the superficial temporal artery and vein and the flap's arterial and venous vessels (**Figure 4.2**). The incision in the right thigh donor area was directly closed. Postoperatively, the transplanted flap showed good blood supply to the head. However, complications such as cerebrospinal fluid leakage, fever, and high intracranial pressure were observed. A lumbar puncture was performed to alleviate intracranial pressure, and signs of intracranial infection were managed with strengthened intravenous antibiotics and continuous lumbar drainage (**Figure 4.3**). The patient's body temperature stabilized, and cerebrospinal fluid analysis normalized. The incision healed well.

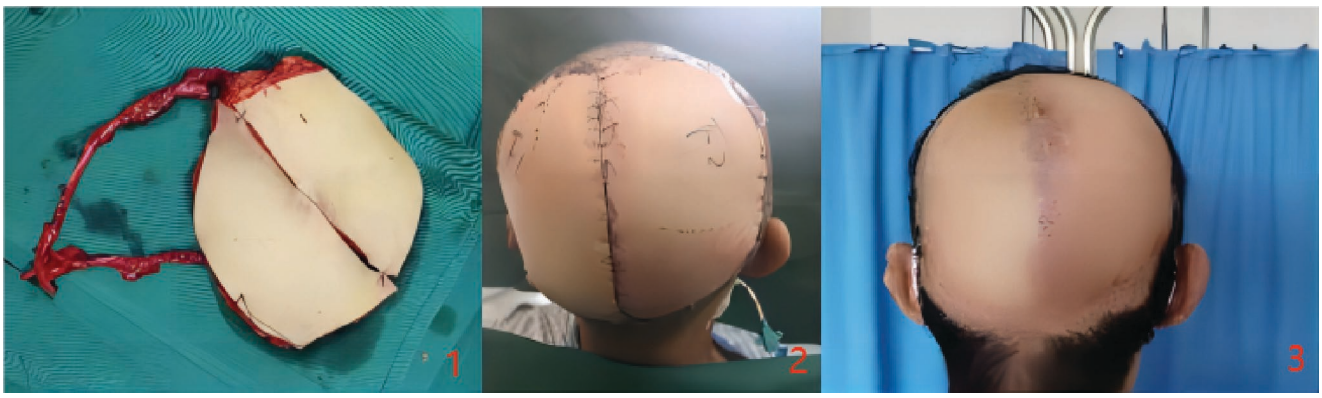

Figure 4. From left to right are pictures of a single pedicle double-island flap, after anastomosis, and after healing

3. Discussion

Repeated breakdown and infection of burn scars can transform into malignant tumors, such as SCC. SCC has a lengthy progression and can invade structures like the skull, dura mater, and brain tissue [4]. Studies indicate that scalp tumors constitute about 5% of all skin tumors, with a rising incidence of malignancies in this region. SCC is particularly prone to local and lymphatic metastasis, as well as neural invasion [5]. Local or systemic application of anti-tumor drugs and radiation therapy may not yield satisfactory results, making surgical intervention the preferred treatment option [6]. Adjuvant radiotherapy and chemotherapy can help reduce the recurrence rate or delay disease progression.

Scalp tumors encompass a variety of types, including hemangiomas, melanomas, neurofibromas, basal cell carcinomas (BCC), SCC, sarcomas, and metastatic tumors. Among these, scalp SCC is the second most common skin cancer following BCC [7,8]. The incidence of scalp tumors is on the rise, in contrast to skin tumors in other areas. Only a small percentage (1% to 2%) of scalp tumors are malignant, and intracranial invasion by SCC is rare [9,10]. However, such an invasion is indicative of a poor prognosis. Surgical treatment remains the preferred method of management. For SCC, a 2 cm margin of excision around the lesion is recommended, while for exophytic fibrosarcoma, a 3 cm margin is necessary. The key to successful treatment is intraoperative pathological analysis to ensure no tumor infiltration at the margins, and complete excision is the standard of care [11]. It is widely accepted that the depth of infiltration correlates positively with the likelihood of metastasis, and complete removal of the lesion can enhance prognosis and lower the recurrence rate [12].

In the presented case, the tumor had infiltrated brain tissue, necessitating extensive resection of the scalp, skull, dura mater, and brain tissue. Postoperative MRI confirmed complete excision. A high-power view of the pathological examination revealed infiltrating SCC cells in the dermis, characterized by significant nuclear pleomorphism, large nucleoli, coarse chromatin, occasional atypical nuclei, and numerous mitotic figures, including atypical mitoses. However, this left defects in the scalp and skull [13-15]. Cranioplasty with titanium plates can be performed. If the tension on the repaired scalp is high, cranioplasty can be temporarily postponed, and direct application of artificial dermis with a pedicled flap can be used for scalp repair. In this case, a large scalp defect necessitated a single pedicle double-island flap design [16]. The anterior-lateral perforator branches of the right thigh were employed for the flap. The rare intramuscular type of perforator vessels, accounting for only 5% of the population, greatly increased the surgical challenge [17]. Each millimeter of dissection risked damaging the vessels and accompanying veins, leading to inadequate blood supply, restricted venous outflow, and consequently, flap necrosis. Despite these challenges, the surgery was successful.

Postoperative radiotherapy and chemotherapy can reduce the recurrence rate. Platinum-based chemotherapy drugs combined with targeted therapy are still the first-line treatment recommended for head and neck SCC in treatment guidelines [18]. With the advancement of immunotherapy, immune checkpoint inhibitors, notably PD-1/PD-L1, have shown promising results in advanced and recurrent head and neck SCC [19,20].

Disclosure statement

The authors declare no conflict of interest.

References

[1] Arginelli F, Salgarelli AC, Ferrari B, et al., 2016, Crescentic Flap for the Reconstruction of the Nose After Skin Cancer Resection. J Craniomaxillofac Surg, 44(6): 703–707. https://doi.org/10.1016/j.jcms.2016.02.008

[2] Cai Q, Liang F, Huang X, et al., 2015, Hypopharynx and Larynx Defect Repair After Resection for Pyriform

Fossa Cancer with a Platysma Skin Flap. Otolaryngol Head Neck Surg, 152(2): 374–376. https://doi.org/10.1177/0194599814559508

[3] Brunetti B, Salzillo R, Tenna S, et al., 2022, Versatility of the Lateral Circumflex Femoral Artery Sparing Perforator-Based Anterolateral Thigh Flaps in Loco-Regional Thigh Reconstruction After Skin Cancer, Melanoma, and Sarcoma Resection. Microsurgery, 42(5): 428–432. https://doi.org/10.1002/micr.30836

[4] Chuang H-C, Su C-Y, Jeng S-F, et al., 2007, Anterior Lateral Thigh Flap for Buccal Mucosal Defect After Resection of Buccal Cancer. Otolaryngol Head Neck Surg, 137(4): 632–635. https://doi.org/10.1016/j.otohns.2007.03.018

[5] Crișan D, Colosi HA, Manea A, et al., 2019, Retrospective Analysis of Complication Rates Associated with Auricular Reconstruction After Skin Cancer Surgery. Journal of Cutaneous Medicine and Surgery, 24(2): 137–143. https://doi.org/10.1177/1203475419890841

[6] Gulati A, Grekin R, Neuhaus I, et al., 2023, Long-Term Appearance-Related Outcomes of Facial Reconstruction After Skin Cancer Resection. Facial Plast Surg Aesthet Med, 25(4): 344–350. https://doi.org/10.1089/fpsam.2022.0170

[7] Halani SH, Ma C, Pierce J, et al., 2021, Nasal Reconstruction After Mohs Cancer Resection: Lessons Learned from 2553 Consecutive Cases. Plast Reconstr Surg, 148(1): 171–182. https://doi.org/10.1097/prs.0000000000008098

[8] Hanada M, Kadota H, Yoshida S, et al., 2019, Large-Defect Resurfacing: A Comparison of Skin Graft Results Following Sarcoma Resection and Traumatic Injury Repair. Wounds, 31(7): 184–192.

[9] Lang Z, Zhao L, Chu Y, 2021, Esthetic Repair of Facial Skin Defect After Resection of Malignant Tumor with Lateral Maxillocervical-Island Fasciocutaneous Flap. J Craniofac Surg, 32(4): e330–e332. https://doi.org/10.1097/scs.0000000000007075

[10] Li X, Li Z, Qi L, et al., 2020, Application of Vermillion Myocutaneous Flap in Restoration After Lip Cancer Resection. Dermatol Ther, 33(6): e14320. https://doi.org/10.1111/dth.14320

[11] Lin J, Wei P, Xu Y, et al., 2022, Use of the O-Z Flap to Repair Scalp Defects After Cancer Tumor Resection. J Craniofac Surg, 33(3): 892–894. https://doi.org/10.1097/scs.0000000000008300

[12] Liu J, Lv D, Deng D, et al., 2019, Free Bipaddled Anterolateral Thigh Flap for Simultaneous Reconstruction of Large Larynx and Prelaryngeal Skin Defects After Resection of the Local Recurrent Laryngeal Cancer Invading the Cricoid Cartilage and Prelaryngeal Skin: A Case Report. Medicine (Baltimore), 98(4): e14199. https://doi.org/10.1097/md.0000000000014199

[13] Mehrara BJ, Disa JJ, Pusic A, 2006, Scalp Reconstruction. J Surg Oncol, 94(6): 504–508. https://doi.org/10.1002/jso.20487

[14] Murillo WL, Fernandez W, Caycedo DJ, et al., 2004, Cheek and Inferior Eyelid Reconstruction After Skin Cancer Ablation. Clin Plast Surg, 31(1): 49–67. https://doi.org/10.1016/s0094-1298(03)00122-6

[15] Qin XJ, Zhang SL, Zhang HL, et al., 2012, Reconstruction with Scrotal Skin Flaps After Wide Local Resection of Penoscrotal Extramammary Paget's Disease. BJU Int, 110(11 Pt C): E1121–E1124. https://doi.org/10.1111/j.1464-410X.2012.11491.x

[16] Rysz M, Grzelecki D, Mazurek M, et al., 2017, Surgical Techniques for Closure of a Scalp Defect After Resection of Skin Malignancy. Dermatol Surg, 43(5): 715–723. https://doi.org/10.1097/dss.0000000000001067

[17] Shinden Y, Nagata A, Nomoto Y, et al., 2020, Surgical Resection with Pedicled Rotation Flap for Post-Mastectomy Locoregional Breast Cancer Recurrence. Anticancer Res, 40(10): 5739–5742. https://doi.org/10.21873/anticanres.14589

[18] Wu Q, Shao Z, Li Y, et al., 2020, A Novel Skin-Stretching Device for Closing Large Skin-Soft Tissue Defects After Soft Tissue Sarcoma Resection. World Journal of Surgical Oncology, 18: 247. https://doi.org/10.1186/s12957-020-02022-3

[19] Xu J-G, Wu M-L, Dai H-Y, et al., 2021, Divisional Reconstruction Strategy: The Repair of Perineal Skin Defect After

Tumor Resection. Scand J Surg, 110(1): 73–77. https://doi.org/10.1177/1457496920903980

[20] Zimmer DI, Wieland AM, Ku JA, 2023, Reconstruction After Skin Cancer Resection of the Head and Neck. Otolaryngol Clin North Am, 56(4): 779–790. https://doi.org/10.1016/j.otc.2023.04.006

Proceedings of Anticancer Research, 2024, Volume 8, Issue 2
http://ojs.bbwpublisher.com/index.php/PAR
ISSN Online: 2208-3553
ISSN Print: 2208-3545

Benign Multicystic Peritoneal Mesothelioma: A Case Report

Yuxuan Shao[1], Shifeng Xiang[2]*, Ya Su[1], Shuyuan Li[1]

[1]Hebei North University, Zhangjiakou 075000, China
[2]CT Room, Handan Central Hospital, Handan 056001, China

Corresponding author: Shifeng Xiang, 13932096565xsf@live.com

Abstract: Benign multicystic peritoneal mesothelioma (BMPM) is a rare tumor originating from peritoneal mesothelial cells. Here, we present a case of an 18-year-old male with right lower abdominal pain. Physical examination revealed a palpable mass with unclear boundaries. Laboratory tests showed elevated levels of monocytes and high-sensitivity C-reactive protein. CT scan revealed a cystic mass in the ileocecal region with multiple septations. Laparoscopic surgery confirmed a cystic solid mass resembling beads on the colon's right side. Immunohistochemistry confirmed BMPM diagnosis. BMPM, especially in the ileocecal region, is uncommon and presents diagnostic challenges. Differential diagnosis includes lymphangioma, peritoneal metastasis, and malignant mesothelioma. CT findings, such as thin cyst walls and septations, aid in diagnosis. Recognition of BMPM's imaging features improves diagnostic accuracy. Surgical resection remains the primary treatment. This case underscores the importance of considering BMPM in young male patients with abdominal pain and emphasizes the value of imaging modalities in accurate diagnosis and management.

Keywords: Benign multicystic peritoneal mesothelioma (BMPM); Imaging; Diagnosis

Online publication: March 28, 2024

1. Case study

The patient, an 18-year-old male, experienced pain in the right lower abdomen for two days. Physical examination revealed a flat abdomen with a palpable tough mass on the right side, exhibiting unclear boundaries and average range of motion. There were no signs of tenderness, rebound tenderness, or muscle tension in the abdomen. The liver from the subcostal position was not palpable. Laboratory tests indicated a monocyte count of 0.78×10^9 g/L, high-sensitivity C-reactive protein (hs-CRP) level of > 10.00 mg/L (normal range: 0–3), cytokeratin level of 0.087 g/L (normal range: 0.2–0.43), and abnormal tumor detection measuring 108.52 μm^2 (in the range of 0–121). Colonoscopy revealed no abnormalities in any segment of the colon or rectum.

The computed tomography (CT) scan showed a cystic mass with a low-density shadow in the paracolic sulcus of the ileocecal region and a clear edge, measuring approximately 7.4 cm × 6.4 cm × 13.3 cm with multiple septations. Mild enhancement of the lesion edges and septations was observed on enhanced scans.

The arterial phase CT value was 25 HU, the venous phase CT value was 28 HU, and the delayed phase CT value was 32 HU (**Figures 1–3**). Additionally, arc-shaped, watery, low-density shadows were visible around the mass. Coronal reconstruction revealed a well-shaped appendix located below the mass with local peritoneal thickening (**Figure 4**).

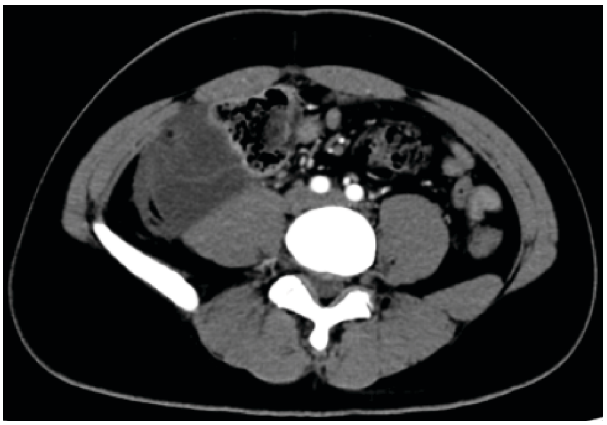

Figure 1. The arterial phase of the enhanced scan shows a cystic mass in the ileocecal paracolic groove, approximately 7.4 cm × 6.4 cm × 13.3 cm in size, with enhancement visible at the edge and separation of the lesion, and a CT value of 25 HU

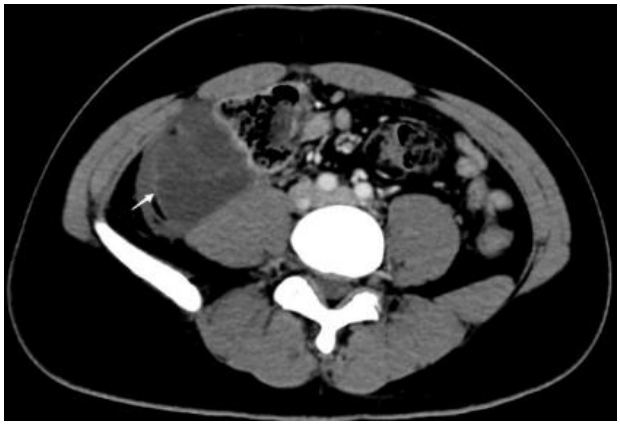

Figure 2. Venous phase of contrast-enhanced scan with a slightly enhanced septa (white arrow) and a CT value of 28 HU

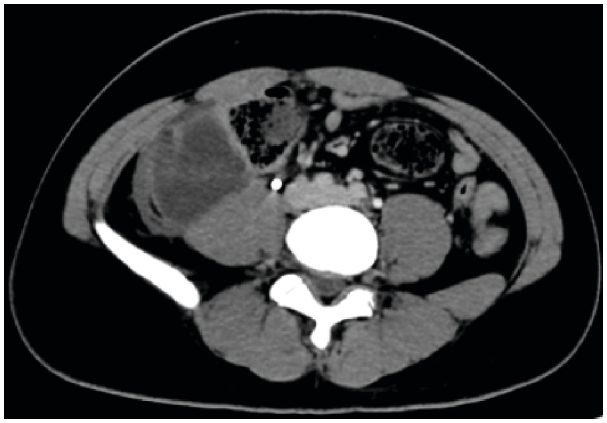

Figure 3. The delay period of the enhanced scan with a CT value of 32 HU

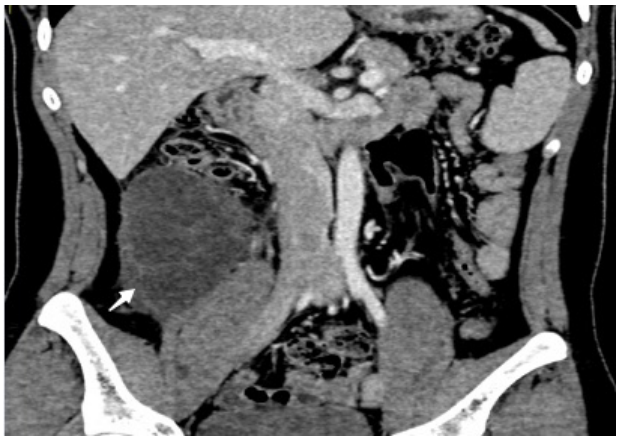

Figure 4. In the CT arterial phase coronal reconstruction image, the lesion edges and septa are enhanced (white arrow), and the right peritoneum is thickened

The diagnosis was a cystic mass occupying the paracolic groove in the ileocecal region with surrounding exudative changes. The patient underwent laparoscopic surgery under general anesthesia, involving laparoscopic abdominal mass resection and intestinal adhesion lysis. During the operation, a large cystic solid mass resembling a string of beads was observed on the right side of the colon. The cystic fluid had a jelly-like consistency and contained septa. The sizes of the tumors submitted for examination post-surgery were 10 cm × 10 cm × 4 cm and 7 cm × 2 cm × 1 cm, respectively. Immunohistochemistry results revealed CR (+), MC (+), CD34 (-), D2-40 (+), CD31 (vascular+), Desmin (partially +), Ki-67 (+ about 25%), EMA (-), P53 (-), Vimentin (+), S-100 (-), MOC31 (-), CK(pan) (+), WT 1 (+), and CK5/6 (+). The pathological diagnosis was benign

cystic peritoneal mesothelioma (BMPM; **Figure 5**).

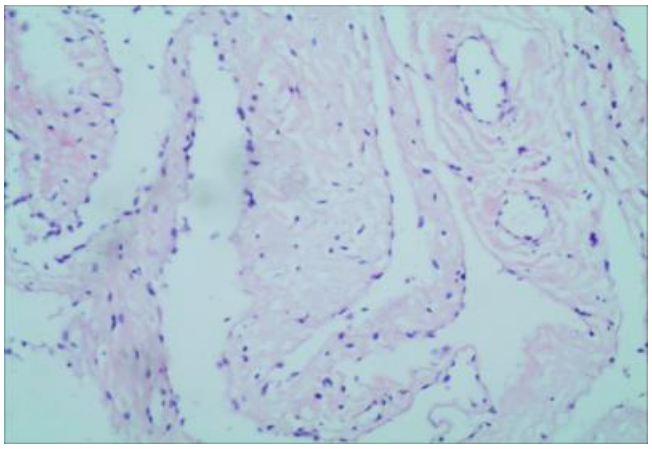

Figure 5. Mass under electron microscope mainly composed of mesothelial cells and stroma (HE×100)

2. Discussion

BMPM is a rare tumor arising from peritoneal mesothelial cells, with the potential to develop in any peritoneal or subperitoneal area. The cyst wall typically consists of a proliferated fibrous stroma, lined with a single or double layer of flat or cuboidal mesothelial cells devoid of atypia. The fibrous stroma often contains edema, mucinous degeneration, and chronic inflammatory cell infiltration. BMPM predominantly affects women under 30 years old [1], manifesting with symptoms like abdominal pain, distension, refractory ascites, and abdominal masses [2]. Reports of BMPM, particularly in the ileocecal region, are scarce.

In this case, CT findings revealed a cystic mass in the ileocecal paracolic groove with distinct boundaries, thin and uniform cyst walls, and multiple internal septations. The enhanced scan displayed mild enhancement along the lesion edges and septations, with internal cyst fluid demonstrating higher density than ordinary water CT values. The diagnostic challenge primarily revolved around accurate localization. Coronal CT reconstruction identified the appendix below the mass, excluding appendiceal origins. Furthermore, colonoscopy ruled out ascending colon involvement, pinpointing the origin to the peritoneum. Differential diagnosis involved distinguishing BMPM from lymphangioma, peritoneal metastasis, and malignant mesothelioma. Notably, lymphangiomas typically located in the retroperitoneum, have irregular shapes, multiple septations, and lack a clear relationship with the peritoneum. Peritoneal metastases present with primary lesions and omental cake signs from thickening of the peritoneum and massive ascites [3], while malignant mesothelioma displays atypical mesothelial cell growth [2,4].

Paracolic BMPM poses diagnostic hurdles, requiring meticulous exclusion of adjacent structures such as the appendix and ascending colon. Recognition of characteristic imaging features, such as thin and uniform cyst wall, multiple septations that are mildly enhanced, and no obvious mural nodules on enhanced scanning, facilitates accurate preoperative diagnosis, with surgical resection serving as the mainstay treatment [5].

Disclosure statement

The authors declare no conflict of interest.

References

[1] Hu H, Wu E, Huang W, et al., 2017, CT Diagnosis and Differential Diagnosis of Peritoneal Mesothelioma. Journal of Clinical Radiology, 2017(9): 1263–1267. https://doi.org/10.13437/j.cnki.jcr.2017.09.015

[2] Wen Z, Long L, Jiang M, et al., 2019, Multi-Phase Enhanced CT Findings and Pathological Basis of Localized Malignant Peritoneal Mesothelioma. Journal of Practical Radiology, 35(4): 576–579. https://doi.org/10.3969/j.issn.1002-1671.2019.04.016

[3] Wang Y, 2019, A Case of MR Manifestations of Pelvic Peritoneal Mesothelioma. Chinese Journal of Medical Imaging, 27(7): 559–560. https://doi.org/10.3969/j.issn.1005-5185.2019.07.019

[4] Li M, Ye C, Ji M, 2017, A Case of MR Manifestations of Pelvic Malignant Peritoneal Mesothelioma. Imaging Diagnosis and Interventional Radiology, 26(3): 244–245. https://doi.org/10.3969/j.issn.1005-8001.2017.03.015

[5] Song D, Dong J, Shi B, et al., 2022, A Case of CT Findings of Multicystic Peritoneal Mesothelioma Combined with Adenomatoid Tumor in the Mesenteric Area. Chinese Journal of Radiology, 56(4): 452–453. https://doi.org/10.3760/cma.j.cn112149-20210415-00377

Proceedings of Anticancer Research, 2024, Volume 8, Issue 2
http://ojs.bbwpublisher.com/index.php/PAR
ISSN Online: 2208-3553
ISSN Print: 2208-3545

The Therapeutic Effect of Biling Weitong Granules Combined with Oryz-Aspergillus Enzyme and Pancreatin Tablet on Reflux Esophagitis with Functional Dyspepsia

Yalan Chen[1†], Ruiyao Wang[2†], Na Zhao[3]*, Jie Liang[1]*

[1]Department of Gastroenterology, The Affiliated Hospital of Hebei University, Baoding 071000, China
[2]Department of Thoracic Surgery, The Affiliated Hospital of Hebei University, Baoding 071000, China
[3]Endoscopy Center, Department of Gastroenterology, The Affiliated Hospital of Hebei University, Baoding 071000, China
[†]*First authors:* Yalan Chen, ziweichen0000@126.com; Ruiyao Wang, baodingdaifu@163.com

***Corresponding authors:** Na Zhao, zhaonaguohui@163.com; Jie Liang, mutoutaozi@163.com

Abstract: *Objective:* To investigate the therapeutic effect of Biling Weitong Granules combined with oryz-aspergillus enzyme and pancreatin tablets on patients with reflux esophagitis with functional dyspepsia. *Methods:* Sixty patients diagnosed with reflux esophagitis with functional dyspepsia who were admitted to the Affiliated Hospital of Hebei University between June 2020 and June 2023 were selected and divided into two groups: the control group and the observation group, each consisting of 30 cases. The control group received oryz-aspergillus enzyme and pancreatin tablets only, while the observation group received Biling Weitong Granules in addition to the tablets. The clinical efficacy, Chinese medicine syndrome points, esophageal kinetic indexes, gastrointestinal hormone levels, and therapeutic safety of both groups were evaluated. *Results:* The total efficiency of the observation group reached 93.33%, significantly higher than the 73.33% of the control group ($P < 0.05$). After treatment, patients in the observation group exhibited significantly lower scores for Chinese medicine symptoms such as early satiety, belching, abdominal distension, abdominal pain, and loss of appetite compared to the control group ($P < 0.05$). Furthermore, the observation group showed significantly higher upper esophageal sphincter pressure, lower esophageal sphincter pressure, and distal esophageal contraction scores compared to the control group ($P < 0.05$). Additionally, levels of gastric motility hormone, vasoactive intestinal peptide, and gastrin were significantly higher in the observation group compared to the control group ($P < 0.05$). Throughout the treatment period, there was no significant difference in the incidence of adverse reactions between the two groups, indicating comparable safety of the two treatment modalities ($P > 0.05$). *Conclusion:* The combination of Biling Weitong Granules with oryz-aspergillus enzyme and pancreatin tablets demonstrates significant efficacy in the treatment of reflux esophagitis with functional dyspepsia, with a better safety profile. This finding warrants further clinical promotion.

Keywords: Biling Weitong Granules; Oryz-aspergillus enzyme and pancreatin tablets; Reflux esophagitis; Functional dyspepsia

Online publication: March 28, 2024

1. Introduction

Reflux esophagitis represents a prevalent digestive disorder characterized by symptoms such as retrosternal or epigastric pain, burning, and acidity, often accompanied by dyspeptic manifestations like belching, nausea, and vomiting. The condition typically arises from the reflux of gastric acid and bile into the esophagus, primarily affecting the esophageal sphincter and mucosa. Pathological changes, including mucosal inflammation, ulceration, and impaired sphincter function, contribute to a compromised esophageal anti-reflux barrier [1]. Diagnostic approaches for reflux esophagitis encompass endoscopy, 24-hour esophageal pH monitoring, and esophageal manometry. Treatment modalities involve medication, dietary adjustments, lifestyle modifications, and surgical interventions.

Oryz-aspergillus enzyme and pancreatin tablet, a medication commonly employed in reflux esophagitis management, combines oryz-aspergillus enzyme extracts with pancreatic enzymes, thereby enhancing gastrointestinal digestive function by supplementing necessary digestive enzymes [2]. Nevertheless, some patients may not achieve lasting relief solely with Western medicine, potentially experiencing disease recurrence. In the realm of Chinese medicine, the spleen and stomach play pivotal roles in digestion and absorption. Dysfunction in these organs leads to compromised digestive function and gastric qi reversal, contributing to reflux esophagitis symptoms. Chinese medical theory attributes the etiology of the disease to factors like liver qi stagnation, spleen deficiency, and disharmony between the spleen and stomach.

Treatment strategies in Chinese medicine often revolve around regulating the spleen and stomach, tonifying the qi and meridian, promoting qi circulation, and resolving qi stagnation. Biling Weitong Granules, a traditional Chinese medicine preparation, holds a venerable status in the treatment of gastroepidermal pain. It exhibits efficacy in promoting qi and blood circulation, harmonizing the stomach, and relieving pain, particularly effective against gastroepidermal pain induced by qi stagnation and blood stasis [3].

This study aims to administer Biling Weitong Granules in combination with oryz-aspergillus enzyme and pancreatin tablets to patients suffering from reflux esophagitis with functional dyspepsia, comprehensively evaluating its therapeutic efficacy.

2. Materials and methods

2.1. General information

Sixty cases of patients diagnosed with reflux esophagitis with functional dyspepsia were recruited from the Affiliated Hospital of Hebei University as research subjects and randomly allocated into two groups, each comprising 30 cases. Inclusion criteria were as follows: (1) age between 18 and 60 years old; (2) clear diagnosis of reflux esophagitis with functional dyspepsia; (3) absence of related treatment for at least three months or discontinued treatment; (4) willingness and ability to comply with study requirements and sign informed consent. Exclusion criteria included: (1) the presence of other serious digestive system diseases such as gastric ulcer or gastric cancer; (2) severe cardiovascular, liver, or kidney dysfunction; (3) pregnancy or lactation; (4) mental illness or cognitive disorders hindering effective study participation; (5) allergies to treatment regimen components including oryz-aspergillus enzyme and pancreatin tablets, Biling Weitong Granules, or other conditions.

2.2. Methods

The control group received treatment with oryz-aspergillus enzyme and pancreatin tablets (enteric-coated tablets) manufactured by Daiichi Sankyo Pharma GmbH, Germany. Each tablet contained 24 mg of mitomycin mycobacterial extract and 220 mg of pancreatic enzyme. Dosage involved oral administration, to be taken

during or after meals, one tablet three times daily.

The observation group underwent combined treatment with oryz-aspergillus enzyme and pancreatin tablets and Biling Weitong Granules (produced by Yangzijiang Pharmaceuticals, 5 g dissolved in boiled water, three times daily). The treatment regimen for oryz-aspergillus enzyme and pancreatin tablets enteric coated tablets was consistent with the control group.

The experiment spanned a duration of two weeks per treatment course, with a total of three treatment courses administered.

2.3. Observation indexes

2.3.1. Clinical efficacy observation indexes

(1) Obvious effect: Symptoms completely subside, with a decline of more than 80% in Chinese medicine symptoms points, and esophageal dynamics indexes return to normal levels.

(2) Effective: Symptoms show significant improvement, with a decrease of 30% to 80% in TCM evidence points and significant improvement in esophageal kinetic indexes.

(3) Ineffective: No significant improvement in symptoms, TCM evidence points, or esophageal kinetic indexes post-treatment.

2.3.2. TCM evidence points

A four-level scoring method is used to evaluate symptoms such as early satiety, abdominal distension, abdominal pain, and loss of appetite:

(1) 0 point: No relevant symptoms or very mild symptoms.

(2) 1 point: Mild symptoms with some impact on daily life but not severe.

(3) 2 points: Moderate symptoms significantly impacting daily life but still tolerable.

(4) 3 points: Severe symptoms greatly impact daily life and seriously interfere with normal functioning.

Scoring these symptoms provides insight into their severity and serves as a reference index for assessing treatment effectiveness.

2.3.3. Esophageal kinetic indexes

One day before and after each treatment course, the Solar GI type gastrointestinal kinetic examination system (Shanghai Hanfei Medical Devices Co., Ltd.) is employed to compare esophageal kinetic indexes. These indicators include:

(1) Upper esophageal sphincter pressure (UESP): Assessing the smoothness of food passage through the upper esophageal sphincter, which should have proper contraction and relaxation under normal conditions.

(2) Lower esophageal sphincter pressure (LESP): Evaluating the smoothness of food passage through the lower esophageal sphincter.

(3) Distal contractile integral (DCI): Reflecting the motor function of the esophagus, indicating the strength and frequency of distal esophageal contraction.

2.3.4. Gastrointestinal hormone indexes

Before and after treatment, fasting venous blood samples (3 mL) are collected and centrifuged using the TDL-SD-5B type laboratory high-speed centrifuge (Shanghai Anting Scientific Instrument Factory) to separate serum supernatant specimens. Enzyme-linked immunosorbent assay is then utilized to detect motilin (MTL), vasoactive intestinal peptide (VIP), and gastrin (GAS) levels. The PT-3502G automatic enzyme labeling

instrument (Beijing Putian Xinqiao Medical Equipment Company) is used for analysis.

(1) MTL: Mainly secreted by entero-endocrine (Mo) cells in the upper small intestine, regulating gastrointestinal motility.
(2) VIP: Secreted by neuroendocrine cells and neurons, promoting peristalsis and increasing gastrointestinal secretion.
(3) GAS: Mainly secreted by G cells in the lining of the stomach and upper small intestine, which can promote gastric acid secretion and gastric contraction and participate in the regulation of gastrointestinal motility.

2.4. Statistical methods

Measurement information is expressed as mean ± standard deviation (SD). Comparison between groups is conducted using the two-sample mean *t*-test or chi-squared test. Data analysis is performed using SPSS software, with significance considered at $P < 0.05$.

3. Results

3.1. Comparison of general information

As shown in **Table 1**, the difference between the two groups of patients' gender, age, average duration of disease, and average body mass index (BMI) data comparison was not statistically significant ($P > 0.05$).

Table 1. Comparison of general data of patients in two groups (mean ± SD)

Group	Gender		Mean age (years)	Mean duration of illness (month)	Mean BMI
	Male	Female			
Control group ($n = 30$)	16	14	43.61 ± 9.73	8.88 ± 2.89	23.16 ± 2.69
Observation group ($n = 30$)	15	15	42.52 ± 9.89	8.67 ± 2.86	23.14 ± 2.81
χ^2 / t	0.067		0.426	0.283	0.028
P	0.800		0.671	0.778	0.978

3.2. Comparison of clinical efficacy between the two groups

Table 2 shows that the observation group has a higher total effective rate ($n = 28$, 93.33%) as compared to the control group ($n = 22$, 77.33%, $P = 0.038$).

Table 2. Comparison of clinical efficacy between the two groups (n)

Group	Obvious effect	Effective	Ineffective	Total effective
Control group ($n = 30$)	13	9	8	22
Observation group ($n = 30$)	16	12	2	28
χ^2				4.320
P				0.038

3.3. Comparison of Chinese medicine symptoms points between the two groups

Before treatment, there was no difference in the TCM symptom scores of both groups ($P > 0.05$). However, after treatment, the TCM symptom points of the observation group were significantly lower than those of the control group ($P < 0.05$), as seen in **Table 3**.

Table 3. Comparison of TCM evidence points between the two groups before and after treatment (mean ± SD, points)

Group (*n*)	Early satiety		Bloating and abdominal pain		Loss of appetite	
	Before	After	Before	After	Before	After
Control group (*n* = 30)	2.57 ± 0.43	0.75 ± 0.16	2.48 ± 0.46	0.85 ± 0.23	2.47 ± 0.49	0.95 ± 0.26
Observation group (*n* = 30)	2.53 ± 0.45	0.65 ± 0.14	2.43 ± 0.48	0.71 ± 0.21	2.41 ± 0.48	0.72 ± 0.23
t	0.352	2.576	0.412	2.462	0.479	3.629
P	0.726	0.013	0.682	0.017	0.634	0.001

3.4. Comparison of esophageal kinetic indexes between the two groups

As shown in **Table 4**, there was no difference between the esophageal kinetic indexes of both groups before treatment ($P > 0.05$). After treatment, the esophageal kinetic indexes of the observation group were significantly higher than those of the control group ($P < 0.05$).

Table 4. Comparison of esophageal kinetic indexes between the two groups before and after treatment (mean ± SD)

Group (*n*)	UESP (mmHg)		LESP (mmHg)		DCI (mmHg/s/cm)	
	Before	After	Before	After	Before	After
Control group (*n* = 30)	35.67 ± 5.73	44.75 ± 5.46	7.68 ± 2.12	10.28 ± 3.13	269.45 ± 29.49	352.95 ± 41.81
Observation group (*n* = 30)	34.81 ± 5.45	49.81 ± 5.54	7.43 ± 2.18	13.95 ± 3.19	266.21 ± 29.48	387.41 ± 45.15
t	0.596	3.563	0.450	3.272	0.426	3.067
P	0.554	0.001	0.654	0.002	0.672	0.003

3.5. Comparison of gastrointestinal hormone levels between the two groups

Table 5 shows that there were no differences between the gastrointestinal hormone levels of both groups before treatment ($P > 0.05$). After treatment, the gastrointestinal hormone levels of the observation group were significantly higher than those of the control group ($P < 0.05$).

Table 5. Comparison of gastrointestinal hormone levels between the two groups before and after treatment (mean ± SD, ng/L)

Group (*n*)	MTL		VIP		GAS	
	Before	After	Before	After	Before	After
Control group (*n* = 30)	104.08 ± 12.13	173.75 ± 18.16	60.84 ± 6.45	95.06 ± 9.38	32.45 ± 5.44	48.25 ± 5.98
Observation group (*n* = 30)	105.53 ± 12.43	190.64 ± 17.28	59.23 ± 6.64	102.34 ± 11.39	32.41 ± 5.41	53.18 ± 5.97
t	0.457	3.690	0.953	2.702	0.029	2.742
P	0.649	0.001	0.345	0.009	0.977	0.008

3.6. Comparison of treatment safety between the two groups

The treatment safety of both groups showed no significant differences ($P = 0.754$), as shown in **Table 6**.

Table 6. Comparison of treatment safety between the two groups of patients (*n*)

Group (*n*)	Nausea and vomiting	Bloating and abdominal pain	Dry mouth	Rash	Total
Control group (*n* = 30)	3	2	1	1	7
Observation group (*n* = 30)	2	2	1	1	6
χ^2					0.098
P					0.754

4. Discussion

Reflux esophagitis, often accompanied by symptoms of functional dyspepsia such as gastric distension, pain, nausea, and vomiting, is commonly viewed through the realms of traditional Chinese medicine as a manifestation of disharmony in the liver-spleen relationship and spleen deficiency. These conditions lead to spleen and stomach qi imbalance, disrupting the spleen qi flow, triggering stomach qi stagnation, and exacerbating symptoms [4]. Poor dietary habits, such as skipping breakfast, overeating, or consuming spicy, high-fat, or high-sugar foods, further burden the spleen and stomach, worsening their function and potentially leading to spleen and stomach deficiency. Psychological stressors can also impact gastrointestinal function, aggravating symptoms like loss of spleen tonicity and gastrointestinal control.

Chinese medicine treatment strategies aim to address these imbalances by promoting liver detoxifying, spleen strengthening, stomach harmonization, and qi regulation [5]. Biling Weitong Granule, a traditional Chinese medicine formulation, contains ingredients including tailed pepper, Chinaberry, *Corydalis yanhusuo* vinegar, Rhubarb liquor, *Coptis chinensis*, and more, known for their ability to promote qi, relieve pain, strengthen the spleen, and harmonize the stomach [6]. This combination effectively clears heat, detoxify toxins, resolves phlegm, dispel dampness, relieve turbidity, activates blood circulation, eliminates qi stagnation, harmonizes the stomach, and alleviates pain [7,8], particularly beneficial for gastric pain and chronic gastritis.

In contrast, oryz-aspergillus enzyme and pancreatin tablet, a digestive medicine, alleviate dyspeptic symptoms by supplementing digestive enzymes, improving pancreatic function, and relieving bloating, stomach pain, nausea, and vomiting. However, there are varying opinions among Chinese medicine scholars regarding the etiology and treatment of functional dyspepsia: (1) Ye posited that the root cause of functional dyspepsia lies in spleen and stomach deficiency, exacerbated by dampness, phlegm, and stasis, which disrupt the organs' receptive and transporting functions. Treatment strategies should vary based on different stages of deficiency and solidity, emphasizing the traditional Chinese medicine principle of "qi transportation and adjustment" [9]. (2) Huang highlighted the impact of acquired dietary habits and emotional factors on functional dyspepsia. Impairment in the spleen and stomach's ability to receive and transport qi leads to imbalances, resulting in the manifestation of functional dyspepsia symptoms [10]. (3) Li proposed that the disease's pathogenesis stems from an imbalance in qi elevation within the Middle Jiao. Treatment focuses on four principles: regulating liver qi to promote elevation of the spleen and stomach qi; balancing cold and heat to regulate qi; harmonizing and transporting qi within the Middle Jiao for balance; and regulating lung qi to support spleen qi elevation and qi clearance [11].

In this study, 60 patients with reflux esophagitis and functional dyspepsia were randomly assigned into two groups: the control group receiving oryz-aspergillus enzyme and pancreatin tablets alone, and the observation group receiving additional Biling Weitong Granules. The combined treatment effectively improved symptoms, enhanced quality of life, and demonstrated safety and reliability without significant side effects. These promising outcomes suggest the potential for clinical application. Future research will delve deeper into the treatment mechanism of this combination therapy, aiming to provide more scientifically

sound and effective clinical interventions. Additionally, efforts will focus on improving patient quality of life and enhancing overall patient care.

Funding

Baoding Science and Technology Plan Project Management (2341ZF318)

Disclosure statement

The authors declare no conflict of interest.

References

[1] Li M, Zhang W, Guo L, et al., 2021, Efficacy and Safety of Vonoprazan versus PPIs in Treating Reflux Esophagitis: A Meta-Analysis. Chinese General Practice, 24(6): 712–717.

[2] Liu Z, Liang S, Qiu L, et al., 2019, A Randomized Controlled Study on the Treatment of Liver Cirrhosis with Reflux Esophagitis Using Oryz-Aspergillus Enzyme and Pancreatin Tablets. Modern Digestion & Intervention, 2019(A02): 2606–2607.

[3] Li M, Wang X, Niu M, et al., 2021, Efficacy of Rabeprazole and Moxapride Combined with Aspergillus Oryzae Trypsin in Treatment of Reflex Esophagitis with Functional Dyspepsia. Chinese Journal of New Drugs and Clinical Remedies, 2021(7): 515–519.

[4] Wang L-H, Wang F-L, Li J, et al., 2021, Thought of Syndrome Differentiation and Countermeasures in Chinese Medical Treatment of Functional Dyspepsia. China Journal of Traditional Chinese Medicine and Pharmacy, 36(9): 5368–5371.

[5] Qu Y-D, Wu S-S, Zhang N-Y, et al., 2022, Clinical Observation of Biling Weitong Granule in the Treatment of Functional Dyspepsia and Epigastric Pain Syndrome in College Students. World Journal of Integrated Traditional and Western Medicine, 17(1): 131–136. https://doi.org/10.13935/j.cnki.sjzx.220126

[6] Mao X, Guo S, Ni W, et al., 2020, Effects of Qizhi Weitong Granules on Gastric Sensitivity and Mental State of Functional Dyspepsia Model Rats. Journal of Traditional Chinese Medicine, 61(22): 1996–2003. https://doi.org/10.13288/j.11-2166/r.2020.22.016

[7] Bai Z, Gao Z, 2021, The Efficacy and Safety Observation of the Combination of Biling Weitong Granules and Pantoprazole Quadruple Therapy in the Treatment of Patients with Chronic Gastritis Complicated with *Helicobacter pylori* Infection. Guizhou Medical Journal, 45(11): 1716–1717.

[8] Hong S, Huang J, Xu S, 2021, Effect of Biling Weitong Granules Combined with Quadruple Therapy on Chronic Atrophic Gastritis with Positive *Helicobacter pylori* Infection. China Medical Herald, 18(29): 122–125.

[9] Wang Z, Ye B, 2019, Experience of Ye Bai's Application of Kaijinsan in the Treatment of Functional Dyspepsia. Journal of Traditional Chinese Medicine, 34(1): 30–32.

[10] Zhong Z, Huang J, Ye Z, et al., 2020, A Study on the Treatment Rules of Professor Huang Suiping's Functional Dyspepsia (FD) Based on Data Mining Technology. Lishizhen Medicine and Materia Medica Research, 2020(3): 753–755.

[11] Zhang H, Li J, 2020, Li Julin's Experience in Recovering Functional Dyspepsia Based on Recovery of Airlift. Journal of Sichuan of Traditional Chinese Medicine, 38(2): 4–7.

Proceedings of Anticancer Research, 2024, Volume 8, Issue 2
http://ojs.bbwpublisher.com/index.php/PAR
ISSN Online: 2208-3553
ISSN Print: 2208-3545

The Application Value of Ultrasound Imaging in the Differential Diagnosis of Benign and Malignant Breast Nodules of BI-RADS 3 and Above

Dongmei Chen*

Physical Examination Department, Baoding No. 1 Central Hospital, Baoding 071030, China

***Corresponding author:** Dongmei Chen, tjk5976676@163.com

Abstract: *Objective:* To explore the diagnostic value of ultrasound imaging for breast nodules of breast imaging-reporting and data system (BI-RADS) category 3 and above. *Methods:* From June 2021 to July 2022, 163 patients with breast nodules of BI-RADS 3 or above were selected as the research subjects. After pathological diagnosis, 24 cases were malignant breast nodules of BI-RADS 3 or above, while 139 cases were benign breast nodules of BI-RADS 3 or above. The diagnosis rate of malignant and benign breast nodules of BI-RADS 3 or above, including 95% CI, was observed and analyzed. *Results:* The malignant and benign detection rates of conventional ultrasound were 88.63% and 75.00%, respectively, and the malignant and benign detection rates of ultrasound imaging were 93.18% and 87.50%, respectively, with 95% CIs greater than 0.7. *Conclusion:* Ultrasound imaging can help improve the diagnostic accuracy of benign and malignant breast nodules of BI-RADS 3 and above and reduce the misdiagnosis rate.

Keywords: Ultrasound; Ultrasound imaging; Breast imaging-reporting and data system (BI-RADS) category 3 and above; Diagnosis

Online publication: March 28, 2024

1. Introduction

Benign breast diseases account for approximately 80% to 90% of breast cancers, among which nodules of breast imaging-reporting and data system (BI-RADS) category 3 and above are one of the important characteristics of breast cancer. However, as the number of nodules of BI-RADS 3 and above increases, ultrasonic examination is also facing more and more challenges, making it difficult for clinicians to judge whether the nodules are benign or malignant. Ultrasound radiomics is a new method that has emerged in recent years. It can use various imaging technologies, including radiomics, computer vision, artificial intelligence, etc., to extract bioinformatics features related to image features from massive images. Based on this, a discriminant model is established to predict the disease's development trend [1,2]. Ultrasound examination, as the main imaging examination method for breast diseases, has the advantages of simple operation, non-invasive, painless, and radiation-free, and is suitable for extensive clinical screening and early diagnosis. The BI-RADS classification

standard was developed by the American College of Radiology and is used to evaluate the likelihood of benign and malignant breast masses. BI-RADS 3 or above nodules indicate a higher possibility of malignancy and require further diagnosis. Ultrasound radiomics can extract many high-dimensional feature information from ultrasound images, including morphological features, hemodynamic features, etc. This information can reflect the nodule's internal structure and blood flow, thereby evaluating its benign and malignant nature. Classifying and identifying features through machine learning algorithms can improve the accuracy and reliability of benign and malignant nodules. In addition, ultrasound imaging can also comprehensively analyze the shape, edge, internal echo, calcification, etc., of breast masses and provide clinicians with a more comprehensive diagnostic basis based on clinical history, age, and other factors. Doctors can formulate more precise treatment plans based on the diagnostic results of ultrasound imaging and the patient's specific conditions. Currently, radiomics research has become one of the hot topics for scholars at home and abroad. This article aims to explore the value of ultrasound imaging in the differential diagnosis of BI-RADS 3 and above nodules to improve clinicians' ability to judge benign and malignant breast cancer and reduce its missed diagnosis and misdiagnosis rates.

2. Materials and methods

2.1. General information

A total of 163 patients with breast nodules of BI-RADS 3 or above in Baoding No.1 Central Hospital from June 2021 to July 2022 were selected as the research subjects. After pathological diagnosis, 24 of them were found to be malignant breast nodules of BI-RADS 3 or above nodules, of which 139 cases were benign breast nodules of BI-RADS 3 or above. There was no statistical difference in the general information of the two groups of patients. The entry criteria were that they were consistent with breast nodules of BI-RADS 3 or above and had no other comprehensive metabolic disease or mental illness. The exclusion criteria were patients with incomplete clinical data and other major diseases.

2.2. Method

2.2.1. Ultrasound imaging

Ultrasound radiomics diagnosis of breast nodules classified as BI-RADS 3 or above mainly involves the following steps: (1) Conducting an ultrasound examination of the breast to obtain ultrasound images; (2) Extracting features relevant to breast nodules from these images, such as morphological and hemodynamic features. These features can reflect the internal structure and blood flow of the nodules, aiding in determining their benign or malignant nature; (3) Among the extracted features, those significantly impacting benign-malignant judgment are selected, effectively reducing the number of features and improving diagnosis efficiency; (4) Appropriate machine learning algorithms, such as support vector machines, decision trees, or neural networks, are utilized to design classifiers for the extracted features and their corresponding benign and malignant nodules; (5) Known benign and malignant breast ultrasound image datasets are employed to train and verify the classifier, significantly enhancing its accuracy and reliability; (6) Based on the classifier's classification results, BI-RADS 3 and above are outputted along with the probability of benign and malignant nodules. This step furnishes doctors with an auxiliary diagnostic basis, aiding them in making more accurate diagnoses.

2.2.2. Ultrasound diagnosis

Ultrasound diagnosis was carried out using color Doppler flow imaging (CDFI) technology and Doppler blood flow perfusion imaging technology to diagnose breast nodules in BI-RADS 3 and above (including papillary,

cystic-solid nodules, and other types of breast nodules in BI-RADS 3 and above).

2.3. Observation indicators

The diagnosis rate of malignant and benign breast nodules of BI-RADS 3 and above, including 95% CI, is shown in **Figure 1**.

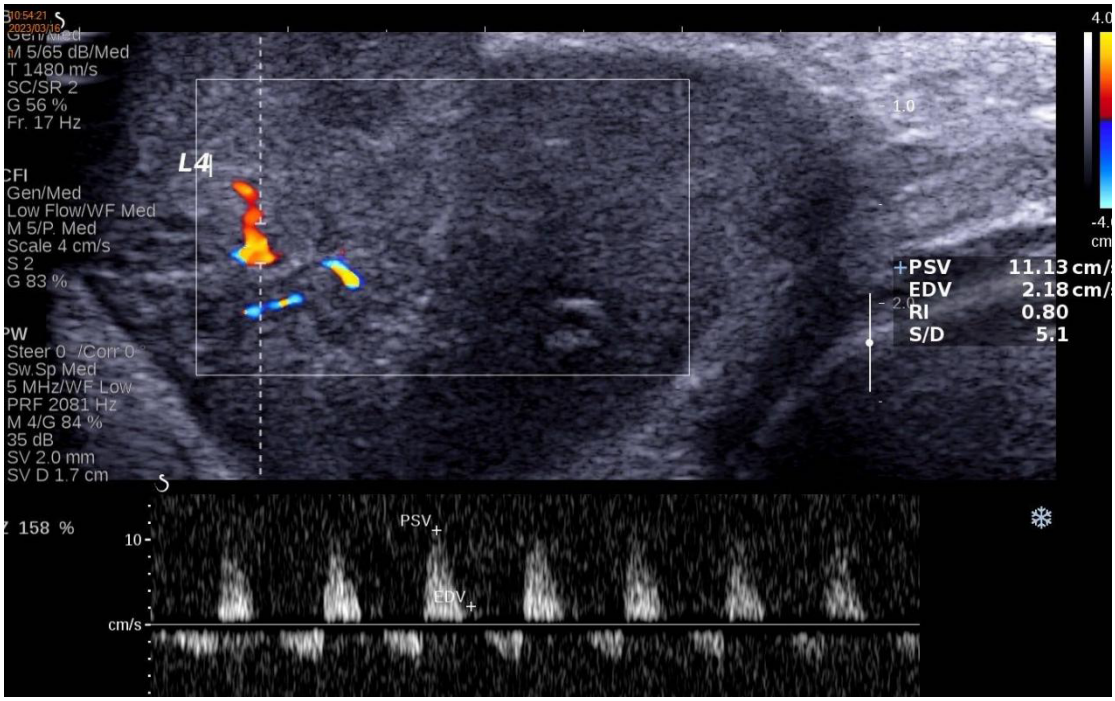

Figure 1. Superficial small organs: bilateral breasts + double axillary soft tissues and axillary veins

2.4. Statistical analysis

SPSS 22.0 statistical software was employed for data analysis. Data were expressed as either mean ± standard deviation (SD) or percentage. The *t*-test and the χ^2 test were utilized for data comparison. Statistical significance was indicated by $P < 0.05$.

3. Results

The patients were diagnosed by pathology, with 24 cases in the malignant group and 139 cases in the benign group. Conventional ultrasound's malignant and benign detection rates were 88.63% and 75.00%, respectively. The malignant and benign detection rates of ultrasound imaging were 93.18% and 87.50%, respectively, and 95% CI are all greater than 0.7, as shown in **Table 1**.

Table 1. Diagnostic performance of ultrasound imaging

Pathological results		Malignant (n = 24)	Benign (n = 139)	Accuracy	95% CI
Conventional ultrasound	Malignant	19	20	79.17%	0.862
	Benign	5	119	85.61%	0.791
Ultrasound imaging	Malignant	23	13	95.83%	0.901
	Benign	1	126	90.65%	0.842

4. Discussion

Breast nodules refer to tumors found during ultrasound examination. Nodules of BI-RADS 3 and above are often accompanied by varying degrees of calcification, which is a typical characteristic of breast cancer. Ultrasound examination has high sensitivity and specificity in the diagnosis of breast cancer and can help clinicians detect nodules early. In clinical work, ultrasonography is mainly used for the diagnosis and differential diagnosis of breast masses. However, in nodules of BI-RADS 3 and above, the sensitivity and specificity of ultrasonic examination are low. Su *et al*. analyzed 337 cases of BI-RADS 3 and above breast nodules. They found that the masses in the high ultrasound density group (0.73 ± 0.19) and the low ultrasound density group (0.58 ± 0.11) had a higher ultrasound diagnosis compliance rate and diagnosis sensitivity. In comparison, the low ultrasound density group (0.56 ± 0.07) and the high ultrasound density group (0.58 ± 0.11) have lower diagnostic coincidence rates and diagnostic sensitivity. Still, it should be noted that the high ultrasound density group and the low ultrasound density group are not independent of each other but influence each other [3]. In addition, nodules of BI-RADS 3 and above usually have a higher risk of malignancy.

The development of radiomics can be traced back to the 1980s. There have been many reports on its application in breast cancer, but most of them are based on pathology reports or clinical data. In recent years, more and more radiomics research has been conducted on breast tumors, and it has gradually begun to be integrated with clinical practice. Currently, there are two main methods for extracting radiomic features: based on computer vision technology and artificial neural network technology. There are two main types of methods based on computer vision technology. One is to segment the image and perform feature analysis based on feature selection and extraction algorithms. The main methods include the fuzzy C-means (FCM) algorithm, principal component analysis (PCA), and neural network methods. The other type uses a gray level co-occurrent matrix (GLCM) on the image to extract texture and color features to build a classification model. The former is more intuitive in extracting features but is time-consuming and laborious; the latter is more effective in extracting features but requires professional knowledge. Currently, methods based on computer vision technology are widely used in ultrasound imaging. Guo's research based on ultrasound imaging found that ultrasound imaging can improve the ability to identify breast cancer, with a sensitivity and specificity of 80% and 85%, respectively [4]. Therefore, research based on ultrasound imaging can improve the ability to identify breast tumors.

In this study, patients were diagnosed pathologically, with 24 cases in the malignant group and 139 cases in the benign group. The malignant and benign detection rates of conventional ultrasound were 88.63% and 75.00%, respectively, and the malignant and benign detection rates of ultrasound imaging were 93.18% and 87.50%, respectively, and the 95% CIs were greater than 0.7. Studies have shown that radiomics is an important part of big data analysis. Ultrasound radiomics can quantify and mine structural features in images to identify benign and malignant breast nodules. Differential diagnosis of knots provides more effective information. This is mainly because when ultrasound imaging studies diagnose BI-RADS 3 and above nodules, multiple technologies are combined, including traditional ultrasound imaging technology, computer vision, artificial intelligence, etc. Current research by Qi [5], Wang [6], Wang [7], Mira [8], Li [9], and Li [10] have shown that ultrasound based on multi-modal fusion radiomics analysis can improve the accuracy of diagnosis of benign and malignant nodules of BI-RADS 3 and above; ultrasound radiomics analysis based on image segmentation method can improve the accuracy of diagnosis of benign and malignant nodules of BI-RADS 3 and above; based on image ultrasound radiomics analysis using feature extraction methods can improve the accuracy of differential diagnosis of benign and malignant nodules of BI-RADS 3 and above. Shi [11], Qu [12], Huang [13], and other researchers have found that multi-modal fusion-based ultrasound image radiomics analysis can improve

the accuracy of benign and malignant diagnosis of BI-RADS 3 and above nodules. Compared with conventional ultrasound image segmentation methods, its prediction accuracy is higher (AUC = 0.842).

Ultrasound, as a non-invasive, simple, and economical examination method, can detect small breast lesions and plays an important role in the early diagnosis and differential diagnosis of breast tumors [14]. However, due to the increase in the number of BI-RADS 3 and above nodules and the varying sizes of breast lesions, the difficulty in the differential diagnosis of benign and malignant breast cancer has increased, making it difficult for clinicians to make judgments [15]. Ultrasound radiomics is a medical data mining method based on ultrasound images. By mining the bioinformatics features related to the benign and malignant breasts in the images, the non-structural information in the images is converted into structured data, thereby assisting clinicians in making correct decisions [16].

In summary, radiomics is a new research method that can identify benign and malignant nodules of BI-RADS 3 and above. However, there are still some problems in current radiomics research, such as the lack of multi-center, large-sample studies. The quality control and analysis methods of research and radiomics are not uniform. Ultrasound imaging mainly utilizes technologies such as computer vision and artificial intelligence, which have the advantages of convenience and speed and do not require pathological diagnosis. With the continuous development of radiomics technology, radiomics will play a greater role in clinical applications. They can be applied to different benign and malignant breast diseases to diagnose them and guide clinical treatment differentially. However, radiomics research is still in its infancy, and more research is needed to verify its diagnostic value. It is believed that as the research of radiomics in the diagnosis of breast cancer gradually deepens, radiomics will play a greater role in the differential diagnosis of benign and malignant breast diseases.

Disclosure statement

The author declares no conflict of interest.

References

[1] Shi L, Zhong L, Ma F, et al., 2023, The Value of Peritumoral Ultrasound Imaging in the Differential Diagnosis of Benign and Malignant Breast Nodules. Oncology Imaging, 32(6): 485–491.

[2] Du Y, Feng X, Wu M, et al., 2023, Constructing a Joint Model Based on Ultrasound Imaging to Predict the Efficacy of Neoadjuvant Chemotherapy for Breast Cancer. Chinese Journal of Ultrasound in Medicine, 39(12): 1353–1356.

[3] Su L, Zhou M, Li Y, et al., 2023, The Application Value of Ultrasound Imaging in the Differential Diagnosis of Benign and Malignant Breast Nodules of BI-RADS 3 and Above. Journal of Bengbu Medical College, 48(8): 1101–1104.

[4] Guo S, 2023, Research on Multi-Regional Elastography and Radiomics Diagnosis of Breast Cancer Based on Ultrasound Images, thesis, Nanchang University.

[5] Qi X, 2023, Research on Breast Cancer Lymph Node Metastasis Prediction Based on Multi-Parameter MRI Imaging, thesis, Shanxi Medical University.

[6] Wang Z, 2023, Research on the Clinical Value of FFDM-Based Radiomics Model in Identifying Benign and Malignant BI-RADS 4 Lesions, thesis, Shanxi Medical University.

[7] Wang H, 2023, Research on the Diagnosis and Metastasis of Breast Cancer and Prediction of HER2 Status Using ABVS Ultrasound Imaging, thesis, Lanzhou University.

[8] Mira Y, 2023, The Value of Ultrasound Imaging and Nomogram Model in Distinguishing Benign and Malignant BI-RADS 4A Irregular Breast Masses, thesis, Xinjiang Medical University.

[9] Li C, Chen C, 2023, Research Progress in Applying Ultrasound Imaging in Breast Tumors. Imaging Research and Medical Applications, 7(5): 5–7.

[10] Li Q, 2022, Research on Building a Prediction Model for Benign and Malignant Breast Tumors Based on Ultrasound Imaging, thesis, Bengbu Medical College.

[11] Shi S, 2022, The Value of Differentiating Benign and Malignant Breast Nodules Based on Ultrasound Imaging Logistic Regression Model, thesis, Jinzhou Medical University.

[12] Qu N, 2021, Study on the Prediction of Benign and Malignant Breast Lesions and Axillary Lymph Node Status of Breast Cancer Using Dynamic Enhanced MRI and Radiomics, thesis, China Medical University.

[13] Huang J, 2021, Research on the Value of Ultrasound Imaging in the Differential Diagnosis of Breast Phyllodes Tumors and Fibroadenomas, thesis, Guangxi Medical University.

[14] Xiao R, 2021, The Value of Radiomics Based on Gray-Scale Ultrasound in Predicting Benign and Malignant Breast Tumors, thesis, Anhui Medical University.

[15] Shi L, 2020, Diagnostic Value of Strain Elastography, Automated Breast Full-Volume Scanning Imaging, and Radiomics for Breast BI-RADS 4 Lesions, thesis, Suzhou University.

[16] Jiang Q, Guo J, 2020, Research Progress of Ultrasound Imaging in Breast Cancer. Chinese Journal of Medical Ultrasound (Electronic Edition), 17(11): 1145–1148.

Proceedings of Anticancer Research, 2024, Volume 8, Issue 2
http://ojs.bbwpublisher.com/index.php/PAR
ISSN Online: 2208-3553
ISSN Print: 2208-3545

Effect of Sequential Early Enteral Nutrition on Postoperative Rehabilitation and Complications in Gastric Cancer Patients

Dongchou Han[1], Qiya Feng[2], Yingmei Fu[2], Feijian Zhang[2], Dazhen Chen[2], Junmei Wu[1]*

[1]The First Affiliated Hospital of Hainan Medical University, Haikou 571000, China
[2]Hainan Medical University, Haikou 571000, China

***Corresponding author:** Junmei Wu, dongye187@tom.com

Abstract: *Objective:* To analyze the effect of sequential early enteral nutrition in patients with gastric cancer after surgery. *Methods:* A total of 139 gastric cancer patients, treated between October 2021 and October 2023, were randomly selected and divided into two groups: Group A (68 cases, receiving early enteral nutrition) and Group B (71 cases, receiving sequential early enteral nutrition), using computer randomization. The effects of the interventions on both groups were compared. *Results:* Seven days post-operation, the levels of nutritional indicators in Group B were significantly higher than those in Group A ($P < 0.05$). Group B showed significantly better levels of inflammatory factors and immune factors compared to Group A seven days post-operation ($P < 0.05$). The postoperative complication rate in Group B was 4.23%, significantly lower than that in Group A, which was 16.18% ($\chi^2 = 5.477$, $P = 0.019$). *Conclusion:* The utilization of sequential early enteral nutrition in gastric cancer patients after surgery demonstrated notable improvements in nutritional status and inflammation markers, along with enhanced immunity, effectively reducing postoperative complications.

Keywords: Sequential early enteral nutrition; Gastric cancer; Postoperative rehabilitation treatment; Complication rate

Online publication: March 28, 2024

1. Introduction

The proportion of gastric cancer patients is relatively high among those with digestive system tumors. In recent years, not only has the number of gastric cancer patients shown an upward trend, but they have also become younger. Due to the nonspecificity of early clinical symptoms of gastric cancer, most patients are diagnosed in the middle and late stages [1].

Currently, gastric cancer is primarily treated through surgery, wherein tumor tissue is removed to control disease progression and reduce metastasis rates. However, the surgical procedure itself inflicts considerable damage on the body. Post-operation, the body enters a high catabolic state, reducing metabolism and increasing the risk of malnutrition [2]. Early postoperative enteral nutrition (EEN) is a commonly employed nutritional

support method for gastric cancer surgery patients. It can mitigate malnutrition incidence and shorten postoperative recovery time. Nevertheless, gastrointestinal dysfunction is prevalent in early postoperative gastric cancer patients, with EEN often leading to adverse symptoms such as abdominal pain and diarrhea [3].

Sequential early enteral nutrition (SEEN) represents a novel EEN approach. Clinicians conduct a comprehensive analysis of the patient's condition and digestive tract function, administering amino acids, peptides, and other substances in the early postoperative period, gradually transitioning to whole protein infusion. This approach not only provides adequate nutrients but aids in restoring normal gastrointestinal functions. Furthermore, incrementally increasing nutrient dosage and infusion rate promotes intestinal peristalsis and expedites the return to normal digestive tract function. Thus, SEEN's nutritional support method aligns more closely with human nutritional absorption rules and facilitates postoperative recovery while effectively reducing gastrointestinal intolerance incidence [4]. This study examines the effect of postoperative SEEN use in gastric cancer patients.

2. Materials and methods

2.1. General information

A total of 139 cases were randomly selected from gastric cancer patients treated between October 2021 and October 2023 and divided into groups using a computer randomization method. Group A comprised 68 cases with an age range of 34 to 75 years, with an average age of 59.48 ± 5.53 years and weights ranging from 45.48 to 87.53 kg, with a mean weight of 63.12 ± 6.79 kg. Thirty-seven cases were classified as stage II and 31 as stage III. Surgical methods included subtotal gastrectomy with RY anastomosis in 36 cases and total gastrectomy with RY anastomosis in 32 cases, with an average operation time of 230.12 ± 69.48 min. The gender distribution was 35 males and 33 females. Group B consisted of 71 cases, with ages ranging from 32 to 78 years and an average age of 59.12 ± 5.47 years, with weights ranging from 45.59 to 87.12 kg and a mean weight of 63.57 ± 6.84 kg. Thirty-eight cases were classified as stage II and 33 as stage III. Surgical methods included subtotal gastrectomy with RY anastomosis in 40 cases and total gastrectomy with RY anastomosis in 31 cases, with an average operation time of 230.84 ± 69.56 min. The gender distribution was 41 males and 30 females. Comparison of general data showed no significant differences ($P > 0.05$).

Inclusion criteria: (1) Patients diagnosed with gastric cancer and meeting indications for surgical treatment; (2) Patients with no history of chemotherapy; (3) Patients with no symptoms of malnutrition before surgery; (4) Patients who did not receive nutritional support or use exogenous albumin preparations before surgery; (5) Complete data and informed consent of patients.

Exclusion criteria: (1) Patients diagnosed with malnutrition before surgery; (2) Patients with severe dysfunction of major organs; (3) Patients with contraindications to enteral nutrition before surgery (intestinal obstruction, intestinal ischemia, etc.); (4) Patients with metastatic cancer lesions; (5) Patients with mental disorders.

2.2. Methods

Group A adopted EEN. Post-operation, 250 mL of glucose injection (5%) was administered through the nasoenteral feeding tube at a rate of 20 mL/h 12 hours after surgery; 500 mL of glucosamine was injected at a rate of 20–30 mL/h 24 hours after surgery; from 2 to 5 days post-operation, the amount of injected nutrients was adjusted according to the patient's needs.

Group B adopted SEEN. Twelve hours after surgery, 250 mL of glucose injection (5%) was administered through the nasoenteral nutrition tube at a rate of 20 mL/h; 24 hours after surgery, when the patient's vital signs

were stable, amino acid enteral nutrition was infused at a rate of 20–30 mL/h (density 1 kcal/mL); 48 hours post-surgery, 600 mL Vivonex was infused at a rate of 40–50 mL/h; 72 hours post-surgery, 300 mL Vivonex and 500 mL short peptide enteral nutrition suspension were infused at a rate of 60–80 mL/h (density 1 kcal/mL); 4 days post-surgery, 1,000 mL of Peptison was infused at a rate of 80–100 mL/h; 5 days post-surgery, 1,000 mL of whole protein enteral nutrition was infused at 80–100 mL/h (density 1 kcal/mL).

2.3. Indicator observation

(1) Nutritional indicators: Seven days post-surgery, 5 mL of venous blood was collected, and the immunoturbidimetric method was used to detect levels of albumin (ALB) and prealbumin (PA). Hemoglobin (Hb) and total protein (TP) levels were also measured.

(2) Inflammatory factors and immune factor indicators: Seven days post-surgery, 5 mL of fasting peripheral venous blood was centrifuged at a speed of 3000 r/min for 15 minutes in the morning, with a centrifugal radius of 10 cm. The double-antibody sandwich enzyme-linked immunosorbent assay (ELISA) was utilized to measure levels of C-reactive protein (CRP) and interleukin-6 levels (IL-6) in the upper serum. An immunoturbidimetric assay was performed to assess immunoglobulin G (IgG) and immunoglobulin M (IgM) in 3 mL of fasting venous blood.

(3) Incidence of postoperative complications: The postoperative complication rate was calculated using the formula Postoperative complication rate = (Abdominal distension and diarrhea + Incision infection + Reflux esophagitis) / Total number of cases × 100%.

2.4. Statistical analysis

The data were processed using SPSS 25.0 software. Measurement data are presented as mean ± standard deviation (SD), while enumeration data are presented as %. The *t*-test and χ^2 test were applied for analysis, with statistical significance set at $P < 0.05$.

3. Results

3.1. Nutritional indicators

Table 1 shows that the ALB, PA, Hb, and TP levels in Group B were significantly higher than those in Group A 7 days after surgery ($P < 0.05$).

Table 1. Comparison of nutritional indicators (mean ± SD)

Group	*n*	ALB (g/L)	PA (ng/L)	Hb (g/L)	TP (g/L)
Group B	71	39.82 ± 2.53	182.53 ± 18.64	119.23 ± 8.46	64.92 ± 2.41
Group A	68	38.54 ± 2.46	160.23 ± 16.72	114.13 ± 9.15	63.15 ± 4.26
t	-	3.022	7.413	3.408	3.031
P	-	0.003	0.000	0.000	0.002

3.2. Inflammatory factors and immune factor indicators

As shown in **Table 2**, the CRP, IL-6, IgG, and IgM of Group B were significantly better than those in Group A 7 days after operation ($P < 0.05$).

Table 2. Comparison of inflammatory factors and immune factor indicators (mean ± SD)

Group	*n*	CRP (mg/L)	IL-6 (ng/L)	IgG (g/L)	IgM (g/L)
Group B	71	24.15 ± 2.37	31.53 ± 12.67	9.92 ± 0.85	0.96 ± 0.15
Group A	68	45.68 ± 20.12	56.31 ± 20.46	8.84 ± 0.82	0.83 ± 0.18
t	-	7.635	12.104	7.618	4.633
P	-	0.000	0.000	0.000	0.000

3.3. Incidence of postoperative complications

The postoperative complication rate in Group B was 4.23%, significantly lower than that in Group A, which was 16.18% ($P < 0.05$), as seen in **Table 3**.

Table 3. Comparison of postoperative complications incidence

Group	*n*	Abdominal distension and diarrhea	Incision infection	Reflux esophagitis	Postoperative complication rate
Group B	71	2	0	1	4.23%
Group A	68	5	3	3	16.18%
χ^2	-				5.477
P	-				0.019

4. Discussion

Gastric cancer constitutes a significant proportion of digestive system tumors and poses a considerable mortality risk. Presently, surgical intervention remains the primary clinical approach for treating gastric cancer patients. However, surgery inflicts substantial bodily damage, coupled with metabolic abnormalities and ongoing tumor cell proliferation, leading to heightened energy demands and increased postoperative complications. The risk of malnutrition escalates accordingly. Postoperative malnutrition in gastric cancer patients predominantly stems from the high catabolic state post-surgery, diminished gastric motility, reduced gastrointestinal secretions, and intolerance of protein preparations by residual gastric tissue and intestinal mucosa in the short term [5]. Malnutrition onset significantly escalates postoperative complication rates and mortality in gastric cancer patients. Hence, early postoperative nutritional support for gastric cancer patients is imperative [6]. Gastrointestinal motility function typically restores within 1–2 days post-surgery, while small intestinal motility, digestion, and absorption functions return within 6–8 hours post-surgery. Consequently, providing nutritional support to gastric cancer patients soon after surgery is deemed highly safe.

Enteral nutritional support currently serves as the primary method for postoperative nutritional supplementation in surgical patients. It not only furnishes the necessary nutrients for physical recovery but also safeguards intestinal mucosa structure, preserving cell integrity. Additionally, postoperative nutritional support accelerates intestinal immune and mechanical function restoration, increases bile secretion, enhances excretion rates, and safeguards liver function. Timely postoperative enteral nutritional support replenishes glutamine and dietary fiber essential for normal physiological activities, thus mitigating malnutrition incidence or ameliorating symptoms. With the advent of rapid surgical recovery, clinical studies corroborate that promptly initiating nutritional supplementation post-surgery effectively reduces hospitalization duration and enhances prognosis.

Currently, EEN predominates in clinical practice for postoperative gastric cancer patients. Although EEN

improves patients' nutritional status, its frequent use in a single dosage form results in high intolerance rates, hindering patients' postoperative recovery [7]. To enhance postoperative nutritional status in gastric cancer patients and diminish intolerance rates, SEEN emerged as a modified nutritional support method based on EEN. This study implemented SEEN for patients in Group B and compared its efficacy with that of patients in Group A receiving EEN. Results indicated that nutritional indicators, inflammatory factors, and immune factor indicators were comparable between the two groups one day pre-surgery ($P > 0.05$). However, Group B exhibited superior indicators compared to Group A ($P < 0.05$). Furthermore, the incidence of postoperative complications in Group B was significantly lower than that in Group A ($P < 0.05$), affirming the benefits of SEEN in postoperative gastrointestinal function restoration, nutritional status improvement, inflammation reduction, and immunity enhancement.

Clinical evaluation of nutritional status predominantly relies on indicators such as ALB and PA. Post-surgery, gastric cancer patients experience heightened catabolism, leading to declining levels of these nutritional indicators. Both EEN and SEEN particularly ameliorate patients' nutritional status post-gastric cancer surgery. SEEN, however, demonstrates a superior efficacy in nutritional status improvement, likely attributed to the incomplete recovery of gastrointestinal absorptive capacity 24–48 hours post-surgery. During this period, intestinal epithelial cells are not able to absorb cellulose effectively [8]. SEEN addresses this by providing Vivonex, which bypasses digestion and better meets gastrointestinal needs within 48 hours post-surgery, facilitating optimal nutrient absorption [9]. Gastric cancer patients typically regain colon function 72 hours post-surgery, allowing for the administration of short peptides that are easily digested and absorbed. These peptides not only provide absorbable nutrients but also offer comprehensive nutrition for subsequent gastrointestinal absorption. This establishes a favorable foundation for gastrointestinal function recovery and augments postoperative nutritional status.

Surgical trauma incites inflammatory reactions and compromises immune function post-surgery in gastric cancer patients. Sole administration of EEN heightens the risk of feeding intolerance symptoms like abdominal pain and bloating, resulting in discontinuation of nutritional support, counterproductive to postoperative recovery. SEEN, by tailoring enteral nutrition preparations to patients' evolving gastrointestinal function recovery post-surgery, minimizes intolerance incidence, thereby fostering not only recovery of gastrointestinal function and nutritional status but also enhancing inflammation and immunity [10]. By furnishing adequate nutrients, SEEN ensures the immune system receives sufficient energy support, facilitating mucosal barrier repair damaged during anesthesia and surgery. This prompts intestinal mucosa repair and regeneration, reinstates immune system function, and ultimately reduces postoperative complication incidence.

In conclusion, SEEN implementation post-gastric cancer surgery enhances nutritional status, inflammation, and immunity, and effectively mitigates postoperative complications.

Disclosure statement

The authors declare no conflict of interest.

References

[1] Bian X, Han F, Wang L, et al., 2020, Comparison of the Predictive Effects of Three Different Enteral Nutrition Support Programs on Gastrectomy Patients for Gastric Cancer. Abdominal Surgery, 33(1): 42–47.

[2] Liu Y, Ge L, Yang J, et al., 2023, The Impact of Staged Nursing Intervention Based on the Concept of Rapid Recovery Surgery Combined with Sequential EEN and Rehabilitation Exercise on the Prognosis of Gastric Cancer

Patients. Journal of Naval Medicine, 44(6): 646–648.

[3] Liu C, Peng H, 2021, Research on the Effect of Early Sequential Enteral Nutrition Support on Nutritional Support for Patients after Subtotal Gastrectomy for Gastric Cancer. Contemporary Nurse (First Month), 28(10): 74–77.

[4] Li X, 2019, Application Effect of Sequential Early Enteral Nutrition in Postoperative Rehabilitation Treatment of Gastric Cancer Patients. World Latest Medical Information Abstracts, 19(81): 7–8 + 10.

[5] Ji H, Liu C, Wang S, et al., 2023, Effects of Bifidobacterium Triple Live Bacteria Combined with Sequential Early Enteral Nutrition on Immune Inflammation Indicators and Body Fat Metabolism Levels in Patients after Gastric Cancer Surgery. Journal of Bengbu Medical College, 48(5): 664–668.

[6] Yang F, 2022, Discussion on the Impact of Sequential Early Enteral Nutrition on the Rehabilitation Effect of Patients after Radical Resection of Gastric Cancer. Reflexology and Rehabilitation Medicine, 3(10): 140–142 + 146.

[7] Wang R, Zan J, He C, et al., 2019, The Role of Sequential Early Enteral Nutrition in Treating Patients with Moderately Severe Acute Pancreatitis. Medical Information, 32(23): 89–92.

[8] Xu J, Liu X, Huang S, et al., 2021, Comparative Study on the Clinical Efficacy of Sequential and Non-Sequential Early Enteral Nutrition in Patients with Postoperative Esophageal Cancer. Oncology Pharmacy, 11(6): 763–768.

[9] He C, Zan J, Song K, et al., 2020, Observation on the Effect of Early Sequential Enteral Nutrition Support after Upper Gastrointestinal Perforation. Journal of the People's Liberation Army Medical College, 41(9): 901–904.

[10] Wang X, Xu Q, Chen L, et al., 2013, Clinical Effect and Health Economics Evaluation of Sequential Early Enteral Nutrition Support after Gastric Cancer Surgery. Parenteral and Enteral Nutrition, 20(6): 348–352.

Proceedings of Anticancer Research, 2024, Volume 8, Issue 2
http://ojs.bbwpublisher.com/index.php/PAR
ISSN Online: 2208-3553
ISSN Print: 2208-3545

EGFR Mutation and FHIT Methylation: Inverse Relationship in Patients with Lung Adenocarcinoma and Tuberculosis

Mireguli Abudureheman, Xiuyou Yan*, Baidurula Ainitu

Department of Oncology, Eighth Affiliated Hospital of Xinjiang Medical University. No. 100, North Lane 1, East Kashi Road, Xinshi District, Urumqi 86830001, Xinjiang, China.

***Corresponding author:** Xiuyou Yan, 18599031019@163.com

Abstract: *Objective:* To investigate the genetic correlations between epithelial growth factor receptor (EGFR) mutation and FHIT methylation in patients diagnosed with lung adenocarcinoma (AC) and pulmonary tuberculosis (TB). *Methods:* The presence of EGFR mutations and the methylation status of the FHIT gene in patients presenting with AC and TB were analyzed. The correlation between TB status and the observed genetic and epigenetic variations was also examined. *Results:* Among the 90 patients included in the study, 38 exhibited EGFR mutations (14 among those with TB and 24 among those without TB), while 29 exhibited FHIT myelination (19 among those with TB and 10 among those without TB). Furthermore, the protein expression levels of EGFR and FHIT were significantly higher in patients diagnosed solely with AC compared to those presenting with both AC and TB. A robust inverse correlation was identified between TB status and the frequency of EGFR mutation ($P < 0.001$). Moreover, significant associations were observed between TB status and FHIT methylation ($P < 0.01$). *Conclusion:* The findings suggest a correlation between TB and the prevalence of EGFR mutation and FHIT methylation in the pathogenesis of AC.

Keywords: Lung cancer; Adenocarcinoma (AC); Tuberculosis (TB); Epithelial growth factor receptor (EGFR); Fragile histidine triad (FHIT)

Online publication: March 28, 2024

1. Introduction

In many countries, lung cancer remains the primary cause of cancer-related deaths. Despite advancements in detection and treatment, the five-year survival rate remains below 15%. China, particularly affected, exhibits a high incidence of malignant tumors, with lung cancer contributing to a significant portion, resulting in approximately 781,000 deaths annually. In Xinjiang, the incidence of lung cancer stands at 17.70 per 100,000 individuals, aligning with the national average [1,2]. Lung cancer is broadly categorized into two histological types: small cell lung carcinoma (SCLC) and non-small cell lung carcinoma (NSCLC), with adenocarcinoma (AC) being the predominant subtype within NSCLC, with its prevalence steadily increasing.

According to the World Health Organization, tuberculosis (TB) remains a significant global health concern, with 10.4 million reported cases in 2016, leading to 1.67 million deaths, including 600,000 cases of multidrug-resistant TB. In China, the incidence was 68 cases per 100,000, resulting in 38,000 fatalities, with a documented rate of multidrug-resistant TB cases at 6.6%. Xinjiang province exhibits the highest incidence nationwide, estimated at 181.42 per 100,000 individuals annually. Approximately 2%–8% of TB cases are complicated by lung cancer [3-5], with TB serving as a strong risk factor for its development. Recent molecular epidemiological studies have started to elucidate the precise gene mutations associated with the progression of cancer in pulmonary TB cases [6,7].

Furthermore, investigations into the connection between TB and DNA methylation have been underway, spurred by findings in animal studies linking DNA methylation and carcinogenesis [8-10]. Carcinomas commonly involve genetic and epigenetic alterations. Previous studies have indicated a prevalence of epithelial growth factor receptor (EFGR) mutations in AC patients [11], while genes associated with TB have shown methylation due to epigenetic modifications. However, data on distinct methylation patterns in AC based on TB status remain limited.

Lung AC harboring mutated EFGR has exhibited significant responses to tyrosine kinase inhibitors (TKIs), indicating a notable survival advantage. The efficacy of TKIs in tumor treatment largely hinges on the status of both EGFR mutation and gene amplification. This study aims to analyze lung AC with or without TB for EGFR mutations and the methylation status of the TB-specific FHIT tumor suppressor gene. The investigation seeks to elucidate the correlation between TB status and the association between genetic mutations and epigenetic alterations in lung AC.

2. Methods

The research comprised the examination of the study population and the subsequent DNA extraction process. A total of 90 lung specimens were acquired through surgical resection following histological diagnosis at the Eighth Affiliated Hospital of Xinjiang Medical University, with participants providing written informed consent. These samples were preserved at -80˚C until further analysis. All patients had not received any chemo- or radiotherapy before the surgery to prevent any changes in cell-cycle proteins due to DNA damage.

2.1. Pulmonary tuberculosis group (Group A)

Between 2020 and 2022, 30 pulmonary TB tissues were collected and confirmed pathologically. The patients, middle-aged or elderly individuals diagnosed with pulmonary TB, had undergone surgical resection or bronchoscopy at the Chest Hospital of Xinjiang Autonomous Region. Among the 30 patients (17 males and 13 females), aged between 45 and 75, with a mean age of 59.8, 4 were newly diagnosed cases, while 26 had received prior treatment. Acid-fast smear test results were positive for 8 cases, while the remaining 22 tested negative.

2.2. Adenocarcinoma group (Group B)

From 2020 to 2022, 30 lung cancer tissues from patients confirmed pathologically and treated with either surgical resection or bronchoscopy at Xinjiang Autonomous Region's Chest Hospital were obtained. The sample consisted of 18 males and 12 females, with an average age of 60.9 years (ranging from 45 to 80 years). Classification based on the 2015 World Health Organization (WHO) Lung Cancer Classification identified 9 stage I+II cases and 21 stage III+IV cases following the 8th edition of UICC's lung cancer staging guidelines (2017). Tumor diameters were ≤ 3 cm for 11 cases and ≥ 3 cm for the remaining 19 cases.

2.3. Tuberculosis plus lung adenocarcinoma group (Group C)

From 2020 to 2022, 30 tissues pathologically verified to have pulmonary TB and lung AC in patients who underwent surgical resection or bronchoscopy at the Chest Hospital of Xinjiang Autonomous Region were gathered. Inclusion criteria encompassed middle-aged or elderly patients meeting diagnostic criteria for both pulmonary TB and lung cancer, or those with a history of TB. The group, diverse in histological types, grades, and pathological stages, comprised 14 males and 16 females, with an average age of 60.5 years (range: 45–84 years). In 24 cases, TB and tumor were on the same side of the lungs, while 6 cases exhibited TB and tumor on opposite lungs. Exclusion criteria included recent myocardial infarction, unstable angina, severe organ complications or failures, Alzheimer's disease, medically proven mental disorders, and inability to undergo bronchoscopy or surgery. Patients with past or suspected HIV infections were also excluded.

2.4. Genomic DNA extraction

Genomic DNA extraction was conducted using a SepaGene kit. The analysis of mutations in exons 19, 20, and 21 of EGFR was conducted through PCR-single strand conformation polymorphism (SSCP) and direct sequencing analyses. Direct sequencing involved using small pieces of the gel containing the shift band detected by SSCP. Gel electrophoresis, data collection, and data analysis were performed using a Genetic Analyzer (PE Applied Biosystems, CA, USA) [12].

Methylation-specific PCR (MSP) determined the methylation status of FHIT after bisulfite treatment of DNA samples. The primer sequences are documented [13], and an unmethylated DAPK primer set verified bisulfite modification of all DNA samples.

2.5. Statistical analysis

Statistical analysis employed either the chi-squared test or Fisher's exact test with the SPSS 24.0 software. A *P*-value less than 0.05 indicated statistical significance.

3. Results

Of all the patients, 38 displayed EGFR mutations (14 patients with TB, and 24 patients without TB), accounting for 42% of cases, while 29 patients had FHIT myelination (19 patients with TB, and 10 patients without TB). Moreover, the protein expression of EGFR and FHIT was significantly higher in patients with AC as compared to the patients with AC and TB (**Figure 1**).

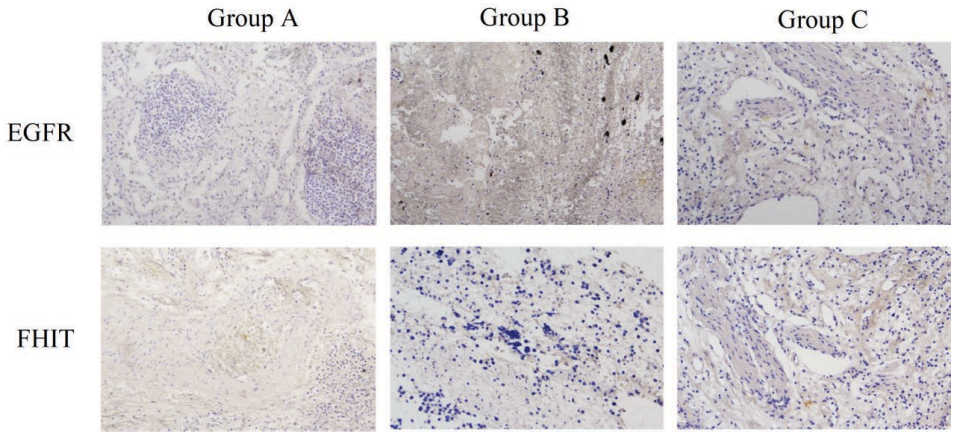

Figure 1. The protein expression of EGFR and FHIT in lung tissue was significantly higher in patients with AC compared to the patients with AC and TB

Among the 38 patients, 23 showed mutations of exon 19, 14 showed mutations of exon 20, and 18 showed mutations of exon 21. Frequencies of EGFR mutations were significantly higher on both exon 21 and exon 19 in patients with AC as compared to the patients with AC and TB, while there was no significant difference in the frequencies of EGFR mutations on exon 20 in patients with AC and patients with AC and TB (**Figure 2**).

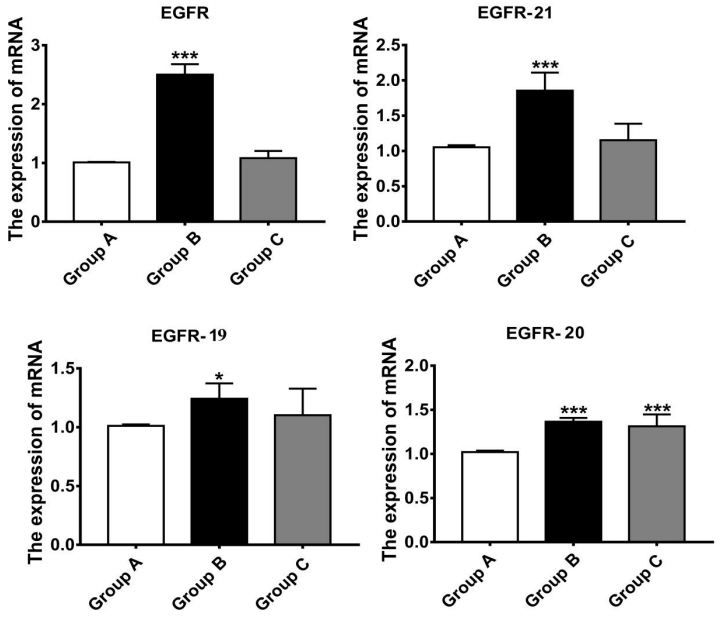

Figure 2. Frequencies of EGFR mutations were significantly higher on exon 19 and 21 in patients with AC compared to the patients with AC and TB

The FHIT gene exhibited methylation. A strong inverse correlation was found between tuberculosis status and frequency of EGFR mutation ($P < 0.001$), while significant correlations were observed between tuberculosis status and methylation of FHIT ($P < 0.01$). Furthermore, FHIT methylation frequency increased with tuberculosis status, while EGFR mutation frequency decreased with tuberculosis status (**Table 1** and **Figure 3**). A reverse correlation was observed between EGFR mutation and FHIT methylation.

Table 1. Status of EGFR mutation and FHIT myelination in patients with AC

		EGFR		*P* value
		Mutant	Wild type	
FHIT	Unmyelinated	32	26	< 0.01
	Myelinated	16	46	

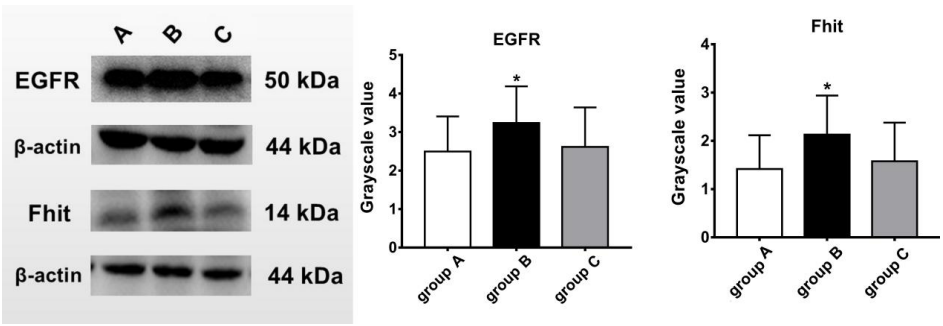

Figure 3. FHIT methylation frequency increased with TB status, while EGFR mutation frequency decreased with TB status

4. Discussion

Recent advances in our understanding of cell signaling pathways controlling cell survival have revealed genetic and regulatory aberrations that suppress cell death, promote cell division, and induce tumorigenesis. Among these discoveries is the EGFR, a transmembrane receptor tyrosine kinase protein expressed in various normal tissues, including epithelial, mesenchymal, and neurogenic tissue. Overexpression of EGFR has been reported in several human malignancies, including NSCLC. Lung AC harboring mutated EGFR has exhibited notable responses to TKIs, suggesting a significant survival advantage. The status of both EGFR mutation and gene amplification may be crucial in determining which tumors effectively respond to TKIs.

The observed pattern concerning TB-related mutations and methylations in this study indicates an increase in the frequency of alterations in FHIT methylation correlated with individual TB status and a tendency for the frequency of EGFR mutations to decrease inversely proportional to TB status. Unique methylation and mutation patterns of EGFR observed in TB and non-TB lung AC patients may be linked to their susceptibility to carcinogen exposure from TB. Based on these findings, our hypothesis suggests that TB may hinder the development of EGFR mutations.

Reports regarding the impact of lung AC and EGFR mutations on the incidence and outcomes of patients with a history of TB are limited. A study in the Taiwan region found a higher incidence of EGFR mutations in patients with lung AC exhibiting radiographic evidence consistent with previous tuberculosis pulmonary lesions (OR: 1.83 [0.92–3.62]) [14]. Another retrospective study analyzed the National Health Insurance Research Database of the Taiwan region and included 8,265 patients with NSCLC who received EGFR-TKIs between 1996 and 2000. This study reported a history of pulmonary TB associated with a poor clinical response to EGFR-TKIs in male patients but a better response in female patients [15].

FHIT methylation in TB patients showed a higher trend, while non-TB patients exhibited a lower trend in the development of EGFR mutation, as per the current study. Therefore, FHIT methylation could potentially suppress EGFR mutation. Studies have reported higher rates of methylation and mean methylation index in TB patients compared to non-TB patients, indicating a relationship between abnormal methylation and TB status [16-19]. Thus, the reduction in the overall methylation rate in TB suggests that methylation is a reversible epigenetic change that does not affect the DNA coding sequence [20]. From this perspective, the inhibition of EGFR mutation could be attributed to FHIT methylation, leading to an increase in EGFR mutations following TB.

Advancements in our understanding of cell signaling pathways have revealed genetic and regulatory abnormalities contributing to tumor formation, including EGFR, expressed in various normal epithelial, mesenchymal, and neurogenic tissues [21,22]. Overexpression of EGFR has been linked to the development of several human malignancies, including NSCLC [23]. Studies have shown that NSCLC patients with EGFR expression have lower survival rates, frequent lymph node metastasis, and poor response to chemotherapy. Lung AC harboring mutated EGFR responds well to TKIs [24-26], but there is a significant survival advantage for non-smoking Asian women with AC, particularly those with bronchioloalveolar carcinoma [27]. Two oral anti-cancer drugs, gefitinib and erlotinib, have been approved for advanced NSCLC treatment, with mutations in EGFR found in some lung cancers [28]. Efforts have been made to identify clinical, morphological, and molecular factors predicting response rates to these drugs. In NSCLC cases, overexpression of EGFR or mutations in intracellular EGFR have been observed in 43%–89% of cases. Other studies report that a quarter of NSCLC cases have mutations in the EGFR tyrosine kinase domain, and these mutations are associated with increased receptor expression in 75% of cases [29]. The majority of known EGFR tyrosine kinase domain mutations involve short deletions in exon 19 or point mutations in exon 21 [30]. Results in our study indicate a significantly higher frequency of EGFR mutation in patients with lung AC secondary to TB, suggesting a poor

response to EGFR-TKIs, resulting in lower survival rates, frequent lymph node metastasis, and poor response to chemotherapy.

However, the study was limited by a small sample size, and approximately 25% of cases showed no evidence of EGFR mutation or FHIT methylation. Further research is needed to confirm these findings. In summary, two distinct pathways are involved in the development of AC in TB patients, namely EGFR mutation and FHIT methylation. The pathogenesis of AC is associated with the frequencies of EGFR mutation and FHIT methylation, which are also correlated with lung TB and inversely correlated with each other.

Acknowledgments

This work was supported by the National Science and Technology Program of PRC. We thank the Local Staff from Xinjiang Chest Hospital for their hard work in data collection.

Ethics approval and consent to participate

This study was approved by the Ethics Committee of the Chest Hospital of Xinjiang Uygur Autonomous Region (Urumqi, China). The methods used in this study were performed in accordance with relevant guidelines and regulations. Written consent was obtained from the participants.

Funding

The Ethnic Minority Science and Technology Program of Xinjiang Autonomous Region (201523122)

Disclosure statement

The authors declare no conflict of interest.

References

[1] Thandra KC, Barsouk A, Saginala K, et al., 2021 Epidemiology of Lung Cancer. Contemp Oncol (Pozn), 25(1): 45–52. https://doi.org/10.5114/wo.2021.103829

[2] Casal-Mouriño A, Ruano-Ravina A, Lorenzo-González M, et al., 2021, Epidemiology of Stage III Lung Cancer: Frequency, Diagnostic Characteristics, and Survival. Transl Lung Cancer Res, 10(1): 506–518. https://doi.org/10.21037/tlcr.2020.03.40

[3] Drapkin BJ, Rudin CM, 2021, Advances in Small-Cell Lung Cancer (SCLC) Translational Research. Cold Spring Harb Perspect Med, 11(4): a038240. https://doi.org/10.1101/cshperspect.a038240

[4] Wu F, Wang L, Zhou C, 2021, Lung Cancer in China: Current and Prospect. Curr Opin Oncol, 33(1): 40–46. https://doi.org/10.1097/CCO.0000000000000703

[5] Rodak O, Peris-Díaz MD, Olbromski M, et al., 2021, Current Landscape of Non-Small Cell Lung Cancer: Epidemiology, Histological Classification, Targeted Therapies, and Immunotherapy. Cancers (Basel), 13(18): 4705. https://doi.org/10.3390/cancers13184705

[6] Abdeahad H, Salehi M, Yaghoubi A, et al., 2022, Previous Pulmonary Tuberculosis Enhances the Risk of Lung Cancer: Systematic Reviews and Meta-Analysis. Infect Dis (Lond), 54(4): 255–268. https://doi.org/10.1080/23744235.2021.2006772

[7] Cabrera-Sanchez J, Cuba V, Vega V, et al., 2022, Lung Cancer Occurrence After an Episode of Tuberculosis: A Systematic Review and Meta-Analysis. Eur Respir Rev, 31(165): 220025. https://doi.org/10.1183/16000617.0025-2022

[8] Li L, Ye Z, Yang S, et al., 2021, Diagnosis of Pulmonary Nodules by DNA Methylation Analysis in Bronchoalveolar Lavage Fluids. Clin Epigenetics, 13(1): 185. https://doi.org/10.1186/s13148-021-01163-w

[9] Malhotra J, Malvezzi M, Negri E, et al., 2016, Risk Factors for Lung Cancer Worldwide. Eur Respir J, 48(3): 889–902. https://doi.org/10.1183/13993003.00359-2016

[10] Sun YQ, Richmond RC, Suderman M, et al., 2021, Assessing the Role of Genome-Wide DNA Methylation Between Smoking and Risk of Lung Cancer Using Repeated Measurements: The HUNT Study. Int J Epidemiol, 50(5): 1482–1497. https://doi.org/10.1093/ije/dyab044

[11] Joshi A, Butle A, Hait S, et al., 2022, Osimertinib for Lung Cancer Cells Harboring Low-Frequency EGFR T790M Mutation. Transl Oncol, 22: 101461. https://doi.org/10.1016/j.tranon.2022.101461

[12] Yanagawa N, Tamura G, Oizumi H, et al., 2002, Frequent Epigenetic Silencing of the p16 Gene in Non-Small Cell Lung Cancers of Smokers. Jpn J Cancer Res, 93(10): 1107–1113. https://doi.org/10.1111/j.1349-7006.2002.tb01212.x

[13] Yanagawa N, Tamura G, Oizumi H, et al., 2007, Promoter Hypermethylation of RASSF1A and RUNX3 Genes as an Independent Prognostic Prediction Marker in Surgically Resected Non-Small Cell Lung Cancers. Lung Cancer, 58(1): 131–138. https://doi.org/10.1016/j.lungcan.2007.05.011

[14] Luo YH, Wu CH, Wu WS, et al., 2012, Association between Tumor Epidermal Growth Factor Receptor Mutation and Pulmonary Tuberculosis in Patients with Adenocarcinoma of the Lungs. J Thorac Oncol, 7(2): 299–305. https://doi.org/10.1097/JTO.0b013e31823c588d

[15] Chang C-H, Lee C-H, Ho C-C, et al., 2015, Gender-Based Impact of Epidermal Growth Factor Receptor Mutation in Patients with Nonsmall Cell Lung Cancer and Previous Tuberculosis. Medicine (Baltimore), 94(4): e444. https://doi.org/10.1097/MD.0000000000000444

[16] Bobak CA, Natarajan H, Gandhi T, et al., 2022, Increased DNA Methylation, Cellular Senescence and Premature Epigenetic Aging in Guinea Pigs and Humans with Tuberculosis. Aging (Albany NY), 14(5): 2174–2193. https://doi.org/10.18632/aging.203936

[17] Kwon MH, Lee GE, Kwon SJ, et al., 2008, Identification of DNA Methylation Markers for NSCLC Using HpaII-MspI Methylation Microarray. Tuberc Respir Dis, 65(6): 495–503. https://doi.org/10.4046/trd.2008.65.6.495

[18] Sharma G, Sowpati DT, Singh P, et al., 2016, Genome-Wide Non-CpG Methylation of the Host Genome During *M. tuberculosis* Infection. Sci Rep, 6: 25006. https://doi.org/10.1038/srep25006

[19] Shell SS, Prestwich EG, Baek SH, et al., 2013, DNA Methylation Impacts Gene Expression and Ensures Hypoxic Survival of *Mycobacterium tuberculosis*. PLoS Pathog, 9(7): e1003419. https://doi.org/10.1371/journal.ppat.1003419

[20] Zheng L, Leung ETY, Wong HK, et al., 2016, Unraveling Methylation Changes of Host Macrophages in *Mycobacterium tuberculosis* Infection. Tuberculosis (Edinb), 98: 139–148. https://doi.org/10.1016/j.tube.2016.03.003

[21] Nishihara S, Yamaoka T, Ishikawa F, et al., 2022, Mechanisms of EGFR-TKI-Induced Apoptosis and Strategies Targeting Apoptosis in EGFR-Mutated Non-Small Cell Lung Cancer. Genes (Basel), 13(12): 2183. https://doi.org/10.3390/genes13122183

[22] Yamaoka T, Arata S, Homma M, et al., 2019, Blockade of EGFR Activation Promotes TNF-Induced Lung Epithelial Cell Apoptosis and Pulmonary Injury. Int J Mol Sci, 20(16): 4021. https://doi.org/10.3390/ijms20164021

[23] Talukdar S, Emdad L, Das SK, et al., 2020, EGFR: An Essential Receptor Tyrosine Kinase-Regulator of Cancer Stem Cells. Adv Cancer Res, 147: 161–188. https://doi.org/10.1016/bs.acr.2020.04.003

[24] Moriya T, Hamaji M, Yoshizawa A, et al., 2022, Epidermal Growth Factor Receptor (EGFR)-Tyrosine Kinase Inhibitors as a First-Line Treatment for Postoperative Recurrent and EGFR-Mutated Non-Small-Cell Lung Cancer.

Interact Cardiovasc Thorac Surg, 34(3): 416–423. https://doi.org/10.1093/icvts/ivab283

[25] Zhou J, Yu X, Hou L, et al., 2021, Epidermal Growth Factor Receptor Tyrosine Kinase Inhibitor Remodels Tumor Microenvironment by Upregulating LAG-3 in Advanced Non-Small-Cell Lung Cancer. Lung Cancer, 153: 143–149. https://doi.org/10.1016/j.lungcan.2021.01.010

[26] Passaro A, Mok T, Peters S, et al., 2021, Recent Advances on the Role of EGFR Tyrosine Kinase Inhibitors in the Management of NSCLC with Uncommon, Non Exon 20 Insertions, EGFR Mutations. J Thorac Oncol, 16(5): 764–773. https://doi.org/10.1016/j.jtho.2020.12.002

[27] Chang Q, Qiang H, Qian J, et al., 2021, Epidermal Growth Factor Receptor Mutation Status and Response to Tyrosine Kinase Inhibitors in Advanced Chinese Female Lung Squamous Cell Carcinoma: A Retrospective Study. Front Oncol, 11: 652560. https://doi.org/10.3389/fonc.2021.652560

[28] Yang Z, Hackshaw A, Feng Q, et al., 2017, Comparison of Gefitinib, Erlotinib and Afatinib in Non-Small Cell Lung Cancer: A Meta-Analysis. Int J Cancer, 140(12): 2805–2819. https://doi.org/10.1002/ijc.30691

[29] Normanno N, De Luca A, Bianco C, et al., 2006, Epidermal Growth Factor Receptor (EGFR) Signaling in Cancer. Gene, 366(1): 2–16. https://doi.org/10.1016/j.gene.2005.10.018

[30] Ortiz AFH, Garland ME, Almarie B, 2022, Clinical and Radiological Characteristics to Differentiate Between EGFR Exon 21 and Exon 19 Mutations in Patients with Lung Adenocarcinoma: A Systematic Literature Review and Meta-Analysis. Cureus, 14(5): e25446. https://doi.org/10.7759/cureus.25446

Proceedings of Anticancer Research, 2024, Volume 8, Issue 2
http://ojs.bbwpublisher.com/index.php/PAR
ISSN Online: 2208-3553
ISSN Print: 2208-3545

A Study on the Influences of the COVID-19 Pandemic-Related Depression, Anxiety, Stress, and Treatment-Crisis on Quality of Life in Cancer Patients – A Secondary Publication

So Hyoung Kim[1], Kyung Hee Lim[2]*

[1]Kungpook National University Chilgok Hospital, Daegu, Republic of Korea
[2]College of Nursing, Keimyung University, Daegu, Republic of Korea

***Corresponding author:** Kyung Hee Lim, khlim7@kmu.ac.kr

Abstract: *Objective:* To investigate the factors affecting the quality of life of cancer patients by examining the degree of the COVID-19 pandemic-related depression, anxiety, stress, and treatment crisis. *Methods:* Data were collected from 132 cancer patients undergoing surgery, chemotherapy, radiotherapy, and hormone therapy at K University Hospital in D City using a structured questionnaire. The period of data collection was from May 6 to May 28, 2022. The collected data were analyzed using descriptive statistics, *t*-test, ANOVA, Pearson's correlation, and stepwise multiple regression. *Results:* The mean scores of quality-of-life, depression, anxiety, stress, and treatment crisis during the COVID-19 pandemic were 84.64 ± 29.09, 15.14 ± 6.49, 4.66 ± 5.27, 75.83 ± 17.70, and 78.52 ± 19.95, respectively. In terms of factors affecting the quality of life related to the COVID-19 pandemic, COVID-19 pandemic-related stress (β = 0.41, $P < 0.001$) appeared to have the greatest impact, followed by COVID-19 pandemic-related treatment-crisis (β = 0.28, P = 0.002), anxiety (β = 0.21, P = 0.002), and gender (β = 0.14, P = 0.009), with a total explanatory power of 67.6%. *Conclusion:* To improve the quality of life during the COVID-19 pandemic, COVID-19 pandemic-related stress, treatment-crisis, and anxiety should be periodically monitored and nursing interventions such as education on infection prevention, management, and emotional support programs should be provided to decrease the COVID-19 pandemic-related stress, treatment-crisis, and anxiety.

Keywords: Cancer; COVID-19; Quality of life

Online publication: March 28, 2024

1. Introduction

1.1. Study purpose

Coronavirus disease 19 (COVID-19) is a new type of acute respiratory infectious disease that first emerged in December 2019 and has since spread globally. In Korea, it spread rapidly locally, starting with the first confirmed case in January 2020, and internationally, it recorded high infection and mortality rates across

countries in just four months, leading the World Health Organization (WHO) to declare a pandemic, the highest classification of infectious disease [1].

Large-scale outbreaks of infectious diseases tend to make people feel more fearful of the potential risk of infection than the actual risk of infection itself [2] and are reported to undermine people's basic sense of security, causing not only fear of infection, but also maladaptive emotional and behavioral responses such as stress, decreased life satisfaction, depression, and anxiety [3]. In particular, the quarantine measures implemented to prevent the spread of COVID-19, such as social distancing, telecommuting, and restrictions on private gatherings, have led to social disconnection and isolation, which have exacerbated a range of COVID-19 pandemic-related psychological and emotional problems, including depression, anxiety, stress, fear, anger, and loneliness [4]. In particular, COVID-19 pandemic-related quality of life, one of the newly emerging terms such as corona blue, refers to an individual's perceived subjective well-being and satisfaction with the physical, social, and emotional domains experienced during the COVID-19 pandemic, as opposed to traditional health-related concepts of quality of life [5]. Psychological and emotional problems caused by the COVID-19 pandemic have been shown to contribute to poor COVID-19 pandemic-related quality of life [6].

The various psychological and emotional problems caused by COVID-19 may be even more severe for cancer patients [7]. Cancer patients are psychologically traumatized by the diagnosis of cancer alone, with 10 to 20 percent reporting depression and anxiety, and stress levels are very high due to the uncertainty of treatment and the burden of the treatment process [8]. In particular, during the COVID-19 pandemic, 64.3% of cancer patients reported depression [9], and 67.5% reported anxiety [10], which is about 2 to 2.5 times higher than the rates of 29.7% of the general population [4], and 18.92% of adolescents [10], respectively. In addition, during the COVID-19 pandemic, 31.6% of cancer patients reported stress [11], which is about three times higher than the rates of about 10% of the general population [12].

In particular, the lack of clear treatment guidelines for cancer patients with impaired physical functioning during COVID-19 infection has led to further anxiety and severe stress for cancer patients [4]. The European Society for Radiotherapy and Oncology (ESRO) has recommended minimizing hospital visits for cancer patients or using telephone consultations instead of in-person visits, which has led 20% of cancer patients to postpone chemotherapy and 5% to postpone additional anti-cancer treatments beyond chemotherapy [13]. These delays or cancellations of care and treatment have created a significant treatment crisis for cancer patients, with 86.5% of cancer patients reporting a sense of crisis that they may not receive adequate cancer care due to COVID-19 [10].

As can be seen, a large-scale infectious disease such as COVID-19 can cause serious psychological and emotional problems across society, and for cancer patients at high risk for COVID-19, pandemic-related depression, anxiety, and stress, as well as feelings of treatment crisis due to delays and interruptions in cancer treatment, can further exacerbate cancer patients' pandemic-related quality of life. However, few studies have examined the extent of COVID-19 pandemic-related depression, anxiety, stress, treatment crisis, and quality of life among cancer patients during the COVID-19 pandemic and how these factors affect COVID-19 pandemic-related quality of life, and none have examined treatment crisis among cancer patients during the pandemic. Therefore, this study aims to investigate the extent of depression, anxiety, stress, and treatment crisis related to the COVID-19 pandemic, determine how these factors affect the quality of life of cancer patients during the COVID-19 pandemic, and provide basic data for the development of nursing interventions that can prevent the development of pandemic-related depression, anxiety, stress, and treatment crisis in cancer patients and improve their quality of life during the pandemic.

1.2. Study objectives

The purpose of this study is to investigate the extent of COVID-19 pandemic-related depression, anxiety, stress, and treatment crisis among cancer patients and to determine how they affect their COVID-19 pandemic-related quality of life, with the following specific objectives:

(1) To determine the level of depression, anxiety, stress, treatment crisis, and quality of life related to the COVID-19 pandemic according to the participants' general characteristics and disease-related characteristics.

(2) To identify differences in COVID-19 pandemic-related quality of life by participants' general and disease-specific characteristics.

(3) To identify relationships among subjects' COVID-19 pandemic-related depression, anxiety, stress, treatment distress, and quality of life.

(4) To determine the impact of subjects' COVID-19 pandemic-related depression, anxiety, stress, and treatment crisis on their COVID-19 pandemic-related quality of life.

2. Research methods

2.1. Study design

This is a descriptive survey study to investigate the extent of depression, anxiety, stress, and treatment crisis related to the COVID-19 pandemic among cancer patients and to identify factors that influence the quality of life related to the COVID-19 pandemic among cancer patients.

2.2. Research subjects

The subjects of the study were cancer patients who have undergone or are currently undergoing surgery, chemotherapy, radiotherapy, hormone therapy, etc. at K University Hospital in D Metropolitan City who met the selection criteria. Specifically, the inclusion criteria were: (1) age 19 or older, (2) having received or undergoing one or more treatments such as surgery, chemotherapy, radiation therapy, or hormone therapy, (3) being able to understand and respond to the questionnaire, and (4) understanding the purpose of the study and voluntarily agreeing to participate. Exclusion criteria were: (1) those who have cognitive impairment due to brain tumor, dementia, intellectual disability, etc., and (2) those with psychiatric history and receiving medication.

The sample size was calculated using the G*power 3.1.9.4 program, and based on the results of a previous study [14], the minimum sample size required for the study was 118, with a moderate effect size of 0.15, a significance level of 0.05, a power of 0.80, and 10 predictor variables (depression, anxiety, stress, treatment crisis, age, gender, occupation, religion, stage, and diagnosis) for regression analysis. Considering a 15% dropout rate, 139 questionnaires were distributed and returned, of which 7 questionnaires with insufficient responses were excluded, leaving 132 for final analysis.

2.3. Research instruments

(1) COVID-19 pandemic-related depression: The depression tool developed by Lovibond and Lovibond [15] was used to measure depression related to the COVID-19 pandemic, which was modified and adapted into Korean by Narigele [16] after receiving approval for use. The tool consists of 6 items, each rated on a 5-point Likert scale with 1 being "not at all" and 5 being "very much so," with a range from a low of 6 to a high of 30, with higher scores indicating higher levels of depression related to the COVID-19 pandemic. The reliability of the tool was 0.89 at the time of development and Cronbach's α was .91 in this study.

(2) Anxiety related to the COVID-19 pandemic: The Coronavirus Anxiety Scale (CAS) developed by

Sherman [17] and adapted by Lee [18] was used to measure anxiety related to the COVID-19 pandemic. The tool is designed to assess anxiety by the extent to which participants experience anxiety symptoms (dizziness, sleep disturbance, lethargy, loss of appetite, digestive distress) when they hear thoughts or information about COVID-19. There are five questions, each rated on a 5-point Likert scale ranging from 0 for "not at all" to 4 for "very much so," and the tool ranges from a low of 0 to a high of 20, with higher scores indicating higher anxiety related to the COVID-19 pandemic. The reliability of the tool was .92 at the time of development and Cronbach's α was 0.93 in this study.

(3) COVID-19 pandemic-related stress: The COVID-19 Stress Scale for Korean People (CSSK) tool developed by Kim *et al.* [19] was used after receiving approval for use. The tool consists of 21 items and is divided into three sub-scales: fear of infection (9 items), difficulty in social distancing (6 items), and anger toward others (6 items). Each item is rated on a 5-point Likert scale with 1 being "not at all" and 5 being "very much so," and the tool ranges from a low of 21 to a high of 105, with higher scores indicating higher levels of pandemic-related stress. The reliability of the tool was 0.91 at the time of development, and Cronbach's α was 0.95 in this study.

(4) COVID-19 pandemic-related treatment crisis: COVID-19 pandemic-related treatment crisis refers to the fear of delayed cancer diagnosis or treatment, delayed appropriate care or referral, and social isolation or lack of social support due to the COVID-19 pandemic [20]. In this study, the COVID-19 pandemic-related treatment crisis instrument was developed by the researcher based on the results of a previous study [20] that investigated the COVID-19 pandemic-related treatment crisis through qualitative research. The tool consisted of 21 questions, including 4 questions about treatment, 4 questions about mental health, 3 questions about cancer diagnosis, 3 questions about the ongoing care process, 4 questions about daily health, and 3 questions about coping and adjustment. The preliminary items were validated by six experts (two cancer center professors, two oncology nursing professors, and two oncology nurse practitioners) for the item content validity index (I-CVI), and items with an I-CVI score of .80 or higher were selected for the instrument. To clarify the meaning of the preliminary items, we revised item 5, "I was worried about being blamed for social isolation due to COVID-19," to "I was worried about being infected with COVID-19 and being blamed as a spreader," based on expert opinions. Question 21, "I was worried that I would not be able to interact with other patients or get support from online support groups due to COVID-19," was reworded to "I was worried that I would not be able to interact with other patients or get support from online support groups due to COVID-19," and the word "online" was removed to "I was worried that I would not be able to interact with other patients or get support from online support groups due to COVID-19." Each question is rated on a 5-point Likert scale with 1 being "not at all true" and 5 being "very true," and the tool ranges from a low of 21 to a high of 105, with higher scores indicating higher levels of COVID-19 pandemic-related treatment crisis. The tool had a Cronbach's α of 0.98 for reliability.

(5) Quality of life related to the COVID-19 pandemic: The COVID-19 pandemic-related quality of life instrument was adapted from the World Health Organization Quality of Life Assessment Instrument (WHOQOL) developed by Min *et al.* [21] and revised by Kim *et al.* [5] after receiving approval for use. The instrument consists of 23 questions and five sub-scales: 7 questions on difficulties due to changes in personal life, 7 questions on difficulties due to changes in external activities, 2 questions on difficulties due to changes in activities with family, 3 questions on difficulties due to changes in work/school, and 4 questions on difficulties with cumbersome procedures. Each question is rated on a 6-point Likert scale with 1 being "not at all" and 6 being "very much so," and the instrument ranges from a low of 23 to a high of 138, with higher scores indicating lower quality of life. The reliability of the tool was

0.93 at the time of development, and Cronbach's α was 0.97 in this study.

2.4. Data collection

The data collection was conducted at K University Hospital in D Metropolitan City from May 6, 2022, to May 28, 2022, and the survey was started after explaining the purpose and objectives of the study to the head of the outpatient department and the ward manager and obtaining their consent to collect data. The subjects of this study were cancer patients who visited the hospital for treatment such as surgery, chemotherapy, radiation therapy, and hormone therapy, and who expressed interest in participating in the study through recruitment advertisements posted on the bulletin boards in front of the outpatient department, chemotherapy injection rooms, and wards. The researcher explained the purpose of the study, questionnaire, and data collection methods and procedures to the patients, and surveyed them after receiving their consent to participate in the study. The researcher read the questionnaire to the subjects if they had poor eyesight or if they wanted to, and recorded their responses. The questionnaire was administered once, and it took about 30 minutes to complete, after completing the questionnaire, a small reward was given as an appreciation token.

2.5. Data analysis

The collected data were analyzed using SPSS/WIN 28.0 version, using the following statistical techniques:

(1) The general and disease-related characteristics of the subjects, depression, anxiety, stress, treatment crisis, and quality of life related to the COVID-19 pandemic were analyzed as frequencies, percentages, means, and standard deviations.

(2) Differences in quality of life related to the COVID-19 pandemic according to general characteristics and disease-related characteristics were analyzed by independent *t*-test and one-way analysis of variance (ANOVA).

(3) Correlations between depression, anxiety, stress, treatment crisis, and quality of life related to the COVID-19 pandemic were analyzed by Pearson's correlation coefficients.

(4) Factors affecting subjects' quality of life related to the COVID-19 pandemic were analyzed by stepwise multiple regression.

2.6. Ethical considerations

This study was conducted after review and approval (IRB. No: 40525-202112-HR-090-02) by the Institutional Review Board of K University. For the ethical protection of research subjects, the purpose of the study, research methods and procedures, benefits and side effects of participating in the study, withdrawal from the study, confidentiality of personal information, access to mandatory records, and inquiries about the study were fully explained to the subjects, and if they agreed to participate in the study, written consent was obtained and data collection began. The collected data were coded by assigning a unique identification number, stored in a double-locked storage box, and shredded after the mandatory retention period of the data (3 years for consent forms and 5 years for other data) under the Bioethics Act.

3. Results

3.1. General and disease-specific characteristics of subjects

The gender of the 132 subjects was 68 (51.5%) female and 45 (34.1%) aged 60 to 69 years, with a mean age of 56.23 ± 10.04 years. In terms of marital status, 109 (82.6%) were married and 108 (81.8%) were living with a partner. Religious affiliation was reported by 70 (53.0%), and occupation was reported by 74 (56.1%).

The most common type of cancer diagnosed was digestive system cancer with 32 (24.2%), and the most common time since diagnosis was less than a year with 80 (60.6%). The most common cancer stage was stage 4 with 49 (37.1%), and the most common current treatment was surgery with 56 (42.4%). 87 (65.9%) and 78 (59.1%) had been diagnosed with COVID-19 and never quarantined, respectively, and 115 (87.1%) had received a COVID-19 vaccine (**Table 1**).

Table 1. Quality of life related to the COVID-19 pandemic according to general and disease-related characteristics of subjects (n = 132)

Characteristics	Categories	n (%) or M ± SD	Quality of life	
			M ± SD	t or F (P)
Gender	Male	64 (48.5)	91.23 ± 28.18	2.58 (0.011)
	Female	68 (51.5)	78.44 ± 28.76	
Age (year)	≤ 49	37 (28.0)	77.16 ± 26.90	1.96 (0.123)
	50 – 59	36 (27.3)	82.97 ± 27.14	
	60 – 69	45 (34.1)	91.96 ± 29.81	
	≥ 70	14 (10.6)	87.79 ± 33.99	
		56.23 ± 10.04		
Marital status	Unmarried	11 (8.3)	71.73 ± 26.56	1.27 (0.285)
	Married	109 (82.6)	86.17 ± 29.03	
	Etc.*	12 (9.1)	82.67 ± 31.09	
Living arrangement	Alone	24 (18.2)	93.46 ± 30.59	1.65 (0.101)
	With	108 (81.8)	82.69 ± 28.52	
Religion	No	62 (47.0)	83.87 ± 27.10	-0.29 (0.775)
	Yes	70 (63.0)	85.33 ± 30.92	
Occupation	No	74 (56.1)	87.00 ± 29.26	1.0 (0.295)
	Yes	58 (43.9)	81.64 ± 28.84	
Diagnosis	Gastrointestinal cancer	32 (24.3)	92.11 ± 32.27	1.03 (0.409)
	Breast cancer	25 (18.9)	91.64 ± 31.08	
	Genital cancer	21 (15.9)	91.00 ± 30.93	
	Lung cancer	18 (13.6)	90.33 ± 34.93	
	Head and neck cancer	16 (12.1)	81.22 ± 24.36	
	Hepatobiliary cancer	14 (10.6)	79.06 ± 25.39	
	Etc.†	6 (4.6)	76.60 ± 30.32	
Period since diagnosis (year)	< 1	80 (60.6)	82.76 ± 30.70	0.45 (0.639)
	1 – < 3	30 (22.7)	88.37 ± 23.85	
	≥ 3	22 (16.7)	86.41 ± 30.17	
Stage	≤ 1	35 (26.5)	84.00 ± 28.66	0.22 (0.881)
	2	30 (22.7)	87.60 ± 30.60	
	3	18 (13.7)	86.72 ± 21.64	
	4	49 (37.1)	82.53 ± 31.37	

Table 1 (Continue)

Characteristics	Categories	*n* (%) or M ± SD	Quality of life	
			M ± SD	*t* or F (*P*)
Type of treatment	Operation	56 (42.4)	81.04 ± 29.11	0.55 (0.651)
	Chemotherapy	55 (41.7)	87.42 ± 29.56	
	Multimodal treatment‡	15 (11.4)	88.60 ± 26.32	
	Radiotherapy	6 (4.5)	83.00 ± 29.09	
COVID-19 infection	No	87 (65.9)	84.17 ± 28.70	-0.26 (0.797)
	Yes	45 (34.1)	85.56 ± 30.13	
Social isolation in COVID-19	No	78 (59.1)	82.95 ± 29.55	-0.80 (0.423)
	Yes	54 (40.)	87.09 ± 28.51	
COVID-19 vaccination	No	17 (12.9)	91.24 ± 28.47	1.00 (0.319)
	Yes	115 (87.1)	83.67 ± 29.18	

M, mean; SD, standard deviation. *Divorce, separation, separation by death; †Osteosarcoma, thymic carcinoma, leukemia, peritoneal carcinoma; ‡The use of two or more kinds of treatments such as operation, chemotherapy, radiation therapy, immunotherapy, and hormonal therapy.

3.2. COVID-19 pandemic-related depression, anxiety, stress, treatment crisis, and quality of life

Participants' depression related to the COVID-19 pandemic was 15.14 ± 6.49 out of 30, with a mean score of 2.52 out of 5. Anxiety related to the COVID-19 pandemic was 4.66 ± 5.27 out of 20, with a mean score of 0.93 out of 4. Stress related to the COVID-19 pandemic was 75.83 ± 17.70 out of 105, with a mean of 3.61 out of 5. Treatment crisis related to the COVID-19 pandemic was 78.52 ± 19.95 out of 105, with a mean score of 3.74 out of 5. Quality of life related to the COVID-19 pandemic was 84.64 ± 29.09 out of 138, with a mean score of 3.68 out of 6 (**Table 2**).

Table 2. The level of depression, anxiety, stress, treatment crisis, and quality of life related to the COVID-19 pandemic (*n* = 132)

Variables	Scale range	M ± SD	Item M ± SD
Depression related to the COVID-19 pandemic	6–30	15.14 ± 6.49	2.5 ± 1.08
Anxiety related to the COVID-19 pandemic	0–20	4.66 ± 5.27	0.93 ± 1.05
Stress related to the COVID-19 pandemic	21–105	75.83 ± 17.70	3.61 ± 0.84
Treatment crisis related to the COVID-19 pandemic	21–105	78.52 ± 19.95	3.74 ± 0.95
Quality of life related to the COVID-19 pandemic	23–138	84.64 ± 29.09	3.68 ± 1.26

M, mean; SD, standard deviation.

3.3. Differences in COVID-19 pandemic-related quality of life by general and disease-related characteristics

When we analyzed the differences in quality of life related to the COVID-19 pandemic according to the general characteristics and disease-related characteristics of the subjects, we found that quality of life was only different by gender, with females scoring 78.44 ± 28.76 significantly lower than males scoring 91.23 ± 28.18 ($t = 2.58$, $P = 0.011$; **Table 1**).

3.4. Correlations between COVID-19 pandemic-related depression, anxiety, stress, treatment crisis, and quality of life

When analyzing the correlations between depression, anxiety, stress, treatment crisis, and quality of life related to the COVID-19 pandemic, we found that quality of life related to the COVID-19 pandemic was significantly positively correlated with treatment crisis ($r = 0.74$, $P < 0.001$), stress ($r = 0.77$, $P < 0.001$), anxiety ($r = 0.64$, $P < 0.001$), and depression ($r = 0.61$, $P < 0.001$). In addition, treatment crisis related to the COVID-19 pandemic was significantly positively correlated with stress ($r = 0.82$, $P < 0.001$), anxiety ($r = 0.54$, $P < 0.001$), and depression ($r = 0.59$, $P < 0.001$), while stress was significantly positively correlated with anxiety ($r = 0.66$, $P < 0.001$) and depression ($r = 0.69$, $P < 0.001$), and anxiety was significantly positively correlated with depression ($r = 0.79$, $P < 0.001$), indicating positive correlations among all variables (**Table 3**).

Table 3. Correlation among depression, anxiety, stress, treatment crisis, and quality of life related to the COVID-19 pandemic ($n = 132$)

Variables	Depression	Anxiety	Stress	Treatment crisis	Quality of life
	r (*P*)	*r* (*P*)	*r* (*P*)	*r* (*P*)	*r* (*P*)
Depression	1				
Anxiety	0.79 (< 0.001)	1			
Stress	0.69 (< 0.001)	0.66 (< 0.001)	1		
Treatment of crisis	0.59 (< 0.001)	0.54 (< 0.001)	0.82 (< 0.001)	1	
Quality of life	0.61 (< 0.001)	0.64 (< 0.001)	0.77 (< 0.001)	0.74 (< 0.001)	1

3.5. COVID-19 pandemic-related quality of life factors

Stepwise regression analyses were conducted to identify factors that influenced the subjects' COVID-19 pandemic-related quality of life. Depression, anxiety, stress, treatment crisis, and gender were selected as independent variables, and the categorical variable gender was analyzed as a dummy variable. Before the stepwise regression analysis, autocorrelation and multicollinearity were checked, and the Durbin-Watson correlation coefficient was 2.53, indicating that the independence of the residuals was satisfied, the tolerance limits were 0.28–0.93, which was greater than 0.1, and the variation inflation factor (VIF) was 1.07–3.58, which was less than 10, indicating that there was no problem with multicollinearity among the independent variables.

In the stepwise regression analysis, the regression model explaining the subjects' COVID-19 pandemic-related quality of life was statistically significant ($F = 69.44$, $P < 0.001$), with an explanatory power of 68.0%. COVID-19 pandemic-related stress ($\beta = 0.41$, $P < 0.001$) was found to be the most influential factor in influencing COVID-19 pandemic-related quality of life, followed by COVID-19 pandemic-related treatment crisis ($\beta = 0.28$, $P = 0.002$), COVID-19 pandemic-related anxiety ($\beta = 0.21$, $P = 0.002$), and gender ($\beta = 0.14$, $P = 0.009$; **Table 4**). These results indicate that higher levels of COVID-19 pandemic-related stress, treatment crisis, and anxiety were associated with lower COVID-19 pandemic-related quality of life for men than for women.

Table 4. Factors affecting the quality of life related to the COVID-19 pandemic (n = 132)

Variables	B	SE	β	t	P	VIF
(Constant)	-7.83	7.55		-1.04	0.302	
Stress	0.68	0.16	0.41	4.39	< 0.001	3.58
Treatment crisis	0.41	0.13	0.28	3.22	0.002	3.03
Anxiety	1.13	0.36	0.21	3.11	0.002	1.75
Gender (male)*	7.97	2.99	0.14	2.67	0.009	1.07
R^2 = 0.69, Adjusted R^2 = 0.68, F = 69.44, P < 0.001						

B, non-standardization coefficient; SE, standard error; VIF, variation inflation factor; β, standardization coefficient; *Dummy variable (female: 0, male: 1).

4. Discussion

This study was conducted to investigate the extent of COVID-19 pandemic-related depression, anxiety, stress, and treatment crisis among cancer patients, and to determine how these variables affect their quality of life during the COVID-19 pandemic, to provide basic data for the development of nursing interventions that can improve the quality of life of cancer patients in the context of an emerging infectious disease pandemic that could reoccur at any time.

In this study, cancer patients reported a COVID-19 pandemic-related quality of life of 84.64 out of 138 (mean 3.68 out of 6). In a study of the general population using the same instrument as this study, Kim [5] found a lower COVID-19 pandemic-related quality of life score of 3.99. These results suggest that cancer patients in this study have better quality of life during the COVID-19 pandemic than the general population, as higher scores are interpreted as lower quality of life during the COVID-19 pandemic. Given that cancer patients generally have a lower quality of life than the general population [12], these results can be considered in several ways. First, we can consider the difference in time points between the two studies. Kim's study was conducted during the fourth wave of the COVID-19 pandemic in 2021 when the number of new COVID-19 cases was at its highest level, and before the introduction of COVID-19 vaccination and treatment for the general adult population. In contrast, this study was conducted in May 2022, after the peak of new COVID-19 cases in Korea and before the start of the gradual return to normal life, which may have reflected the expectation of returning to normal life as the COVID-19 pandemic situation improved, resulting in higher COVID-19 pandemic-related quality of life for cancer patients than for the general population in 2021. This is consistent with a study by Lee [22] that examined changes in quality of life according to the COVID-19 pandemic situation and found that quality of life tended to worsen as the COVID-19 pandemic situation worsened, indicating that the severity of the COVID-19 pandemic may have a significant impact on quality of life. Therefore, since the COVID-19 pandemic-related quality of life of cancer patients during the pandemic may be worse than that of the general population, future studies should identify how the quality of life of cancer patients changes according to the severity of the pandemic, and develop effective interventions to prevent, maintain, and improve the quality of life of cancer patients.

Another possible explanation for the higher COVID-19 pandemic-related quality of life among cancer patients than the general population is that cancer patients may be less likely to take their discomfort with physical, social, and emotional problems caused by COVID-19 less seriously due to the severity of their health-related quality of life, such as worries about the cancer diagnosis and treatment itself, side effects, and cancer

symptoms. Therefore, we suggest that future research should examine the extent to which cancer patients' health-related quality of life, as well as their COVID-19 pandemic-related quality of life, represent pandemic-related well-being during the pandemic.

In this study, the factors that influenced COVID-19 pandemic-related quality of life in cancer patients were COVID-19 pandemic-related stress, treatment crisis, anxiety, and gender, and the explanatory power of these factors for COVID-19 pandemic-related quality of life in cancer patients was 68.0%. Of these factors, COVID-19 pandemic-related stress was found to have the greatest impact on cancer patients' COVID-19 pandemic-related quality of life, which is consistent with previous studies [23] that have examined quality of life among COVID-19 survivors and found stress to be the most important factor affecting quality of life.

In this study, cancer patients reported COVID-19-related stress at 75.83 out of 105 (3.61 out of 5), which was higher than the 3.26 score in a previous study of the general population using the same tool [24]. Cancer patients are considered a high-risk group for COVID-19 due to their compromised immunity from chemotherapy, and COVID-19 vaccination is recommended for cancer patients, especially since COVID-19 infection can be severe and has been reported to have a 30% higher mortality rate than the general population.1 However, due to controversy over the effectiveness and safety of COVID-19 vaccines, cancer patients have been shown to experience stress in deciding whether to get vaccinated [25], so outreach and education about the benefits of COVID-19 vaccination should be conducted to increase vaccination rates and reduce stress about the possibility of COVID-19 infection among cancer patients.

In the present study, contagion liability stress, which is the worry that one's own COVID-19 infection will cause their family to become infected with COVID-19, was significantly higher than other stress items. Considering the characteristics of Korean society, which is highly family-oriented and family-oriented [4], these results may be due to the strong influence of guilt and responsibility for infection and worry that one's own COVID-19 infection may spread COVID-19 to family members. Therefore, in the event of a COVID-19 infection in the family, strict self-isolation, adherence to infection prevention measures, and information and education on the symptoms of infection should be strengthened to reduce stress related to COVID-19 transmission.

The second factor affecting the quality of life during the COVID-19 pandemic in cancer patients was perceived treatment crisis, which is limited by the lack of prior research examining treatment crisis and quality of life during the COVID-19 pandemic in cancer patients, both domestically and internationally, which limits the ability to directly compare results. However, an international study found that 52% of cancer patients had their outpatient appointments changed to telephone or telemedicine during the COVID-19 pandemic, 12% of patients on treatment had their treatment schedule postponed or interrupted, and 62% of these patients reported a sense of treatment crisis, such as fear that their disease would progress or recur due to the change in treatment schedule, which is similar to our findings [26]. On the other hand, some domestic studies showed that the number of hospital visits for mild illnesses or infectious diseases decreased by 20%–46% after the COVID-19 pandemic, but patients with serious diseases such as cancer, brain disease, and heart disease increased by 1.94% compared to pre-COVID-19, which is different from international studies [27]. However, this study did not directly investigate patients' sense of treatment crisis, so it is difficult to compare it with the sense of treatment crisis in this study, but it is necessary to investigate whether the COVID-19 pandemic increased worries and sense of crisis about cancer treatment, which led to more hospital visits in future studies.

Previous studies examining the quality of life in cancer patients have found that cancer patients report increased care needs and a sense of crisis that they may not receive adequate care when they experience physical symptoms during cancer treatment, when they do not receive timely treatment for cancer recurrence,

when their physical needs are not met, when they are worried about their cancer prognosis and health, and when they perceive a decrease in the frequency of contact with health care providers [28]. This study also found that cancer patients have a high sense of treatment crisis regarding the postponement or interruption of their cancer treatment schedule due to infection with COVID-19, and in particular, among the treatment crisis questions, they most often complain of difficulties in following infection prevention measures that have been strengthened due to the COVID-19 pandemic. In particular, the Korean Society of Critical Illness has suggested improvements such as a shortage of beds for critically ill patients, a lack of manuals for managing critically ill patients, and chaos in the medical care system for the failure to provide adequate care to critically ill patients, including cancer patients, during the COVID-19 pandemic [29]. Based on this, to reduce the sense of medical crisis among cancer patients, which is one of the severe diseases, it is necessary to apply strict and strengthened infection prevention guidelines when using hospitals, strengthen the access system for cancer patients to receive continuous medical care with peace of mind, and prepare a manual for managing cancer patients according to the type of cancer diagnosed and the symptoms of cancer if they become infected with COVID-19. In particular, as cancer patients are more likely to become critically ill, establishing infectious disease hospitals with enough professional staff and high-risk medical equipment to care for cancer patients, establishing a close cooperation system between local organizations and infectious disease hospitals to smoothly coordinate the supply and demand of beds, and preparing to support treatment resources can be a good strategy to reduce the sense of urgency of treatment for cancer patients. The third factor affecting cancer patients' quality of life related to the COVID-19 pandemic was anxiety related to the COVID-19 pandemic. These findings are not directly comparable as no prior studies have examined the association between COVID-19 pandemic-related quality of life and COVID-19 pandemic-related anxiety in cancer patients, but they are consistent with previous studies that have examined quality of life in cancer patients and found COVID-19-related anxiety to be a factor in quality of life [8].

Previous studies of COVID-19-related anxiety in the general population have shown that infectious disease outbreaks caused by new, unknown pathogens and the lack of a cure increase infectious disease anxiety [4], and in this study, cancer patients reported higher levels of anxiety about COVID-19, a new, unknown infectious disease, with a mean score of 3.62 out of 5. To reduce COVID-19-related anxiety, it will be important to provide evidence-based infectious disease information and educate patients on what to do if they experience symptoms of suspected COVID-19 infection so that early detection and treatment can occur. In addition, cancer patients with high levels of COVID-19-related anxiety should be provided with psychological support to understand the causes of their anxiety, provide psychological prevention programs such as emotional support, and provide professional counseling for anxiety symptoms.

The final factor affecting COVID-19 pandemic-related quality of life in cancer patients was gender. These findings were consistent with previous studies examining quality of life among COVID-19 survivors, which found that men had lower pandemic-related quality of life than women [23]. This could be explained by the fact that the COVID-19 pandemic reduced the social activities of men, who are more socially active than women, and reduced or limited the number of relationships between people, leading to a relatively higher level of social isolation among men than before the pandemic [30], resulting in a further decline in quality of life compared to women. In addition, the socioeconomic changes caused by COVID-19 and the increase in household debt [30] may have exacerbated the psychological burden on men who are primarily responsible for the household economy, and the financial losses, reduced income, and loss of economic ability caused by the cancer diagnosis may have further worsened the quality of life of male cancer patients. Therefore, since the quality of life of men may be more negatively affected during the epidemic, it is necessary to identify the changes in the quality of

life of male cancer patients, identify economic factors and psychosocial factors that may affect the quality of life, and provide nursing interventions for patients, such as financial support, social services, and psychological counseling services. However, a previous study [13] that examined COVID-19 illness attitudes and quality of life in the general population using the same instrument as this study found that women experienced more stress, anxiety, and depression about COVID-19 than men, resulting in lower quality of life, so it is necessary to repeat the study to confirm the association between gender and quality of life related to the COVID-19 pandemic.

In this study, depression related to the COVID-19 pandemic showed a significant correlation with the quality of life of cancer patients, but it did not appear as a contributing factor. These results may reflect the gradual return to normal life and the anticipation of the end of the COVID-19 situation, which occurred in May 2022 when this study was conducted. It is presumed that the low depression scores are related to this and are not significantly impacting the quality of life of patients. However, since the COVID-19 pandemic situation has not yet completely ended, and the era of living with COVID-19 continues to impact society with pandemic-related depression like "COVID blues," it is necessary to regularly assess depression in cancer patients and continuously monitor changes in depressive symptoms to detect depression in cancer patients early.

The results of this study, which examined the impact of COVID-19 pandemic-related depression, anxiety, stress, and treatment crisis on the quality of life in patients with advanced cancer, showed that COVID-19 pandemic-related stress, treatment crisis, anxiety, and gender were factors affecting the quality of life in cancer patients. These results are significant in that they provide a basis for developing nursing interventions to improve COVID-19 pandemic-related quality of life in cancer patients during an emerging infectious disease epidemic such as COVID-19. In particular, as the treatment crisis was shown to be an influential factor in COVID-19 pandemic-related quality of life in cancer patients, it is expected to provide evidence as a variable for improving COVID-19 pandemic-related quality of life in cancer patients and to promote further research on interventions that can reduce treatment crisis in cancer patients. In addition, it is of great significance that we identified quality-of-life influencing factors in the context of a few COVID-19 pandemic-related quality-of-life studies in Korea.

Limitations of this study include the fact that the study was conducted during the transition period of daily life recovery from the COVID-19 pandemic, so it is necessary to be cautious in interpreting the results and applying them to cancer patients during the COVID-19 pandemic and future pandemics, and the fact that the study was cross-sectional, which limits the ability to infer changes in quality of life in cancer patients reflecting the situation at different times of the COVID-19 pandemic. Furthermore, the reliability and validity of the instrument used to measure treatment crisis related to the COVID-19 pandemic have not been previously validated, and further validation of the instrument is needed. Finally, this study collected data on all cancer patients and did not take into account the diagnosis name, time of diagnosis, and stage of cancer, so there are limitations in generalizing the results to patients of each cancer type and stage, so it is recommended that future studies should investigate the subjects in detail and investigate not only the quality of life related to the COVID-19 pandemic but also the health-related quality of life of cancer patients in general.

5. Conclusions and recommendations

This study was conducted to identify factors affecting COVID-19-related quality of life in cancer patients during the COVID-19 pandemic to provide a basis for developing nursing interventions to improve COVID-19-related quality of life in cancer patients. The results of this study showed that COVID-19 pandemic-related quality of life in cancer patients was significantly and positively correlated with COVID-19 pandemic-related

stress, treatment crisis, anxiety, and depression, and that COVID-19 pandemic-related stress, treatment crisis, anxiety, and gender were significant factors affecting COVID-19 pandemic-related quality of life. Therefore, to improve the COVID-19 pandemic-related quality of life of cancer patients during the pandemic, it is necessary to periodically assess the level of COVID-19 pandemic-related stress, treatment crisis, and anxiety, and to identify the patterns of psychological and emotional changes. In particular, to reduce COVID-19 pandemic-related stress and anxiety, it is necessary to strengthen publicity and education on infectious disease information and the benefits of infectious disease vaccination, and to educate patients on infection prevention measures and what to do if an infectious disease occurs, so that early detection and treatment of infectious diseases can be achieved. It will also be necessary to provide psychological support to cancer patients in need of psychological and emotional interventions, including the provision of psychological prevention programs and access to professional counseling.

Based on the above findings, we make the following recommendations: First, there is little prior research on factors affecting pandemic-related quality of life in cancer patients, so replication studies are needed to generalize the findings of this study. Second, since this study was conducted as a cross-sectional study and could not reflect the changes in the COVID-19 pandemic situation, it is necessary to conduct a longitudinal study to identify the psychological reactions and quality of life of cancer patients according to the changing patterns of the pandemic situation and to identify the influencing factors by time. Third, we propose a study that identifies the quality-of-life influencing factors by separating patients by cancer type and stage, considering the diagnosis name, time of diagnosis, and stage of cancer, and a study that investigates the health-related quality of life of cancer patients.

Acknowledgment

This article is a condensed form of the first author's master's thesis from Keimyung University.

Disclosure statement

The authors declare no conflict of interest.

References

[1] World Health Organization (WHO), Numbers at a Glance, viewed September 26, 2022, http://www.who.int/emergencies/diseases/novel-coronavirus-2019

[2] Kim J, Kang J, 2021, Who is to Blame for Infection? Emotional Discourse in Editorial Articles during the Emerging Infectious Diseases Epidemics in Korea. J Korea Contents Assoc, 12: 816–827.

[3] Kimhi S, Eshel Y, Marciano H, et al., 2020, Distress and Resilience in the Days of COVID-19: Comparing Two Ethnicities. Int J Environ Res Public Health, 17(11): 3956. https://doi.org/10.3390/ijerph17113956

[4] Lee DH, Kim YJ, Lee DH, et al., 2020, The Influence of Public Fear, and Psycho-Social Experiences During the Coronavirus Disease 2019 (COVID-19) Pandemic on Depression and Anxiety in South Korea. Korean J Couns Psychother, 32: 2119–2156.

[5] Kim HA, 2021, The Effects of Illness Attitude on Quality of Life in the COVID-19 Era, thesis, Hanyang University.

[6] Salari N, Hosseinian-Far A, Jalali R, et al., 2020, Prevalence of Stress, Anxiety, Depression Among the General Population During the COVID-19 Pandemic: A Systematic Review and Meta-Analysis. Global Health, 16(1): 57. https://doi.org/10.1186/s12992-020-00589-w

[7] Wang C, Pan R, Wan X, et al., 2020, A Longitudinal Study on the Mental Health of General Population During the COVID-19 Epidemic in China. Brain Behav Immun, 87: 40–48. https://doi.org/10.1016/j.bbi.2020.04.028

[8] Pitman A, Suleman S, Hyde N, et al., 2018, Depression and Anxiety in Patients with Cancer. BMJ, 361: k1415. https://doi.org/10.1136/bmj.k1415

[9] Madkhali NA, Ameri A, Al-Naamani ZY, et al., 2022, Has the COVID-19 Pandemic Affected the Psychological State of Arab Cancer Patients? Curr Psychol, 21: 1–12. https://doi.org/10.1007/s12144-022-03414-2

[10] Chen G, Wu Q, Jiang H, et al., 2020, Fear of Disease Progression and Psychological Stress in Cancer Patients Under the Outbreak of COVID-19. Psychooncology, 29(9): 1395–1398. https://doi.org/10.1002/pon.5451

[11] Miaskowski C, Paul SM, Snowberg K, et al., 2020, Stress and Symptom Burden in Oncology Patients During the COVID-19 Pandemic. J Pain Symptom Manage, 60(5): e25–e34. https://doi.org/10.1016/j.jpainsymman.2020.08.037

[12] Park HY, 2021, Mental Health in Patients with Coronavirus Disease-19 and the Quarantined People. J Korean Neuropsychiatr Assoc, 60: 11–18.

[13] Ciążyńska M, Pabianek M, Szczepaniak K, et al., 2020, Quality of Life of Cancer Patients During Coronavirus Disease (COVID-19) Pandemic. Psychooncology, 29(9): 1377–1379. https://doi.org/10.1002/pon.5434

[14] Choi HK, 2021, Factors Influencing Health-Related Quality of Life of Pregnant Women: A Comparative Study. J Korean Data Inf Sci Soc, 32: 501–514.

[15] Lovibond PF, Lovibond SH, 1995, The Structure of Negative Emotional States: Comparison of the Depression Anxiety Stress Scales (DASS) with the Beck Depression and Anxiety Inventories. Behav Res Ther, 33(3): 335–343. https://doi.org/10.1016/0005-7967(94)00075-u

[16] Narigele N, Bae SY, 2021, The Impact of Depression from COVID-19 and Career Anxiety on Career Indecision among College Students Majoring in Hospitality and Tourism. Journal of Tourism and Leisure Research, 33(7): 275–291. https://doi.org/10.31336/jtlr.2021.7.33.7.275

[17] Lee SA, 2020, Coronavirus Anxiety Scale: A Brief Mental Health Screener for COVID-19 Related Anxiety. Death Stud, 44(7): 393–401. https://doi.org/10.1080/07481187.2020.1748481

[18] Lee R, 2021, Factors Related to COVID-19 Anxiety and Stress: Focusing on Demographic Characteristics and Neighborhood Satisfaction. J Korea Contents Assoc, 21: 71–80.

[19] Taylor S, Landry CA, Paluszek MM, et al., 2020, Development and Initial Validation of the COVID Stress Scale for Korean People. J Anxiety Disord, 72: 102232. https://doi.org/10.1016/j.janxdis.2020.102232

[20] Moraliyage H, De Silva D, Ranasinghe W, et al., 2021, Cancer in Lockdown: Impact of the COVID-19 Pandemic on Patients with Cancer. Oncologist, 26: e342–e344. https://doi.org/10.1002/onco.13604

[21] Min SK, Kim KI, Lee CI, et al., 2002, Development of the Korean Versions of WHO Quality of Life Scale and WHOQOL-BREF. Qual Life Res, 11(6): 593–600. https://doi.org/10.1023/a:1016351406336

[22] Lee ER, 2021, Changes in the Quality of Life of University Students in Daegu and Gyeongbuk in the Epidemic of COVID-19: The Relationship with COVID-19 Stress, Neuroticism, Anxiety Control, thesis, Daegu University.

[23] Ji HY, 2022, Effects of Post-Traumatic Stress Disorder (PTSD): Social Stigma and Social Support on COVID-19 Survivors' Quality of Life, thesis, Incheon Catholic University.

[24] Kim SY, Kang JS, 2022, Factors Influencing COVID-19 Stress Among Tertiary Hospital Workers. Stress, 30: 252–259.

[25] Villarreal-Garza C, Vaca-Cartagena BF, Becerril-Gaitan A, et al., 2021, Attitudes and Factors Associated with COVID-19 Vaccine Hesitancy Among Patients with Breast Cancer. JAMA Oncol, 7(8): 1242–1244. https://doi.org/10.1001/jamaoncol.2021.1962

[26] de Joode K, Dumoulin DW, Engelen V, et al., 2020, Impact of the Coronavirus Disease 2019 Pandemic on Cancer Treatment: The Patients' Perspective. Eur J Cancer, 136: 132–139. https://doi.org/10.1016/j.ejca.2020.06.019

[27] Byun JY, 2021, Impact of the COVID-19 Pandemic on the Utilization of Medical Care Services, thesis, Seoul National University.

[28] Choi E, Kim SH, Lee YW, et al., 2021, Supportive Care Needs and Health-Related Quality of Life of Esophageal Cancer Survivors. Asia Pac J Oncol Nurs, 8: 164–171. https://doi.org/10.4103/apjon.apjon_60_20

[29] Korean Society of Critical Care Medicine, Notification Website, viewed December 1, 2021, https://www.ksccm.org/html/?pmode=BBBS0006700005&smode=view&seq=2560

[30] Ministry of Health and Welfare (KR), The Results of the COVID-19 National Mental Health Survey in the Second Quarter of 2022 are Announced, viewed March 10, 2023, http://www.mohw.go.kr/react/al/sal0301vw.jsp?PAR_MENU_ID=04&MENU_ID=0403&page=1&CONT_SEQ=372545

Proceedings of Anticancer Research, 2024, Volume 8, Issue 2
http://ojs.bbwpublisher.com/index.php/PAR
ISSN Online: 2208-3553
ISSN Print: 2208-3545

Arterial Embolization: A Superior Treatment for Massive Urinary Tract Bleeding in Emergency Care

Bo Chen, Donghong Shi, Min Ai, Longjiang Zhang*

Department of Medical Imaging, General Hospital of the Eastern Theater Command of the Chinese People's Liberation Army, Nanjing 210002, China

***Corresponding author:** Longjiang Zhang, kevinzhlj@163.com

Abstract: *Objective:* To analyze the effect of arterial embolism (AE) in patients with massive urinary system bleeding (MBUS). *Methods:* From September 2018 to September 2023, 175 cases of MBUS patients in the emergency department of the hospital were randomly selected and divided into groups according to the length of stay. Among them, 85 cases (September 2018 – September 2020) underwent bladder irrigation treatment with aluminum potassium sulfate solution through a catheter (Group A), and 90 cases (October 2020 – September 2023) underwent AE treatment (Group B). The treatment effects of the two groups were compared. *Results:* The treatment effectiveness of Group B is higher than that of Group A ($P < 0.05$). The urinary hemoglobin level of Group B is lower than that of Group A at 1, 6, 12, and 24 hours after treatment ($P < 0.05$). Among the 90 cases treated with AE, 7 cases had a fever, with body temperatures ranging from 37.3°C to 38.9°C, with a mean temperature of 38.2 ± 0.3°C. Four cases experienced local pain, nausea, and vomiting, while two cases of intra-iliac AE showed transient buttock pain. These patients with adverse reactions were treated symptomatically for 7 days. All patients recovered after treatment. Intravenous urography of 87 patients in June showed that the renal pelvis and calyces were in good condition, the renal function returned to normal, and the blood urea nitrogen and blood creatinine test results were within the normal range. After 1 year of follow-up, no hypertension occurred. *Conclusion:* AE treats MBUS patients in the emergency department with remarkable efficacy. It has the advantages of less damage to the body, rapid hemostasis, high safety, and maximum preservation of organ function.

Keywords: Emergency; Arterial embolism; Urinary tract bleeding

Online publication: March 28, 2024

1. Introduction

Massive bleeding of the urinary system (MBUS) encompasses various bleeding sites, including the kidneys, ureters, bladder, and urethra, among others, and constitutes a significant portion of clinical emergency cases. Additionally, MBUS can arise from systemic diseases or conditions affecting adjacent organs [1]. The predominant symptom in most MBUS cases is hematuria, though some patients may primarily present with pelvic and abdominal bleeding without evident hematuria. Without prompt and effective intervention, MBUS patients are at risk of succumbing to hemorrhagic shock. Therefore, a pressing challenge for urology

departments is expedited hemostasis in MBUS patients.

Historically, clinical management of MBUS has relied on systemic hemostatic agents, continuous bladder irrigation, and similar approaches. While these methods can mitigate bleeding to a certain extent, patients with substantial hemorrhage often necessitate surgical intervention or ligation of major blood vessels to achieve hemostasis. However, swiftly identifying the bleeding source poses challenges and may result in increased bodily harm. Advancements in digital subtraction angiography (DSA) technology have facilitated the widespread adoption of arterial embolism (AE) in clinical practice for MBUS patients, offering simplicity of procedure, high efficacy, and safety [2,3]. This study aims to analyze the efficacy of AE in treating MBUS patients.

2. Materials and methods

2.1. General information

MBUS patients from the emergency department of the hospital between September 2018 and September 2023 were randomly selected and categorized based on their duration of stay. Among them, Group A comprised 85 cases (September 2018 – September 2020), while Group B included 90 cases (October 2020 – September 2023). In Group A, the age range is between 20 and 65 years, with a mean age of 43.68 ± 4.52 years, and their weight ranging from 45.62 to 87.95 kg, with a mean weight of 63.17 ± 6.59 kg. The predominant bleeding types were pelvic fracture combined with massive urethral bleeding (27 cases), bleeding after percutaneous nephrolithotomy (43 cases), and traumatic closed renal contusion and laceration bleeding (15 cases). The male/female ratio was 41/44. In Group B, the age range is between 21 and 63 years, with a mean age of 43.15 ± 4.49 years, and their weight ranging from 45.56 to 87.82 kg, with a mean weight of 63.69 ± 6.63 kg. The predominant bleeding types were pelvic fracture combined with urethral bleeding (28 cases), bleeding after percutaneous nephrolithotomy (45 cases), and traumatic closed renal contusion and laceration bleeding (17 cases). The male/female ratio was 43/47. General data comparison showed no significant difference ($P > 0.05$).

Inclusion criteria: (1) Patients diagnosed with MBUS; (2) Patients providing voluntary participation with complete medical history; (3) Patients providing informed consent for study participation and signing relevant documentation.

Exclusion criteria: (1) Individuals with mental illness; (2) Patients diagnosed with malignant tumors; (3) Individuals with severe disorders of major organs such as liver and kidney; (4) Patients with incomplete medical history data; (5) Individuals who dropped out midway.

2.2. Methods

Group A: Treatment involved bladder irrigation with aluminum potassium sulfate solution via a urinary catheter. Preparation of potassium aluminum sulfate solution: The Pharmacy Department's preparation room utilized 0.9% sodium chloride injection to prepare potassium aluminum sulfate into a 1.0% aluminum solution, autoclaved for sterility. For patients with cystostomy tubes, continuous irrigation was administered using an irrigation device at a rate of 50 mL/min. Retention flushing involved connecting a three-lumen balloon catheter to the bladder flushing device, followed by injecting 150–250 mL of aluminum solution into the bladder, retaining for 10 minutes, and subsequently flushing. The irrigation volume ranged from 2,000–3,000 mL, administered once daily, ceasing when urine clarity was achieved.

Group B: AE involved local anesthesia using the Seldinger technique, with femoral artery puncture and cannulation. DSA guided the identification of damaged and bleeding vessels. For example, patients with pelvic fractures and urethral rupture underwent bilateral internal iliac artery angiography, while those with kidney damage underwent bilateral renal artery angiography. Following ultra-smooth loach guidewire insertion, a

4–5F Cobra catheter was advanced to the bleeding artery branch, and embolization materials were selected based on arterial injury severity. Successful embolization was confirmed via DSA examination, indicating interrupted bleeding, absent blood flow, intact contrast agent containment, and stable vital signs postoperatively. Compression and bandaging were applied to the puncture site, with a prescribed 24-hour limb immobilization period and 7-day bed rest with close monitoring of urine and vital signs.

2.3. Observation indicators

(1) Treatment effectiveness: Calculated as the sum of the markedly effective rate and the effective rate, with markedly effective indicating clear urine, urinary Hb < 0.1 g/L, and 24-hour urinary blood loss < 2 mL; effective indicating slightly mixed urine, urinary Hb 0.1–1 g/L, 24-hour urinary blood loss 2–20 mL; ineffective indicating no change in fluid color, urine Hb > 1 g/L, and 24-hour urinary blood loss > 20 mL.

(2) Urinary hemoglobin (Hb) level: Urine occult blood test assessed urinary Hb levels before treatment, and at 1 h, 6 h, 12 h, and 24 h post-treatment.

(3) Analysis of patient response after AE.

2.4. Statistical analysis

SPSS 25.0 was used for data analysis. Measurement data were expressed as mean ± standard deviation (SD) and processed with the *t*-test. Count data were presented as *n* (%) and processed with the χ^2 test. A *P*-value of less than 0.05 is considered as statistically significant.

3. Results

3.1. Treatment effectiveness

Table 1 shows that the treatment effectiveness of Group B was significantly higher than Group A ($P < 0.05$).

Table 1. Comparison of treatment effectiveness [*n* (%)]

Group	*n*	Markedly effective	Effective	Ineffective	Total effective rate
Group B	90	54 (60.00)	34 (37.78)	2 (2.22)	88 (97.78)
Group A	85	33 (38.82)	41 (48.24)	11 (12.94)	74 (87.06)
χ^2	-	-	-	-	7.303
P	-	-	-	-	0.006

3.2. Urine hemoglobin levels

As seen in **Table 2**, there were no significant differences in the urinary Hb levels between the two groups before treatment ($P > 0.05$). However, Group B showed significantly lower urinary Hb levels than Group A at 1, 6, 12, and 24 hours after treatment ($P < 0.05$).

Table 2. Comparison of urine hemoglobin levels (mean ± SD, g/L)

Group	*n*	Before treatment	1 hour after treatment	6 hours after treatment	12 hours after treatment	24 hours after treatment
Group B	90	15.38 ± 5.64	0.52 ± 0.14	0.38 ± 0.12	0.19 ± 0.10	0.11 ± 0.06
Group A	85	15.67 ± 5.58	3.76 ± 0.25	1.64 ± 0.23	0.68 ± 0.37	0.53 ± 0.15
t	-	0.341	106.537	45.794	12.106	24.566
P	-	0.733	0.000	0.000	0.000	0.000

3.3. Patient response after AE

Out of the 90 cases treated with AE, 7 experienced post-operative fever, with body temperatures ranging from 37.3°C to 38.9°C, with a mean temperature of 38.2 ± 0.3°C. Additionally, 4 cases reported local pain, nausea, and vomiting, while 2 cases showed transient buttock pain following internal iliac AE. All patients with adverse reactions recovered after receiving 7 days of symptomatic treatment. Intravenous urography conducted on 87 patients in June revealed favorable conditions of the renal pelvis and calyces, with normalized renal function and blood urea nitrogen and blood creatinine levels within the normal range. No instances of hypertension were observed during the 1-year follow-up period.

4. Discussion

In cases of MBUS where bleeding is not excessive, conservative treatment can suffice for achieving hemostasis. However, if bleeding is rapid or extensive, and hemodynamics become unstable, surgical intervention becomes necessary to halt the bleeding. Yet, surgical procedures entail greater bodily damage and risk factors for patients. Complicated bleeding scenarios post-surgery may impede quick identification of damaged blood vessels and prompt cessation of bleeding, potentially leading to organ dysfunction. With ongoing advancements in interventional radiology, DSA-guided AE emerges as a simple, highly effective, and safe approach for treating various major hemorrhages [4,5]. Urology has increasingly adopted AE to treat MBUS patients, achieving notable efficacy and safety through clinical practice. In this study, AE treatment in 90 MBUS patients resulted in rapid hemostasis and significant hemostatic effects.

Successful AE treatment for MBUS hinges on swiftly and accurately locating the damaged blood vessels for intubation [6]. This study utilizes DSA to pinpoint damaged blood vessels, providing precise anatomical understanding and bleeding extent assessment, thereby ensuring patients do not miss optimal treatment opportunities: (1) where MBUS patients show no significant improvement after 6 hours of conservative treatment; (2) in cases of substantial bleeding and persistent blood pressure instability post-conservative treatment; and (3) instances where patients experience bleeding recurrence post-effective conservative treatment, prompting AE combined with stabilizing vital signs and anti-shock measures. In this study, 7 patients with unstable blood pressure and heart rhythm underwent AE following DSA examination, leading to stabilized vital signs and urine color improvement [7]. Additionally, four patients developed MBUS post-percutaneous nephrolithotomy, stabilized after active symptomatic treatment. Subsequent DSA examination located bleeding vessels, facilitating successful AE completion.

During AE treatment, after successful intubation, appropriate embolization materials selection based on damaged blood vessel conditions (diameter, blood flow, etc.) is crucial [8]. For MBUS patients with larger blood vessel branch damage, especially arteriovenous fistulas or pseudoaneurysms, non-transparent X-ray coils are preferred for easier monitoring during the operation. This allows for quick collateral circulation reconstruction post-AE, preventing organ necrosis in most patients. Gelatin sponge, as an AE material, is cost-effective, readily available, and effectively stops bleeding, with most patients absorbing it within about 3 weeks post-AE. Beyond this period, inflammatory packaging of damaged tissues and organs begins, aiding in tissue repair and minimizing further bleeding risk, particularly beneficial for organ function recovery [9]. In this study, 13 patients with thin blood vessels and bleeding were treated with Gelfoam sponge strips or gelatin sponge particles, achieving prompt bleeding cessation and ideal hemostatic effects with no recurrence observed post-AE. Furthermore, five patients with thick blood vessels and extensive bleeding were treated with spring steel coils in AE. As a result, 3 patients with severe closed renal contusion and laceration had a large degree of vascular damage. To address damaged capillaries, a small amount of gelatin sponge particles was used in conjunction

with spring steel coils, and no further bleeding or ectopic embolism was observed post-AE.

Complications post-AE treatment included fever in 7 patients, with temperatures ranging from 37.3°C to 38.9°C, averaging 38.2 ± 0.3°C, and local pain, nausea, and vomiting in 4 cases. Following symptomatic treatment within 7 days, complication symptoms resolved. Common complications after AE include bleeding recurrence, embolism syndrome, and ectopic embolism. Nausea, vomiting, fever, and low back pain are key manifestations of embolism syndrome, potentially resulting from local tissue edema and necrosis due to ischemia and hypoxia post-AE. Ensuring the catheter enters the bleeding vessel during intubation and placing the catheter tip as close to the bleeding site as possible helps reduce the risk of embolization of other arterial branches, particularly in embolizing renal-damaged blood vessels. Bleeding recurrence, mainly due to thrombus absorption and emboli shedding, necessitates a second AE or conversion to open surgery. Using metal springs to embolize damaged, thick blood vessels effectively reduces the bleeding recurrence rate [10].

In conclusion, AE proves highly effective in the emergency treatment of MBUS patients, offering the advantages of minimally bodily harm, rapid hemostasis, high safety, and optimal organ function preservation.

Disclosure statement

The authors declare no conflict of interest.

References

[1] Wang Y, Yi J, Luo Y, 2021, Application of Electronic Urine Volume Monitor Equipment to Observe Urine Volume in Patients with Urinary Tract Bleeding. Contemporary Medicine, 27(20): 183–184.

[2] Huang D, Meng X, Zhao J, et al., 2022, The Efficacy of Arterial Embolization Combined with Thoracoscopic Lobectomy in the Treatment of Pulmonary Tuberculosis Accompanied by Massive Hemoptysis and Its Impact on Patients' Lung Function and Arterial Blood Gases. Hainan Medicine, 33(15): 1931–1934.

[3] Wang Q, Wu G, 2023, Preventive Effect of Uterine Artery Embolization and Conservative Treatment on Postoperative Massive Bleeding in Patients with Scar Pregnancy. Chinese Maternal and Child Health Care, 38(5): 787–790.

[4] Wang H, Li G, Chen Q, et al., 2023, Occurrence and Influencing Factors of Massive Bleeding During Uterine Curettage After Uterine Artery Embolization in Early Cesarean Scar Pregnancy. Journal of Interventional Radiology, 32(5): 436–440.

[5] Shi J, Wang L, Du L, et al., 2023, Renal Capsular Artery Embolization Combined with Super-Selective Renal Artery Embolization in Treating Injured Renal Hemorrhage. Journal of Practical Radiology, 39(9): 1503–1513.

[6] Liu S, Liu M, Wang Q, et al., 2023, Efficacy and Safety of CalliSpheres Drug-Loaded Microspheres Through Prostatic Artery Chemoembolization in the Treatment of Advanced Prostate Cancer with Bleeding. Journal of Jiangsu University (Medical Edition), 33(5): 380–385.

[7] He X, Chi R, Wang W, et al., 2023, Analysis of the Therapeutic Effect and Influencing Factors of Uterine Artery Embolization in Patients with Refractory Postpartum Hemorrhage. Chinese Maternal and Child Health Care, 38(13): 2425–2428.

[8] Zheng Z, Zhang Y, Zhou C, 2022, Effects of Uterine Artery Embolization and Methotrexate Treatment on Uterine Artery Hemodynamic Indicators and Adverse Reactions in Patients with Uterine Bleeding in Scar Pregnancy. Chinese and Foreign Medicine, 41(34): 86–89 + 98.

[9] Wu S, 2023, Clinical Observation on Using Spring Coils Combined with Gelatin Sponge Particles for Renal Artery Embolization in Treating Traumatic Renal Bleeding. Zhejiang Trauma Surgery, 28(8): 1424–1427.

[10] Dai Z, Wang D, Li J, 2023, Clinical Observational Study on NBCA Glue Combined with Spring Coil Super-Selective Renal Artery Embolization in Treating Bleeding After Percutaneous Nephroscopy. Modern Chinese Doctors, 61(23): 52–54.

Integrated Services Platform of International Scientific Cooperation

Innoscience Research (Malaysia), which is global market oriented, was founded in 2016.Innoscience Research focuses on services based on scientific research. By cooperating with universities and scientific institutes all over the world, it performs medical researches to benefit human beings and promotes the interdisciplinary and international exchanges among researchers.

Innoscience Research covers biology, chemistry, physics and many other disciplines. It mainly focuses on the improvement of human health. It aims to promote the cooperation, exploration and exchange among researchers from different countries. By establishing platforms, Innoscience integrates the demands from different fields to realize the combination of clinical research and basic research and to accelerate and deepen the international scientific cooperation.

Cooperation Mode

Clinical Workers

In-service Doctors

Foreign Researchers

China Collaborators

Oversea Collaborators

Hospital

University

Scientific institutions

Our Journals

The *Journal of Architectural Research and Development* is an international peer-reviewed and open access journal which is devoted to establish a bridge between theory and practice in the fields of architectural and design research, urban planning and built environment research.

Topics covered but not limited to:

- Architectural design
- Architectural technology, including new technologies and energy saving technologies
- Architectural practice
- Urban planning
- Impacts of architecture on environment

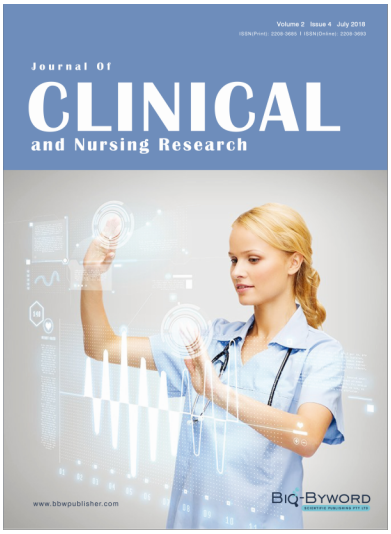

Journal of Clinical and Nursing Research (JCNR) is an international, peer reviewed and open access journal that seeks to promote the development and exchange of knowledge which is directly relevant to all clinical and nursing research and practice. Articles which explore the meaning, prevention, treatment, outcome and impact of a high standard clinical and nursing practice and discipline are encouraged to be submitted as original article, review, case report, short communication and letters.

Topics covered by not limited to:

- Development of clinical and nursing research, evaluation, evidence-based practice and scientific enquiry
- Patients and family experiences of health care
- Clinical and nursing research to enhance patient safety and reduce harm to patients
- Ethics
- Clinical and Nursing history
- Medicine

Journal of Electronic Research and Application is an international, peer-reviewed and open access journal which publishes original articles, reviews, short communications, case studies and letters in the field of electronic research and application.

Topics covered but not limited to:

- Automation
- Circuit Analysis and Application
- Electric and Electronic Measurement Systems
- Electrical Engineering
- Electronic Materials
- Electronics and Communications Engineering
- Power Systems and Power Electronics
- Signal Processing
- Telecommunications Engineering
- Wireless and Mobile Communication